

An Inertia-Free Filter Line-Search Algorithm for Large-Scale Nonlinear Programming

Nai-Yuan Chiang · Victor M. Zavala

Abstract We present a filter line-search algorithm that does not require inertia information of the linear system. This feature enables the use of a wide range of linear algebra strategies and libraries, which is essential to tackle large-scale problems on modern computing architectures. The proposed approach performs curvature tests along the search step to detect negative curvature and to trigger convexification. We prove that the approach is globally convergent and we implement the approach within a parallel interior-point framework to solve large-scale and highly nonlinear problems. Our numerical tests demonstrate that the inertia-free approach is as efficient as inertia detection via symmetric indefinite factorizations. We also demonstrate that the inertia-free approach can lead to reductions in solution time because it reduces the amount of convexification needed.

Keywords inertia · nonlinear programming · filter line-search · nonconvex · large-scale

1 Introduction

Filter line-search strategies have proven effective at solving large-scale, constrained nonlinear programs (NLPs) [6,12,16,37,30]. This algorithmic approach is implemented in the widely used IPOPT package [38]. In a filter line-search setting, it is essential to detect the presence of negative curvature and to regularize the Hessian of the Lagrangian when such is present. This ensures that the computed step is a descent direction when the constraint violation is sufficiently small. This in turn prevents the filter from accepting iteration subsequences that only improve the constraint violation.

The ability to handle negative curvature is essential when dealing with highly nonlinear and inherently ill-conditioned problems [43]. In a constrained NLP setting, the presence of negative curvature is detected using inertia information of the augmented matrix. Inertia informa-

Nai-Yuan Chiang
Mathematics and Computer Science Division, Argonne National Laboratory
9700 South Cass Avenue, Argonne, IL 60439
Tel.: +1-630-252-3343
E-mail: nychiang@mcs.anl.gov

Victor M. Zavala
Department of Chemical and Biological Engineering, University of Wisconsin-Madison
1415 Engineering Hall, Madison, WI 53706
Tel.: +1-608-262-6934
E-mail: victor.zavala@wisc.edu

tion is provided by symmetric indefinite factorization routines such as MA27, MA57, MUMPS, and PARDISO [2,20,21,35]. An inertia-revealing preconditioning strategy based on incomplete factorizations has also been proposed that enables the use of iterative linear strategies such as QMR [36]. Unfortunately, many modern and efficient linear algebra strategies and libraries are not capable of providing inertia information. Examples include iterative techniques such as multigrid (geometric and algebraic) and Lagrange-Newton-Krylov [7,8]; parallel libraries for graphics processing units (GPUs) and distributed-memory systems such as MAGMA, ELMENTAL, Trilinos, and PETSc [1,29,4]; and decomposition strategies for stochastic optimization, optimal control, and network problems that are widely used in convex optimization [22,26,32–34,41,45]. Consequently, the need for inertia information hinders modularity, application scope, and scalability. Byrd, Curtis, and Nocedal recently proposed a line-search exact penalty framework that does not require inertia information [11]. In their approach, termination tests are included to guarantee that the search step provides sufficient progress in the merit function. This approach can also deal with inexact linear algebra and has been extended to deal with rank-deficient Jacobians [17]. The strategy has also proven to be effective when used within an interior-point framework [18].

Trust-region strategies provide a natural mechanism to detect negative curvature. Modern trust-region implementations for constrained NLP decompose the search step into tangential and normal components. The tangential step is computed by approximately solving a trust-region subproblem [10,23,28]. This is typically done by using a projected conjugate gradient (PCG) scheme that detects negative curvature at the inner iterates. In the presence of a direction of negative curvature, the PCG path is continued along this direction until it reaches the trust-region boundary. This approach is guaranteed to be globally convergent because it can always improve the Cauchy step (or revert to it) [15]. It is well-known, however, that the quality of the step can be poor when the PCG procedure is terminated prematurely and this can result in excessive shrinking of the trust-region and slow progress. A Lanczos approach can be used to improve the quality of the PCG step when this hits the trust-region boundary but this requires a more expensive procedure [24]. Under a trust-region setting, one is limited in the linear algebra techniques that can be used to compute the search step. In particular, one requires schemes that are compatible with the globalization approach (i.e., improve the progress of the Cauchy step). Linear algebra strategies such as direct factorizations, GMRES, and QMR are not compatible in this sense. This is important because some of these linear algebra strategies might handle difficult linear systems more efficiently than PCG. This observation has in fact motivated the implementation of a hybrid trust-region and line-search strategy in the widely used KNITRO package [40]. In addition, trust-region settings require tailored preconditioners that project (exactly or inexactly) the iterates onto the nullspace of the constraint Jacobian [23,28]. This can be a limitation when the preconditioner does not have the required projection properties or when it involves an iterative scheme such as multigrid. A line-search setting has the practical advantage that any linear algebra scheme can be used to compute the step (as long as the computed step is a descent direction) and this provides computational flexibility. Such flexibility motivates our interest in line-search approaches. The price to pay in a line-search setting is that regularization of the Hessian matrix (convexification) might be needed and this tends to decrease the quality of the computed step and increase the number of trial step computations. Trust-region settings, on the other hand, have the advantage that no explicit regularization is needed (this is done implicitly through the trust-region constraint) and this can enable more efficient handling of ill-posed problems such as those arising in parameter estimation [3]. Motivated by this property, we are interested in deriving step acceptance tests for line-search settings that limit the amount of regularization needed and that can better handle ill-posed problems.

In this work, we present an inertia-free filter line-search strategy for nonconvex NLPs. Motivated by curvature tests used in trust-region settings, the approach performs a curvature test along the tangential component of the computed step. The curvature test guarantees descent when the constraint violation is sufficiently small. When the test is not fulfilled, it triggers regularization of the Hessian matrix. We prove that global convergence of the algorithm can be guaranteed and that the norm of the step is a consistent criticality metric if the computed step satisfies the curvature test and if the iteration matrix is nonsingular at each iteration. These requirements are significantly less restrictive than the positive definiteness assumption for the reduced Hessian used in the standard filter line-search algorithm. We implement our developments in an interior-point framework and perform extensive numerical tests which include small-scale CUTE and Schittkowski problems as well as large-scale and highly nonlinear problems arising from power grid and natural gas networks. We demonstrate that two variants of the inertia-free approach are as efficient as the standard inertia detection strategy based on symmetric indefinite LBL^T factorizations in terms of iteration counts. We also demonstrate that the inertia-free variants can reduce the number of trial factorizations and solution times because of increased flexibility. We also demonstrate that such flexibility enables us to handle ill-posed problems more efficiently.

The paper is structured as follows. Section 2 presents the filter line-search algorithm of Wächter and Biegler [38,39] in an interior-point framework and discusses assumptions needed to guarantee global convergence. Section 4 presents the new inertia-free strategies and establishes global convergence. Section 5 compares the numerical performance of both strategies. Section 6 presents concluding remarks.

2 Interior-Point Framework

Consider the NLP of the form

$$\min_{x \in \mathbb{R}^n} f(x) \quad (1a)$$

$$\text{s.t. } c(x) = 0 \quad (1b)$$

$$x \geq 0. \quad (1c)$$

Here, $x \in \mathbb{R}^n$ are primal variables, and the objective and constraint functions are $f : \mathbb{R}^n \rightarrow \mathbb{R}$ and $c : \mathbb{R}^n \rightarrow \mathbb{R}^m$, respectively. We use a logarithmic barrier framework with subproblems of the form

$$\min_{x \in \mathbb{R}^n} \varphi^\mu(x) := f(x) - \mu \sum_{j=1}^n \ln x^{(j)} \quad (2a)$$

$$\text{s.t. } c(x) = 0 \quad (2b)$$

where $\mu > 0$ is the barrier parameter and $x^{(j)}$ is the j th entry of vector x . We consider a framework that solves a sequence of barrier problems (2) and drives the barrier parameter μ monotonically to zero.

To approximately solve each barrier problem, we apply Newton's method to its optimality conditions:

$$\nabla_x \varphi^\mu(x) + \nabla_x c(x) \lambda = 0 \quad (3a)$$

$$c(x) = 0 \quad (3b)$$

while enforcing $x \geq 0$ along the search. Here, $\lambda \in \mathfrak{R}^m$ are multipliers for equality constraints. The primal variables and multipliers at iteration k are denoted as (x_k, λ_k) . Their corresponding search directions $(d_k, \lambda_k^+ - \lambda_k)$ can be obtained by solving the linear system

$$\begin{bmatrix} W_k & J_k^T \\ J_k & 0 \end{bmatrix} \begin{bmatrix} d_k \\ \lambda_k^+ \end{bmatrix} = - \begin{bmatrix} g_k \\ c_k \end{bmatrix}. \quad (4)$$

We refer to this system as the augmented system. Here, $c_k := c(x_k)$, $J_k := \nabla_x c(x_k)^T \in \mathfrak{R}^{m \times n}$, $g_k := \nabla_x \varphi_k^\mu$, $W_k := H_k + \Sigma_k$, $H_k := \nabla_{xx} \mathcal{L}(x_k, \lambda_k) \in \mathfrak{R}^{n \times n}$, $\mathcal{L}(x_k, \lambda_k) := \varphi^\mu(x_k) + \lambda_k^T c(x_k)$, and $\Sigma_k := X_k^{-2}$ with $X_k := \text{diag}(x_k)$. One can show that the primal-dual approximation $\Sigma_k \approx X_k^{-1} V_k$, where $V_k := \text{diag}(\nu_k)$ and ν_k are multiplier estimates for the bounds (1c), can be used as long as the products $x_k^{(j)} \nu_k^{(j)}$ remain proportional to μ [39,18]. To enable compact notation, we define the augmented matrix

$$M_k := \begin{bmatrix} W_k & J_k^T \\ J_k & 0 \end{bmatrix}. \quad (5)$$

We can also consider the computation of the search directions d_k using the decomposition

$$d_k = n_k + t_k. \quad (6)$$

Here, n_k is computed from

$$\begin{bmatrix} W_k & J_k^T \\ J_k & 0 \end{bmatrix} \begin{bmatrix} n_k \\ \cdot \end{bmatrix} = - \begin{bmatrix} 0 \\ c_k \end{bmatrix}, \quad (7)$$

and t_k is computed from

$$\begin{bmatrix} W_k & J_k^T \\ J_k & 0 \end{bmatrix} \begin{bmatrix} t_k \\ \lambda_k^+ \end{bmatrix} = - \begin{bmatrix} g_k + W_k n_k \\ 0 \end{bmatrix}, \quad (8)$$

where λ_k^+ is the multiplier update.

We define a two-dimensional filter of the form $\mathcal{F} := \{(\theta(x), \varphi(x))\}$ with $\theta(x) = \|c(x)\|$, $\varphi(x) := \varphi^\mu(x)$ for a fixed barrier parameter μ , where $\|\cdot\|$ is the Euclidean norm. At each value of μ , the filter is initialized as

$$\mathcal{F}_0 := \{(\theta, \varphi) \mid \theta \geq \theta^{max}\} \quad (9)$$

with a given parameter $\theta^{max} > 0$. The filter at iteration k is denoted as \mathcal{F}_k . Given a search step d_k , a line search is started from counter $l \leftarrow 0$ and $\alpha_{k,0} = \alpha_k^{max} \leq 1$ to define trial iterates $x_k(\alpha_{k,l}) := x_k + \alpha_{k,l} d_k$.

We define

$$m_k(\alpha) := \alpha g_k^T d_k \quad (10)$$

as the linear model of $\varphi(x_k + \alpha d_k) - \varphi(x_k)$. We note that d_k is a descent direction¹ if $m_k(\alpha) < 0$. Having constants $\kappa_\theta > 0$, $s_\theta > 1$, $s_\varphi \geq 1$, $\gamma_\theta \in (0, 1)$, and $\eta_\varphi \in (0, 1)$, we consider the following conditions to check whether a trial iterate should be accepted.

– *Filter Condition FC:*

$$(\theta(x_k(\alpha_{k,l})), \varphi(x_k(\alpha_{k,l}))) \notin \mathcal{F}_k$$

¹ We use the expression “descent direction” with respect to the barrier function.

– *Switching Condition SC*:

$$-m_k(\alpha_{k,l}) > 0 \quad \text{and} \quad [-m_k(\alpha_{k,l})]^{s_\varphi} [\alpha_{k,l}]^{1-s_\varphi} > \kappa_\theta [\theta(x_k)]^{s_\theta}$$

– *Armijo Condition AC*:

$$\varphi(x_k(\alpha_{k,l})) \leq \varphi(x_k) + \eta_\varphi m_k(\alpha_{k,l}).$$

– *Sufficient Decrease Condition SDC*:

$$\theta(x_k(\alpha_{k,l})) \leq (1 - \gamma_\theta)\theta(x_k) \quad \text{or} \quad \varphi(x_k(\alpha_{k,l})) \leq \varphi(x_k) - \gamma_\varphi\theta(x_k).$$

The filter condition FC is the first requirement for accepting a trial iterate $x_k(\alpha_{k,l})$. If the pair $(\theta(x_k(\alpha_{k,l})), \varphi(x_k(\alpha_{k,l}))) \in \mathcal{F}_k$ (i.e., the trial iterate is contained in the filter), then the step is rejected, and we decrease the stepsize. If the trial iterate is not contained in the filter, then we continue testing additional conditions. We have two possible cases:

- If SC holds, then the step d_k is a descent direction, and we check whether AC holds. If AC holds, then we accept the trial point $x_k(\alpha_{k,l})$. If not, we decrease the stepsize.
- If SC does not hold and SDC holds, then we accept the trial iterate $x_k(\alpha_{k,l})$. If not, we decrease the stepsize.

If the trial iterate $x_k(\alpha_{k,l})$ is accepted in the second case, then the filter is augmented as

$$\mathcal{F}_{k+1} \leftarrow \mathcal{F}_k \cup \{(\theta, \varphi) \mid \varphi \geq \varphi(x_k) - \gamma_\varphi\theta(x_k), \theta \geq (1 - \gamma_\theta)\theta(x_k)\} \quad (11)$$

with parameters $\gamma_\varphi \in (0, 1)$; otherwise, we leave the filter unchanged (i.e., $\mathcal{F}_{k+1} \leftarrow \mathcal{F}_k$). If the trial stepsize $\alpha_{k,l}$ becomes smaller than α_k^{min} and the step has not been accepted in either case, then we revert to feasibility restoration, and the filter is augmented. A strategy to obtain α_k^{min} is proposed in [39]. We define the set \mathcal{R}_{inc} as the set of iteration counters k in which feasibility restoration is called.

We refer to the first condition of SDC as SDCC to emphasize that this condition accepts the trial iterate if it improves the constraint violation. Similarly, we refer to the second condition as SDCO to emphasize that this condition accepts the trial iterate if it improves the objective function. We refer to successful iterates in which the filter is not augmented (iterates in which the switching condition SC holds) as *f-iterates*. The filter line-search algorithm is summarized below.

FILTER LINE-SEARCH ALGORITHM

0. **Given** starting point x_0, λ_0 , constants $\theta_{max} \in (\theta(x_0), \infty]$, $\gamma_\theta, \gamma_\varphi \in (0, 1)$, $\eta_\varphi \in (0, 1)$, $\kappa_\theta > 0$, $s_\theta > 1$, $s_\varphi \geq 1$ and $0 < \tau_1 \leq \tau_2 < 1$.
1. **Initialize** filter $\mathcal{F}_0 := \{(\theta, \varphi) : \theta \geq \theta_{max}\}$ and iteration counter $k \leftarrow 0$.
2. **Check Convergence.** Stop if x_k is a stationary point (i.e., satisfies (3)).
3. **Compute Search Direction.** Compute step $(d_k, \lambda_k^+ - \lambda_k)$ from (6)-(8).
4. **Backtracking Line-Search.**
 - (a) **Initialize.** Set $\alpha_{k,0} \leftarrow \alpha_k^{max}$ and counter $\ell \leftarrow 0$.
 - (b) **Compute Trial Point.** If $\alpha_{k,\ell} \leq \alpha_k^{min}$ revert to feasibility restoration in Step 8. Otherwise, set trial point $x_k(\alpha_{k,\ell}) \leftarrow x_k + \alpha_{k,\ell}d_k$.
 - (c) **Check Acceptability to the Filter.** If FC does not hold, reject trial point $x_k(\alpha_{k,\ell})$, and go to Step 4e.
 - (d) **Check Sufficient Progress.**
 - i. If SC and AC hold, accept trial point $x_k(\alpha_{k,\ell})$ and go to Step 5.
 - ii. If SC does not hold and SDC hold, accept trial point $x_k(\alpha_{k,\ell})$, and go to Step 5. Otherwise, go to Step 4e.

- (e) **New Trial stepsize.** Choose $\alpha_{k,\ell+1} \in [\tau_1\alpha_{k,\ell}, \tau_2\alpha_{k,\ell}]$, set $\ell \leftarrow \ell + 1$, and go to Step 4b.
5. **Accept Trial Point.** Set $\alpha_k \leftarrow \alpha_{k,\ell}$ and $x_{k+1} \leftarrow x_k(\alpha_{k,\ell})$.
 6. **Augment Filter.** If SC is not satisfied, augment filter using (11). Otherwise, leave filter unchanged.
 7. **Next Iteration.** Increase iteration counter $k \leftarrow k + 1$ and go to Step 2.
 8. **Feasibility Restoration.** Compute an iterate x_{k+1} that satisfies FC and SDC. Augment filter using (11), and go to Step 7.

The above algorithm seeks to solve the barrier subproblem (2) approximately for a fixed μ . Once this problem is solved, we decrease the barrier parameter μ and we reset the filter (9). This outer loop is repeated until we find a stationary point for the original NLP (1). We highlight that the global convergence analysis of the filter line-search algorithm discussed in the next section does not require a particular stepsize rule for the multipliers (it only requires boundedness of the multiplier updates λ_k^+). Consequently, we do not provide a explicit stepsize rule in the above algorithm. This is left as an implementation issue at this point that is discussed in Section 5.

3 Inertia-Based Strategy

The global convergence analysis of the filter line-search algorithm provided in [39] assumes a step decomposition of the form

$$d_k = Y_k \bar{q}_k + Z_k \bar{p}_k \quad (12a)$$

$$\bar{q}_k := -(J_k Y_k)^{-1} c_k \quad (12b)$$

$$\bar{p}_k := -(Z_k^T W_k Z_k)^{-1} Z_k^T (g_k + W_k Y_k \bar{q}_k), \quad (12c)$$

where $Y_k \in \mathbb{R}^{n \times m}$ and $Z_k \in \mathbb{R}^{n \times (n-m)}$ are matrices such that the columns of $[Y_k \ Z_k]$ form an orthonormal basis for \mathbb{R}^n and the columns of Z_k are the basis of the null space of J_k (i.e., $J_k Z_k = 0$). The convergence analysis also relies on the criticality measure

$$\chi_k := \|Z_k \bar{p}_k\| = \|\bar{p}_k\|, \quad (13)$$

where the last identity follows from the orthonormality of Z_k (i.e., $Z_k^T Z_k = I$). The analysis requires assumptions (G) in [39]. To facilitate the discussion, we state the relevant assumptions here:

Assumptions (G)

- (G1) There exists an open set $\Omega \subseteq \mathbb{R}^n$ with $[x_k, x_k + d_k] \subseteq \Omega$ for all $k \notin \mathcal{R}_{inc}$ in which $\varphi(\cdot)$ and $c(\cdot)$ are twice differentiable and their values and derivatives are bounded.
- (G2) The matrices W_k are uniformly bounded for all $k \notin \mathcal{R}_{inc}$.
- (G3) The matrices W_k are uniformly positive definite on the null space of the Jacobian J_k .
- (G4) There exists a constant $c_A > 0$ so that for all $k \notin \mathcal{R}_{inc}$, the smallest singular value of J_k is bounded by $c_A > 0$.
- (G5) There exists a constant $\theta_{inc} > 0$ such that $k \notin \mathcal{R}_{inc}$ whenever $\theta(x_k) \leq \theta_{inc}$.

Assumptions (G3) and (G4) are needed to guarantee that χ_k is a valid criticality measure in the sense that it converges to zero as we approach a first-order stationary point. To see this, consider a subsequence $\{x_{k_i}\}$ with $\lim_{i \rightarrow \infty} \chi_{k_i} = 0$ and $\lim_{i \rightarrow \infty} x_{k_i} = x^*$ for some feasible point x^* . If the Jacobian is of full row rank (implied by assumption (G4)) and (12b) holds, we have that $\lim_{i \rightarrow \infty} \bar{q}_{k_i} = 0$ as $\lim_{i \rightarrow \infty} x_{k_i} = x^*$. From $\lim_{i \rightarrow \infty} \chi_{k_i}$, (12c), and (13); and because

(G3) guarantees nonsingularity of the reduced Hessian we have that $\lim_{i \rightarrow \infty} \|Z_{k_i}^T g_{k_i}\| = 0$. In Section 4 we will prove that a decomposition of the form (12) can always be obtained when the Jacobian is of full row rank and the augmented matrix is nonsingular (these are less restrictive assumptions). Consequently, the step computed from the augmented system (8) is equivalent to that obtained with (12).

Positive definiteness of the reduced Hessian (G3) also guarantees that the search direction is of descent when the constraint violation is sufficiently small and the criticality measure is nonzero (see Lemma 2 in [39]). As we will discuss in Section 4, this *descent lemma* is essential for establishing global convergence. Assumption (G3) can be enforced in a practical setting by monitoring the inertia (number of positive, negative, and zero eigenvalues) of the augmented matrix M_k and correcting it (if necessary) by regularizing the Hessian matrix as $W_k \leftarrow W_k + \delta I$ for $\delta \geq 0$. This *convexification* approach is justified from the results of Gould [25], which show that the reduced Hessian is positive definite if and only if the augmented matrix M_k has n positive, m negative, and no zero eigenvalues. We state this condition formally as

$$\text{Inertia}(M_k) = \{n, m, 0\}. \quad (14)$$

The augmented matrix M_k can be decomposed as LBL^T by using symmetric indefinite factorizations where L is a unit lower triangular matrix and B is a block diagonal matrix composed of 1×1 and 2×2 diagonal blocks. From Sylvester's law of inertia we know that the eigenvalues of M_k are the eigenvalues of B . Furthermore, because each 2×2 block is constructed by having one positive and one negative eigenvalue, the inertia of M_k can be estimated from the inertia of B [9].

We can enforce assumption (G3) using the following procedure. The matrix M_k is decomposed as LBL^T for $\delta = 0$ and the search direction d_k is computed using this decomposition. If the inertia is correct (i.e., condition (14) is satisfied), the search direction d_k is used as trial step in the line-search procedure. If the inertia is not correct, the regularization parameter δ is increased, the augmented matrix is refactorized and a new direction d_k is obtained. The procedure is repeated until the matrix M_k has the correct inertia. Heuristics are incorporated to accelerate the rate of increase/decrease of δ in order to ensure that the number of trial factorizations is not too large (because each factorization is computationally expensive). The inertia-based regularization strategy implemented in the current version of IPOPT [38] is shown below.

INERTIA-BASED REGULARIZATION (IBR)

- IBR-1 Factorize M_k with $\delta = 0$. If (14) holds, compute d_k and stop.
- IBR-2 If $\delta^{last} = 0$, set $\delta \leftarrow \bar{\delta}^0$, otherwise set $\delta \leftarrow \max\{\bar{\delta}^{min}, \kappa^- \delta^{last}\}$.
- IBR-3 Factorize M_k with current δ . If (14) holds, set $\delta^{last} \leftarrow \delta$, compute d_k and stop.
- IBR-4 If $\delta^{last} = 0$, set $\delta \leftarrow \hat{\kappa}^+ \delta$, otherwise set $\delta \leftarrow \kappa^+ \delta$ and go to IBR-3.

Here, $0 < \bar{\delta}^{min} < \bar{\delta}^0$, $0 < \kappa^- < 1 < \kappa^+ < \hat{\kappa}^+$ are given constants.

4 Inertia-Free Strategies

Estimating the inertia of M_k can be complicated or impossible when a decomposition of the form LBL^T is not available. As we noted in the introduction, this situation limits our options for computing the search step and motivates us to consider inertia-free strategies. If we take one step back, we realize that the primary practical intention of inertia correction is to guarantee that the direction d_k is of descent when the constraint violation is sufficiently small. This approach,

however, introduces a disconnect between the regularization procedure (IBR) and the filter line-search globalization procedure. In particular, the inertia test (14) is based solely on the structural properties of M_k and not on the computed direction d_k . Hence, the regularization procedure IBR can implicitly discard productive descent directions in attempting to enforce a correct inertia. We thus consider another route to enforce descent.

We first discuss a inertia-free strategy that uses the step decomposition (6), system (7)-(8), and the criticality measure

$$\Psi_k^t := \|t_k\|. \quad (15)$$

As we will argue in Section 4.1, a step decomposition is not strictly necessary, but it is advantageous for the analysis and can be used to enable the use of PCG strategies [23].

For our analysis we make the following assumptions.

Assumptions (RG)

- (RG1) There exists an open set $\Omega \subseteq \mathfrak{R}^n$ with $[x_k, x_k + d_k] \subseteq \Omega$ for all $k \notin \mathcal{R}_{inc}$ in which $\varphi(\cdot)$ and $c(\cdot)$ are twice differentiable and their values and derivatives are bounded.
- (RG2) The matrices W_k are uniformly bounded for all $k \notin \mathcal{R}_{inc}$.
- (RG3) There exists a constant $\alpha_t > 0$ such that the step components n_k, t_k satisfy the following *curvature condition* (RG3a):

$$t_k^T W_k t_k + \max\{t_k^T W_k n_k - g_k^T n_k, 0\} \geq \alpha_t t_k^T t_k. \quad (16)$$

Furthermore, the augmented matrix M_k is nonsingular and its inverse is bounded for all $k \notin \mathcal{R}_{inc}$ (RG3b).

- (RG4) There exists a constant $c_A > 0$ so that for all $k \notin \mathcal{R}_{inc}$, the smallest singular value of J_k is bounded by $c_A > 0$.
- (RG5) There exists a constant $\theta_{inc} > 0$ such that $k \notin \mathcal{R}_{inc}$ whenever $\theta(x_k) \leq \theta_{inc}$.

The key difference between assumptions (RG) and assumptions (G) used in the standard filter line-search algorithm is that we do not require positive definiteness of the reduced Hessian (G3). This requirement is replaced by assumptions (RG3) and we now show that these are less restrictive and sufficient to guarantee global convergence. We begin by showing that conditions (RG3b) and (RG4) are sufficient to guarantee that the reduced Hessian is nonsingular and that (15) is a valid criticality measure.

Lemma 1 *Let (RG3b) and (RG4) hold and define $M = M_k$, $W = W_k$, $Z = Z_k$, and $J = J_k$. Then (i) the reduced Hessian $Z^T W Z$ is nonsingular and (ii) the inverse of M can be expressed as*

$$M_{inv} = \begin{bmatrix} W & J^T \\ J & 0 \end{bmatrix}^{-1} = \begin{bmatrix} P & (I - PW)J^T V^{-1} \\ V^{-1}J(I - WP) & -V^{-1}J(W - W P W)J^T V^{-1} \end{bmatrix} \quad (17)$$

with

$$P = Z(Z^T W Z)^{-1} Z^T \quad (18)$$

and $V = J J^T$.

Proof: Part (i) follows from Lemmas 3.2 and 3.4 in [25]. These results establish that if the Jacobian is of full row rank (RG4) there exists a nonsingular matrix R such that

$$RMR^T = \begin{bmatrix} & I \\ Z^T W Z & \\ I & \end{bmatrix}. \quad (19)$$

From Sylvester's law of inertia and the structure of RMR^T we have that

$$\text{Inertia}(M) = \text{Inertia}(Z^T W Z) + \{m, m, 0\}. \quad (20)$$

Consequently, the number of zero eigenvalues of M is equal to the number of zero eigenvalues of $Z^T W Z$. By assumption (RG3b) we know that M is nonsingular and thus we know that it does not have zero eigenvalues. Consequently, $Z^T W Z$ does not have zero eigenvalues either and therefore is nonsingular.

To prove (ii), we first note that (RG3b) and (RG4) guarantee that P exists. We denote the blocks of $M_{inv}M$ as A_{11} , $A_{12} = A_{21}^T$, A_{22} , and we seek to prove that $M_{inv}M = I$. By direct calculation and by noticing that $J^T(JJ^T)^{-1}J = I - ZZ^T$ [5, p. 20] and $JZ = 0$, we obtain

$$\begin{aligned} A_{11} &= WP + J^T V^{-1} J(I - WP) \\ &= WP + (I - ZZ^T)(I - WP) \\ &= I - ZZ^T + ZZ^T W Z (Z^T W Z)^{-1} Z^T \\ &= I \end{aligned} \quad (21a)$$

$$\begin{aligned} A_{12} &= W(I - PW)J^T(JJ^T)^{-1} - J^T(JJ^T)^{-1}J(W - WPW)J^T(JJ^T)^{-1} \\ &= ZZ^T(W - WPW)J^T(JJ^T)^{-1} \\ &= (ZZ^T W - ZZ^T W Z (Z^T W Z)^{-1} Z^T W) J^T(JJ^T)^{-1} \\ &= 0 \end{aligned} \quad (21b)$$

$$\begin{aligned} A_{22} &= J(I - PW)J^T(JJ^T)^{-1} \\ &= J(I - Z(Z^T W Z)^{-1} Z^T W)J^T(JJ^T)^{-1} \\ &= JJ^T(JJ^T)^{-1} - JZ(Z^T W Z)^{-1} Z^T W J^T(JJ^T)^{-1} \\ &= I. \end{aligned} \quad (21c)$$

The proof is complete. \square

From (7), (8), and the explicit form of the inverse of M_k in (17) we have that,

$$n_k = -(I - Z_k(Z_k^T W_k Z_k)^{-1} Z_k^T W_k) J_k^T (J_k J_k^T)^{-1} c_k, \quad (22)$$

and

$$t_k = -Z_k(Z_k^T W_k Z_k)^{-1} Z_k^T (g_k + W_k n_k). \quad (23)$$

We thus see that the tangential step is equivalent to the tangential component $Z_k \bar{p}_k$ obtained from the decomposition (12). Consequently, Lemma 1 implies that an expression for the tangential step of the form in (12) can always be obtained if the Jacobian is of full row rank and the augmented matrix is nonsingular. We also note that the expression for the normal component in (12) is not equivalent to that in (22) but this is not necessary as long as n_k obtained from (7) is bounded and decays to zero as we approach a feasible point (equivalence can be achieved by replacing W_k with I in (7)). These observations allow us to prove that the measure (15) is a valid criticality measure under assumptions (RG), as stated in the next result.

Theorem 1 Consider a subsequence $\{x_{k_i}\}$ with $\lim_{i \rightarrow \infty} x_{k_i} = x^*$ for a feasible x^* , let (RG3b) and (RG4) hold, let n_{k_i} solve (7), and let t_{k_i} solve (8). Then

$$\lim_{i \rightarrow \infty} \Psi_{k_i}^t = 0 \implies \lim_{i \rightarrow \infty} \|Z_{k_i}^T g_{k_i}\| = 0$$

for Z_{k_i} spanning the null space of J_{k_i} .

Proof: Define $M := M_{k_i}$, $W := W_{k_i}$, $J := J_{k_i}$, and $Z := Z_{k_i}$. Boundedness of n_k follows from (RG1), which guarantees that the right-hand side of the augmented system (7) is bounded and from (RG3b) which guarantees that the inverse of M_k is bounded. Boundedness of n_k together with (RG1) and (RG2) guarantee that the right hand side of (8) is bounded. This fact, together with (RG3b), guarantee that t_k is bounded. We thus have that condition $\lim_{i \rightarrow \infty} x_{k_i} = x^*$ for feasible x^* ensures $\lim_{i \rightarrow \infty} n_{k_i} = 0$. From Lemma 1 we know that $Z^T W Z$ is nonsingular and therefore the projection matrix P_{k_i} exists and is nonsingular. From (15), (23), and $\lim_{i \rightarrow \infty} n_{k_i} = 0$ as $\lim_{i \rightarrow \infty} x_{k_i} = x^*$ we obtain the result. \square

We now show that the curvature condition of assumption (RG3a) is sufficient to ensure that the step d_k is a descent direction.

Lemma 2 Let assumptions (RG1)-(RG5) hold. If x_{k_i} is a subsequence of iterates for which $\Psi_{k_i}^t \geq \epsilon$ with a constant ϵ independent of i , then there exist positive constants ϵ_1, ϵ_2 such that

$$\theta_{k_i} \leq \epsilon_1 \implies \frac{m_{k_i}(\alpha)}{\alpha} \leq -\epsilon_2.$$

Proof: Define $W := W_{k_i}$, $J := J_{k_i}$, $g := g_{k_i}$, $d := d_{k_i}$, $\Psi := \Psi_{k_i}^t$, $\theta := \theta_{k_i}$, $n := n_{k_i}$, and $t := t_{k_i}$. Multiplying the first row of (8) by t^T and recalling that $Jt = 0$, we obtain

$$t^T W t = -g^T t - t^T W n.$$

We know that $g^T d = g^T n + g^T t$. Thus, combining terms, we obtain

$$-g^T d = t^T W t + t^T W n - g^T n.$$

We consider two cases. In the first case we have that $t^T W n - g^T n < 0$, and the curvature condition (16) guarantees that $t^T W t \geq \alpha_t t^T t$ and $-g^T d \geq \alpha_t t^T t + t^T W n - g^T n$. From (RG1) we can obtain the bounds $|t^T W n| \leq \bar{c}_1 \Psi \theta$ and $|g^T n| \leq \bar{c}_2 \theta$ for $\bar{c}_1, \bar{c}_2 > 0$. From (15) we have that $\|t\| = \Psi$, and we thus have

$$\begin{aligned} g^T d &\leq -\alpha_t \Psi^2 + \bar{c}_1 \Psi \theta + \bar{c}_2 \theta \\ &\leq \Psi \left(-\alpha_t \epsilon + \bar{c}_1 \theta + \frac{\bar{c}_2}{\epsilon} \theta \right). \end{aligned}$$

Defining $\epsilon_1 := \min \left\{ \theta_{inc}, \frac{\epsilon^2 \alpha_t}{2(\bar{c}_1 \epsilon + \bar{c}_2)} \right\}$ with θ_{inc} from (RG5), it follows that for all $\theta \leq \epsilon_1$ we have $m(\alpha) \leq -\alpha \epsilon_2$ with $\epsilon_2 := \frac{\epsilon^2 \alpha_t}{2}$. In the second case, we have that $t^T W n - g^T n \geq 0$ and the curvature condition guarantees that $t^T W t + t^T W n - g^T n \geq \alpha_t t^T t$ and $-g^T d \geq \alpha_t t^T t$. In this case the result follows with $\epsilon_1 := \theta_{inc}$ because $\bar{c}_1 = \bar{c}_2 = 0$ and for ϵ_2 defined previously. \square

The descent lemma guarantees that the objective function will be improved at a subsequence of nonstationary iterates (i.e., those with $\Psi_{k_i}^t \geq \epsilon$) having a sufficiently small constraint violation

θ_{k_i} . This implies that f -iterates will eventually be accepted and the filter is eventually not augmented. This in turn implies that an infinite subsequence of nonstationary iterates cannot exist. We now prove that assumptions (RG) guarantee global convergence of the filter line-search algorithm.

Theorem 2 *Let assumptions (RG) hold. The filter line-search algorithm delivers a sequence $\{x_k\}$ satisfying*

$$\lim_{k \rightarrow \infty} \theta(x_k) = 0 \quad (25a)$$

$$\liminf_{k \rightarrow \infty} \Psi^t(x_k) = 0. \quad (25b)$$

Proof: We go through the results leading to the proof of Theorem 2 in [39] and argue that our assumptions (RG) are sufficient. Unless otherwise stated, all lemmas refer to those in [39]. Boundedness of d_k follows from boundedness of its components n_k and t_k which in turn follow from (RG1), (RG2), and (RG3b), as was argued in the proof of Theorem 1. We can also use similar arguments to prove that boundedness of λ_k^+ follows from boundedness of n_k , and from (RG1), (RG2) and (RG3b). Boundedness of $|m_k(\alpha)|$ follows from (RG1). Lemma 2 is replaced by the descent Lemma 2 of this work. Lemma 3 are standard bounding results that follow from Taylor's theorem and require only (RG1). Lemma 4 follows from the descent Lemma 2 of this work. Lemma 6 requires only (RG1). Lemma 8 requires the descent Lemma 2 of this work. Lemma 10 establishes that for a subsequence of nonstationary iterates the filter is eventually not augmented. This requires the descent Lemma 2 of this work. The result follows. \square

The curvature condition (16) of assumption (RG3a) can hold even if the reduced Hessian matrix is not positive definite, as required by assumption (G3) in the standard filter line-search algorithm. Consequently, the curvature condition is less restrictive. If the curvature condition does not hold for the computed step, we can enforce it by regularizing the Hessian matrix $W_k \leftarrow W_k + \delta I$. Specifically, the curvature condition (16) can always be satisfied for sufficiently large δ and sufficiently small α_t satisfying $\alpha_t \leq \lambda_{\min}(Z_k^T W_k Z_k)$. The reason is that t_k lies on the null space of J_k and, consequently, can always be expressed as $t_k = Z_k u$ for a given nonzero vector u and the curvature condition then implies that $u^T Z_k^T W_k Z_k u \geq \alpha_t u^T u$. We also know that an appropriate α_t exists for any δ because $\lambda_{\min}(Z_k^T W_k(\delta) Z_k)$ is an increasing function of δ . Note also that the term $(\max\{t_k^T W_k n_k - g_k^T n_k, 0\})$ does not affect these properties. This is because, if the argument is negative, then this is set to zero; and, if the argument is positive, it provides additional flexibility to satisfy the curvature condition.

We can enforce nonsingularity of M_k and boundedness of its inverse, as required by assumption (RG3b), by regularizing the Hessian W_k as well while making sure that (RG2) holds. This is necessary to guarantee that both n_k and t_k are bounded. Note also that nonsingularity of M_k can be monitored using a linear solver and boundedness of n_k and t_k can be monitored directly. These observations lead to the following inertia-free regularization (IFR) procedure:

INERTIA-FREE REGULARIZATION (IFR)

- IFR-1 Given constant $\alpha_t > 0$, factorize M_k with $\delta = 0$ and compute n_k, t_k from (7) and (8). If t_k satisfies the curvature condition (16) and M_k satisfies (RG3b), set $d_k = t_k + n_k$, and terminate.
- IFR-2 If $\delta^{last} = 0$, set $\delta \leftarrow \bar{\delta}^0$, otherwise set $\delta \leftarrow \max\{\delta^{min}, \kappa^- \delta^{last}\}$.
- IFR-3 Given constant $\alpha_t > 0$, factorize M_k with current δ and compute n_k, t_k from (7) and (8). If t_k satisfies (16) and M_k satisfies (RG3b), set $d_k \leftarrow n_k + t_k$, and terminate.
- IFR-4 If $\delta^{last} = 0$, set $\delta \leftarrow \hat{\kappa}^+ \delta$, otherwise set $\delta \leftarrow \kappa^+ \delta$ and go to IFR-3.

We make the following remarks:

- The curvature condition (16) is enforced at every iteration. In principle, however, one can enforce it only at iterations in which the constraint violation is less than a certain small threshold value θ_{sml} . This approach is consistent with the observation that the switching condition SC needs to be checked only at iterations with small constraint violation [39]. In either case, however, we might need to regularize the Hessian in order to enforce nonsingularity of M_k at every iteration.
- A potential caveat of the inertia-free strategy is that it cannot guarantee that the step computed via the augmented system is a minimum of the associated quadratic program (the inertia-based approach guarantees this). Consequently, while enabling global convergence with enhanced flexibility is a great benefit of inertia-free strategy, the potential price to pay is the possibility of having a larger proportion of steps that are accepted because of improvements on constraint violation and not on the objective function. This situation might ultimately manifest as a tendency to get attracted to first-order stationary points with larger objective values than those obtained with the inertia-based strategy. We provide numerical results in Section 5 to discuss this issue further.
- As seen in Lemma 2, the term $(\max\{t_k^T W_k n_k - g_k^T n_k, 0\})$ in the curvature condition is harmless and is included only to provide additional flexibility. Because of this, one might also consider the simpler test $t_k^T W_k t_k \geq \alpha_t t_k^T t_k$ and still guarantee convergence.
- The normal component n_k can also be computed from system (7) by replacing W_k with I . This, in fact, is a more natural choice than our approach because the normal and tangential components correspond to the decomposition (12) for $Y_k = J_k^T$. Moreover, this approach naturally guarantees that the corresponding augmented matrix is bounded and that the normal step is bounded. This, approach, however, would require the solution of a linear system with a different coefficient matrix as the one used to compute the tangential step.
- Assumption (RG3b) is needed to guarantee that the tangential step is bounded. In practice, however, this condition might be unnecessarily strong if the normal step is guaranteed to be bounded. This is because, in principle, one could still compute a productive tangential step that satisfies (RG3a) even if (RG3b) does not hold. Establishing convergence in this case, however, would require a more sophisticated analysis.
- Assumption (RG1) can be guaranteed to hold only if all iterates x_k remain strictly in the interior of the nonnegative orthant. This condition guarantees that the barrier function $\varphi^\mu(x_k)$ and its derivatives are bounded. One can show that Theorem 3 in [39] holds under assumptions (RG). This result establishes that the iterates x_k remain in the strict interior of the feasible region if the maximum stepsize α_k^{max} is determined by using the following fraction-to-the-boundary rule

$$\alpha_k^{max} := \max\{\alpha \in (0, 1] : x_k + \alpha d_k \geq (1 - \tau)x_k\}, \quad (26)$$

for a fixed parameter $\tau \in (0, 1)$. The full row rank assumption of J_k (RG4), together with the assumption that its rows and the corresponding rows of the active bounds of x_k are linearly independent as well as the nonsingularity of the reduced Hessian (which follows from (RG3b) and Lemma 1), is sufficient for establishing the result.

4.1 Alternative Inertia-Free Tests

Computing the normal and tangential components of the step separately can be beneficial in certain situations. For instance, the use of a PCG scheme provides a mechanism to perform the

curvature test

$$t_{k,j}^T W_k t_{k,j} \geq \alpha_t t_{k,j}^T t_{k,j} \quad (27)$$

on the fly at each PCG iteration j and thus terminate early and save some work if the test does not hold for the current regularization parameter δ . This approach can also be beneficial because more test directions are used to identify negative curvature. This approach, however, requires a preconditioner that projects the iterations onto the null space of the Jacobian, which might not be available in certain applications.

In some applications it might be desirable to operate directly on the full step d_k . In this case, we can impose a curvature condition of the form

$$d_k^T W_k d_k + \max\{-(\lambda_k^+)^T c_k, 0\} \geq \alpha_d d_k^T d_k, \quad (28)$$

with d_k computed from (4).

To argue that test (28) is consistent, we use the criticality measure

$$\Psi_k^d := \|d_k\|. \quad (29)$$

If (RG3b) and (RG4) hold, we have from Lemma 1 and equation (4) that

$$\begin{aligned} d_k &= -P_k g_k - (I - P_k W_k) J_k^T (J_k J_k^T)^{-1} c_k \\ &= -Z_k (Z_k^T W_k Z_k)^{-1} Z_k^T (g_k - W_k J_k^T (J_k J_k^T)^{-1} c_k) - J_k^T (J_k J_k^T)^{-1} c_k. \end{aligned} \quad (30)$$

If we set $Y_k = J_k^T$, we have that d_k has the same structure as the step decomposition in (12). Moreover, we have that

$$\Psi_k^d = \Psi_k^t + O(\|c_k\|). \quad (31)$$

Consequently, the results of Theorem 1 still hold and Ψ_k^d is a valid criticality measure. If $-(\lambda_k^+)^T c_k < 0$, from (28), (RG1), (RG4), and (RG3b) we have that $\|\lambda_k^+\| \leq \kappa$ for some $\kappa > 0$ and, therefore,

$$\begin{aligned} g_k^T d_k &= -d_k^T W_k d_k + d_k^T J_k^T \lambda_k^+ \\ &= -d_k^T W_k d_k + c_k^T \lambda_k^+ \\ &\leq -\alpha_d (\Psi_k^d)^2 + \kappa \theta_k. \end{aligned} \quad (32)$$

Consequently, the results of Lemma 2 hold with appropriate constants. If $-(\lambda_k^+)^T c_k \geq 0$ holds the result follows with $\kappa = 0$.

The curvature condition (28) holds for any δ and $\alpha_d \geq \lambda_{\min}(W_k)$, and we note that the term $\max\{-(\lambda_k^+)^T c_k, 0\}$ is harmless and is used only to enhance flexibility.

5 Numerical Results

In this section we benchmark the inertia-based and inertia-free strategies using the PIPS-NLP interior-point framework [14]. We first describe the implementation used to perform the benchmarks. We then present results for small-scale problems and large-scale problems arising from different applications.

5.1 Implementation

PIPS-NLP is an object-oriented interior-point framework implemented in C++ that facilitates the communication of model structures and the development of linear algebra strategies. These capabilities enable us to solve large-scale problems on parallel computing architectures. The algorithmic framework of PIPS-NLP follows along the lines of that of IPOPT [38] but we do not implement a feasibility restoration phase and watchdog heuristics. If the restoration phase is reached, we terminate the algorithm. We prefer to use this approach to isolate the effects of inertia correction on performance. As in IPOPT [38], we allow steps that are very small in norm $\|d_k\|$ to be accepted even if they do not satisfy SDC or SAC, we use the same stepsize for both primal and equality constraint multipliers, use a primal-dual Hessian, and use a different stepsize for the bound multipliers. We have validated the performance of our implementation by comparing it with that of IPOPT, and we have obtained nearly identical results.

We compare three regularization strategies: (1) IBR: inertia-based regularization, (2) IFRT: inertia-free regularization with the curvature test (16), and (3) IFRd: inertia-free regularization with the curvature test (28). We use the same parameters for IBR and IFR to increase/decrease the regularization parameter δ . For IFRd and IFRT we set both α_t and α_d to 10^{-12} as default. We also scale these parameters using the barrier parameter μ , as suggested in [18]. Strategy IFRd has been implemented in the latest version of IPOPT <https://projects.coin-or.org/Ipopt>.

For the IFRT strategy, we compute the normal step by solving the linear system (7) by factorizing M_k using MA57 [20], and we reuse the factorization to compute the tangential component from (8). For IBR we estimate the inertia of the augmented matrix using MA57.

We use the optimality error described in [38, Section 2] with a convergence tolerance of 10^{-6} , we perform iterative refinement for the augmented system with a tolerance of 10^{-12} , and we set the maximum number of iterations to 1,000. If the line search cannot find an acceptable point within 50 trials, the last trial stepsize is used in the next iteration. We use a pivoting tolerance of 10^{-4} for MA57.

Of the entire set of test problems studied in Section 5.2, 13% have Jacobians that are nearly rank-deficient. To deal with these instances, we regularize the (2,2) block of the augmented matrix as in IPOPT whenever we detect the augmented matrix to be singular [38, Section 3.1]. We emphasize that the convergence theory of this work and the supporting theory in [39] do not hold in this case. In particular, the tangential step computed in IFRT no longer lies exactly on the null-space of the Jacobian and the inverse expression of the augmented matrix of Lemma 1 does not hold. The regularization parameter of the (2,2) block is, however, very small ($10^{-8} - 10^{-11}$) and this is often sufficient to avoid singularity issues. The numerical results obtained indicate that the performance of IFRd and IFRT are not strongly affected by this regularization.

5.2 Small-Scale Tests

We consider 929 test problems: 738 CUTE instances <http://orfe.princeton.edu/~rvdb/ampl/nlmodels/cute/index.html>, 188 Schittkowski instances <http://orfe.princeton.edu/~rvdb/ampl/nlmodels/cute/index.html>, and three additional optimal power flow instances based on IEEE data. The power flow models are accessible at <http://zavalab.engr.wisc.edu/data/testinertia>. Out of the 929 test problems, PIPS-NLP can solve 828 problems with at least one of the regularization strategies implemented (89% of all the tests). This demonstrates the robustness of our implementation. The rest of the problems cannot be solved with any of the strategies considered because the solver either: 1) reaches the limit of

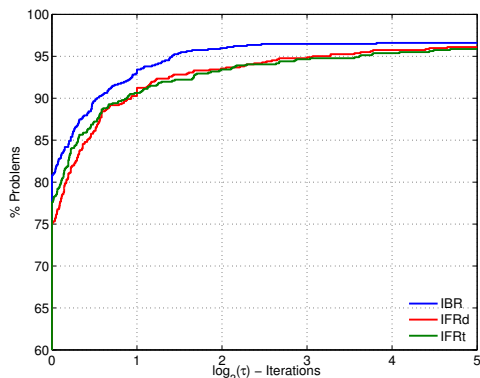


Fig. 1 Number of iterations

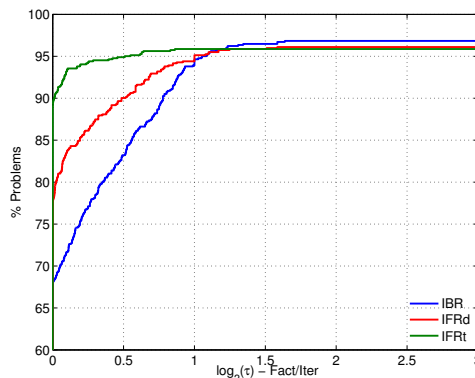


Fig. 2 Number of factorizations per iteration

iterations; 2) requires feasibility restoration; 3) encounters an evaluation error in the problem functions; 4) requires regularization that reaches the maximum limit of 1×10^{12} . We only compare the performance of inertia-based and inertia-free strategies for the 828 problems for which at least one strategy was successful.

The performance of the three strategies is presented in Table A1 in the Appendix. Here, we report the optimal objective (OBJ), the number of iterations (Iter), number of regularizations (Reg), and solution time in seconds. The total number of factorizations is equal to the number of iterations plus the number of regularizations. We use “-” to denote the tests that cannot be solved within the limit of iterations. The last three instances in the table are the energy problems.

We present the numerical results in Table A1. From these results we have that 802, 796, and 794 test problems can be solved with IBR, IFRd and IFRt, respectively. Moreover, there are several instances that can only be solved with the inertia-free strategies (e.g., *fletcher*, and *steenbrf*). We can thus conclude that the inertia-free strategies are competitive. In Figures 1 and 2 we present Dolan-Moré profiles [19] for the total number of iterations and the average number of factorizations per iteration. In Figure 1 we can see that IBR requires fewer iterations to converge, but the differences are negligible. In Figure 2 we can see that IFRd and IFRt significantly outperform IBR in terms of the average number of factorizations required per iteration. From the tests reported in Table A1 we also estimate the average number of regularizations per iteration. We have that IBR requires 0.61 regularizations per iteration while IFRd and IFRt require 0.37 and 0.43 regularizations per iteration, respectively. We thus conclude that IFR strategies significantly reduce the amount of regularization needed.

The inertia-free strategies yield the same final objective value as IBR in 85% of the instances. The performance in this respect is rather surprising. IBR yields better final objective values than IFRd and IFRt in 81 instances (e.g., instances *hatfldd* and *hatflde*), while IFRd and IFRt yield better objective values than IBR in 40 and 41 instances (e.g., instances *s295* and *s296*), respectively. We could, in principle, attribute the tendency of IBR to reach better final objective values to the fact that the solutions of the augmented system are actual minimizers of the associated quadratic program at each iteration, whereas the solutions obtained with the inertia-free strategies are not. Consequently, we would expect that steps computed with IBR should yield improvements in the objective more often. Interestingly, we have found this not necessarily to be the case. To demonstrate this, we compared the percentages of steps accepted by the filter for the three strategies as a result of improvements in the objective function and in the constraint violation. We recall that a trial stepsize can be accepted under three cases: (1) SAC: both SC and

AC hold, (2) SDCO: SDC holds because of sufficient decrease in the objective, and (3) SDCC: SDC holds because of sufficient reduction in the constraint violation. In Table A2 we present the percentage of successful trial steps obtained for each case. We note that the percentages do not add to 100% in some cases because we allow the line search to accept very small steps and because we round the percentages to the nearest integer. To perform this comparison, we consider only problems in which all strategies are successful, and we consider only problems with constraints (the unconstrained instances have a percentage of acceptance for SAC of 100%). The last row presents the average percentages for all problems and from this we can see that IBR accepts 46% of the steps due to SAC. The corresponding percentages are 49% and 51% for IFRd and IFRt, respectively. If we add the total percentages in which the steps are accepted because of improvements in the objective (i.e., add SAC and SDCO), we have that the percentages are 76%, 75%, and 79% for IBR, IFRd, and IFRt, respectively. This result indicates that both inertia-free strategies are competitive with inertia-based strategy in achieving productive steps for the objective value. Moreover, we recall that IFRd and IFRt yield better final objective values than IBR in 40 and 41 instances. Because of this, we cannot draw general conclusions on the tendency of the strategies to provide better final objective values. This can be attributed to the presence of multiple local minima.

We elaborate on the behavior of the strategies in instance `IEEE_162` which is a highly non-linear optimal power flow problem. From Table 1 we can see that IFRt and IFRd do not require regularization and converge in 23 iterations whereas IBR requires 145 iterations and 183 regularizations. This instance is an ill-posed problem that does not seem to have an isolated local minimum (inertia is not correct at the solution). In this instance, significant regularization is observed for IBR during the entire search. This degrades the quality of the steps and results in slow convergence. On the other hand, from the behavior of IFR we can see that productive steps can be achieved without regularizing the system. We observed similar behavior in other instances (e.g., `static3`, `s368`, and `s389`). For the `IEEE_162f` instance we performed an additional experiment in which we change the pivoting tolerance of MA57. In Table 1 we compare the performance of IFRd, IFRt and IBR. We note that the number of iterations and regularizations for IBR vary quite drastically as we change the pivoting tolerance. This is an indication that the inertia estimates provided by MA57 become unreliable. This parasitic behavior is confirmed when we compare against the performance of the inertia-free approaches, which require the same number of iterations in all cases. As can be seen, inertia-free strategies can be beneficial in solving ill-posed problems. In this respect, inertia-free strategies inherit some of the desirable features of trust-region settings.

Table 1 Performance of inertia-based and inertia-free strategies for `IEEE_162` under different pivoting tolerances.

Pivoting Tolerance	Strategy	Iter	Reg
1×10^{-2}	IBR	138	182
	IFRd	23	0
	IFRt	23	0
1×10^{-4}	IBR	109	132
	IFRd	23	0
	IFRt	23	0
1×10^{-6}	IBR	178	236
	IFRd	23	0
	IFRt	23	0
1×10^{-8}	IBR	592	883
	IFRd	23	0
	IFRt	23	0

We highlight that IFRt requires two backsolves to compute the search step (one for the normal component and one for the tangential component) while IFRd requires only one. The factorization of the augmented matrix is reused. The overhead of the additional backsolve is often one to two orders of magnitude smaller than the factorization overhead. We can see this from Table A1 if one considers large instances that do not require regularization and take the same number of iterations for IFRt and IFRd. For example, `cvxqp3` requires one more second for IFRt than for IFRb out of 371 seconds of total time. For `cvxqp2`, IFRt requires 12 more seconds than IFRd while the total time is 123 seconds.

5.3 Large-Scale Tests

We now demonstrate that the inertia-free strategies remain efficient in large-scale problems. We use large-scale stochastic optimization problems arising from security-constrained optimal power flow and stochastic optimal control of natural gas networks [13,42]. Because of the large dimensionality of these instances we solve them using a distributed-memory Schur decomposition strategy implemented in PIPS-NLP.

5.3.1 Structured NLPs and Schur Decomposition

We are interested in solving NLPs with the following structure:

$$\min f_0(x_0) + \sum_{\omega \in \Omega} f_\omega(x_\omega, x_0) \quad (33a)$$

$$\text{s.t.} \quad c_0(x_0) = 0 \quad (\lambda_0) \quad (33b)$$

$$c_\omega(x_\omega, x_0) = 0, \omega \in \Omega \quad (\lambda_\omega) \quad (33c)$$

$$x_0 \geq 0 \quad (\nu_0) \quad (33d)$$

$$x_\omega \geq 0, \omega \in \Omega \quad (\nu_\omega) \quad (33e)$$

The augmented matrix (4) of the structured NLP (33) can be permuted into the following block-bordered diagonal form:

$$\hat{M} = \begin{bmatrix} \hat{M}_1 & & & B_1^T \\ & \hat{M}_2 & & B_2^T \\ & & \ddots & \vdots \\ & & & \hat{M}_{|\Omega|} & B_{|\Omega|}^T \\ B_1 & B_2 & \cdots & B_{|\Omega|} & M_0 \end{bmatrix}, \quad (34)$$

where $\Omega := \{0, 1, 2, \dots, |\Omega|\}$ is the scenario set [22,44,32]. The zero index corresponds to coupling variables. We refer to this coupling scenario as the zero scenario. We use \hat{M} to denote the permuted form of the augmented matrix M_k . The matrices

$$\hat{M}_\omega = \begin{bmatrix} W_\omega & J_\omega^T \\ J_\omega & 0 \end{bmatrix} \quad (35)$$

for $\omega \in \Omega$ have a saddle-point structure. Here, W_ω and J_ω are the corresponding Hessian and Jacobian contributions of each scenario and the border matrices B_ω define coupling between scenarios and the zero scenario.

The permuted augmented system can be represented as

$$\hat{M}\hat{w} = \hat{r}, \quad (36)$$

where $\hat{w} = (\hat{w}_1, \dots, \hat{w}_{|\Omega|}, \hat{w}_0)$ are the permuted search directions for primal variables and multipliers, respectively, and $\hat{r} = (\hat{r}_1, \dots, \hat{r}_{|\Omega|}, \hat{r}_0)$ are the permuted right-hand sides. To solve the structured augmented system (36) in parallel, we use Schur decomposition. The solution of (36) can be obtained from

$$\hat{z}_\omega = \hat{M}_\omega^{-1}\hat{r}_\omega \quad \omega \in \Omega \setminus \{0\}, \quad (37a)$$

$$\hat{w}_0 = C(\delta)^{-1} \left(\hat{r}_0 - \sum_{\omega \in \Omega} B_\omega \hat{z}_\omega \right), \quad (37b)$$

$$\hat{w}_\omega = \hat{z}_\omega - \hat{M}_\omega^{-1}B_\omega^T \hat{w}_0, \quad \omega \in \Omega \setminus \{0\}, \quad (37c)$$

where

$$C = \hat{M}_0 - \sum_{\omega \in \Omega} B_\omega \hat{M}_\omega^{-1} B_\omega^T, \quad (38)$$

is the Schur complement. Each slave processor is allocated with the information of certain blocks ω , and performs step (37a) by factorizing the local blocks \hat{M}_ω in parallel. A master processor gathers the contributions of each worker to assemble the Schur complement in (38) and computes the stepsize for the coupling variables using (37b). Having the coupling step \hat{w}_0 , the slave processors compute the local steps \hat{w}_ω in parallel using (37c).

Because an LBL^T factorization of the entire matrix \hat{M} is not available, its inertia can be inferred by using Haynsworth's inertia additivity formula [27]:

$$\text{Inertia}(\hat{M}) = \text{Inertia}(C) + \sum_{\omega \in \Omega} \text{Inertia}(\hat{M}_\omega). \quad (39)$$

We perform the factorization of the subblocks and of the Schur complement and check that the addition of their inertias satisfies the inertia condition $\text{Inertia}(\hat{M}) = \{n, m, 0\}$. If this is not the case, all the Hessian terms W_ω are regularized by using a common parameter δ until \hat{M} has the correct inertia. We note that obtaining the inertia of the Schur complement C by factorizing it with a sparse symmetric indefinite routine such as MA57 is not efficient because this matrix tends to be dense. More efficient parallel codes such as MAGMA or ELEMENTAL can be used but these are based on dense factorizations schemes that do not provide inertia information [1,31]. This situation illustrates a practical complication that can be encountered when inertia information is required and motivates the development of inertia-free strategies. In our implementation we use MA57 to factorize the Schur complement (even if this is not the most efficient choice) because we seek to compare the performance of IFR with that of IBR.

We note that the serial bottleneck of the Schur complement is associated to the formation and factorization of the Schur complement. Because the Schur complement must be re-assembled and factorized whenever the regularization term δ is adjusted, regularization can increase not only total work per iteration but also parallel performance.

5.3.2 Natural Gas and Power Grid Problems

The stochastic optimal control problem for gas networks has the form presented in (40). This problem determines compressor policies $\Delta\theta_{\omega,\ell}(\tau)$ up to a preparation time T_d that build up enough gas in the network to sustain demand profiles $d_j^{target}(\omega, \tau)$ under multiple scenarios

$\omega \in \Omega$. The objective function is the expected cost of compression plus an error term between the actual delivered demands and the targets. The PDEs (40b)-(40d) are transport equations that describe flow, pressure, and temperature variations inside the pipelines comprising the network. These equations also capture the dynamic response of the gas stored inside the pipelines when gas is added/withdrawn at network nodes. The boundary conditions and the network constraints (40f)-(40i) couple the pipelines. The constraint (40j) is used to compute the power consumed by each compressor station and the constraints (40l) bound the discharge and suction pressures at network nodes. The constraint (40k) enforces periodicity in the average flow of the system. Constraint (40m) are the so-called non-anticipativity constraints that require the compressor policies to be the same for each scenario. For more details in the problem formulation the reader is referred to [42]. We discretize the PDEs in space and time using finite differences and implicit Euler schemes, respectively. After discretization, we obtain an NLP of the form (33) with 128 scenarios and that contains a total of 1,024,651 variables and 1,023,104 constraints. We refer to this problem instance as `STOCH_GAS`.

The security-constrained optimal power flow (SCOPF) problem has the form shown in (41). The SCOPF problem seeks to minimize the power generation cost under a base condition (zero scenario) while guaranteeing that the operation of the network is feasible under predetermined contingencies caused by the loss of different transmission lines. Here, Ω is the set of contingencies (scenarios) and each contingency $\omega \in \Omega$ gives rise to a different network topology (reflected in the sets of links \mathcal{L}_ω). The voltage angle differences between nodes i and j are defined as $\delta_{\omega,ij} := \delta_{\omega,i} - \delta_{\omega,j}$. Constraints (41b)-(41e) are derived from Kirchhoff's laws, which establish the conservation of energy in the power network. Constraints (41b) and (41c) assert that the sum of incoming power flows and power generation at any particular node (bus) must be equal to the sum of outgoing power flow and power consumption. Constraints (41d) and (41e) are power balances at each node. Constraint (41f) forces the phase angle at a reference bus b_0 to be zero. Constraints (41g)-(41j) are physical limits of the system. Constraints (41l)-(41k) are non-anticipativity constraints and state that the voltage level and real power generation at the PV buses (control buses) should remain at their base condition. The only correction action after a failure occurs in the real power generation at the reference bus, which is used to refill the power transmission loss occurring in each contingency. We use the IEEE 300 bus system with 239 contingencies as case study (we refer to the resulting problem as `IEEE_300`). This gives a structured NLP of the form (1) with 878,650 variables and 734,406 constraints. The gas and power flow instances are accessible at <http://zavalab.engr.wisc.edu/data/testinertia>.

All parallel numerical tests were performed on the Fusion computing cluster at Argonne National Laboratory. Fusion contains 320 computing nodes, and each node has two quad-core Nehalem 2.6 GHz CPUs. The results are presented in Table 2. Here, #MPI denotes the number of MPI processes used for parallelization. All strategies converge to the same objective values; consequently, we report only one value. For these problem instances we have used parameter values $\alpha_t = 10^{-10}$, $\alpha_d = 10^{-10}$ (scaled by μ) because the default values of 10^{-12} resulted in high variability in the number of iterations for `STOCH_GAS`. We have observed that increasing α_t, α_d enhances efficiency. As expected, however, this comes at the expense of additional regularizations.

$$\min \mathbb{E} \left[\int_0^T \left(\sum_{\ell \in \mathcal{L}_a} \alpha_\ell^P P_{\omega,\ell}(\tau) + \sum_{j \in \mathcal{D}} \alpha_j^d (d_{\omega,j}(\tau) - d_{\omega,j}^{target}(\tau))^2 \right) d\tau \right] \quad (40a)$$

s.t.

$$\frac{\partial p_{\omega,\ell}(x,\tau)}{\partial \tau} + \frac{ZRT_{\omega,\ell}(x,\tau)}{A_\ell} \frac{\partial f_{\omega,\ell}(x,\tau)}{\partial x} = 0, \ell \in \mathcal{L}, \omega \in \Omega, x \in \mathcal{X}_\ell, \tau \in \mathcal{T} \quad (40b)$$

$$\frac{1}{A_\ell} \frac{\partial f_{\omega,\ell}(x,\tau)}{\partial \tau} + \frac{\partial p_{\omega,\ell}(x,\tau)}{\partial x} + \frac{8\lambda_\ell}{\pi^2 D_\ell^5} \frac{f_{\omega,\ell}(x,\tau) |f_{\omega,\ell}(x,\tau)|}{\rho_{\omega,\ell}(x,\tau)} = 0, \ell \in \mathcal{L}, \omega \in \Omega, x \in \mathcal{X}_\ell, \tau \in \mathcal{T} \quad (40c)$$

$$\begin{aligned} \rho_{\omega,\ell}(x,\tau) c_p & \left(\frac{\partial T_{\omega,\ell}(x,\tau)}{\partial \tau} + \nu_{\omega,\ell}(x,\tau) \frac{\partial T_{\omega,\ell}(x,\tau)}{\partial x} \right) \\ & - \left(\frac{\partial p_{\omega,\ell}(x,\tau)}{\partial \tau} + \nu_{\omega,\ell}(x,\tau) \frac{\partial p_{\omega,\ell}(x,\tau)}{\partial x} \right) \\ & + \frac{\pi D_\ell U_\ell}{A_\ell} (T_{\omega,\ell}(x,\tau) - T_\omega^{amb}(x,\tau)) = 0, \ell \in \mathcal{L}, \omega \in \Omega, x \in \mathcal{X}_\ell, \tau \in \mathcal{T} \end{aligned} \quad (40d)$$

$$\frac{p_{\omega,\ell}(x,\tau)}{\rho_{\omega,\ell}(x,\tau)} = ZRT_{\omega,\ell}(x,\tau), \ell \in \mathcal{L}, \omega \in \Omega, x \in \mathcal{X}_\ell, \tau \in \mathcal{T} \quad (40e)$$

$$p_{\omega,\ell}(L_\ell, \tau) = \theta_{\omega,rec}(\ell)(\tau), \ell \in \mathcal{L}, \omega \in \Omega, \tau \in \mathcal{T} \quad (40f)$$

$$p_{\omega,\ell}(0, \tau) = \theta_{\omega,snd}(\ell)(\tau), \ell \in \mathcal{L}_p, \omega \in \Omega, \tau \in \mathcal{T} \quad (40g)$$

$$p_{\omega,\ell}(0, \tau) = \theta_{\omega,snd}(\ell)(\tau) + \Delta\theta_{\omega,\ell}(\tau), \ell \in \mathcal{L}_a, \omega \in \Omega, \tau \in \mathcal{T} \quad (40h)$$

$$\begin{aligned} \sum_{\ell \in \mathcal{L}_n^{rec}} f_{\omega,\ell}(L_\ell, \tau) - \sum_{\ell \in \mathcal{L}_n^{snd}} f_{\omega,\ell}(0, \tau) \\ + \sum_{i \in \mathcal{S}_n} s_{\omega,i}(\tau) - \sum_{j \in \mathcal{D}_n} d_{\omega,j}(\tau) = 0, n \in \mathcal{N}, \omega \in \Omega, \tau \in \mathcal{T} \end{aligned} \quad (40i)$$

$$P_{\omega,\ell}(\tau) = c_p \cdot T \cdot f_{\omega,\ell}(0, \tau) \left(\left(\frac{\theta_{\omega,snd}(\ell)(\tau) + \Delta\theta_{\omega,\ell}(\tau)}{\theta_{\omega,snd}(\ell)(\tau)} \right)^{\frac{\gamma-1}{\gamma}} - 1 \right), \ell \in \mathcal{L}_a, \omega \in \Omega, \tau \in \mathcal{T} \quad (40j)$$

$$\int_0^{L_\ell} f_{\omega,\ell}(x, T) dx \geq \int_0^{L_\ell} f_{\omega,\ell}(x, 0) dx, \ell \in \mathcal{L}_a, \omega \in \Omega, \tau \in \mathcal{T} \quad (40k)$$

$$\theta_n \leq \theta_{\omega,n}(\tau) \leq \bar{\theta}_n, n \in \mathcal{N}, \omega \in \Omega, \tau \in \mathcal{T} \quad (40l)$$

$$\Delta\theta_{\omega,\ell}(\tau) = \Delta\theta_{0,\ell}(\tau), \ell \in \mathcal{L}_a, \omega \in \Omega \setminus \{0\}, \tau \in [0, T_d]. \quad (40m)$$

We can see that, despite the high nonlinearity of the large-scale instances, the inertia-free approaches IFRd and IFRT converge in all instances. This provides evidence that the tests can scale to large-scale instances. In general, IFRd and IFRT require more iterations than IBR does but the number of factorizations is reduced, resulting in faster solutions. These problem instances are highly ill-conditioned, particularly STOCH_GAS as is evident from the variability of the number of iterations as we increase the number of MPI processes. This is the result of linear system errors introduced by Schur decomposition. The performance, however, is satisfactory in all cases. For IEEE_300 we note that the number of iterations for IBR does not vary as we add MPI processors whereas those of IFRd and IFRT do. While it is difficult to isolate a specific source of

Table 2 Performance of inertia-based and inertia-free strategies on large-scale instances.

Problem	#MPI	IBR				IFRd			IFRt		
		Obj	Iter	Fact	Time(s)	Iter	Fact	Time(s)	Iter	Fact	Time(s)
IEEE_300	16	1.36E+03	112	274	627	173	190	476	209	241	651
IEEE_300	24	1.36E+03	112	274	424	208	238	403	232	255	475
IEEE_300	40	1.36E+03	112	274	263	160	169	181	168	178	206
IEEE_300	80	1.36E+03	112	274	174	183	203	119	177	190	127
IEEE_300	120	1.36E+03	112	274	126	192	224	91	201	227	103
IEEE_300	240	1.36E+03	113	274	65	170	185	47	219	240	80
STOCH.GAS	8	1.26E-02	153	278	832	122	144	621	93	106	491
STOCH.GAS	16	1.26E-02	136	251	363	245	277	789	109	122	315
STOCH.GAS	32	1.26E-02	146	274	209	211	250	301	99	112	143
STOCH.GAS	64	1.26E-02	157	286	123	112	137	74	101	114	79
STOCH.GAS	128	1.26E-02	145	275	64	127	158	52	109	125	52

such behavior, we attribute this behavior to the stabilizing effect that additional regularizations of IBR provide on the linear system.

$$\min \sum_{g \in \mathcal{G}} (c_{0g} + c_{1g} p_{base,g} + c_{2g} p_{base,g}^2) \quad (41a)$$

s.t.

$$\sum_{g|o_g=b} p_{\omega,g} - d_b^P = \sum_{(i,j) \in \mathcal{L}_\omega} f_{\omega,(i,j)}^P, \quad b \in \mathcal{B}, \omega \in \Omega \quad (41b)$$

$$\sum_{g|o_g=b} q_{\omega,g} - d_b^Q = \sum_{(i,j) \in \mathcal{L}_\omega} f_{\omega,(i,j)}^Q - \frac{(V_b)^2}{2} \sum_{(i,j) \in \mathcal{L}_\omega} \gamma_{(i,j)}, \quad b \in \mathcal{B}, \omega \in \Omega \quad (41c)$$

$$f_{\omega,(i,j)}^P = \begin{cases} \alpha_l V_{\omega,i}^2 - V_{\omega,i} V_{\omega,j} [\alpha_l \cos(\delta_{\omega,ij}) + \beta_l \sin(\delta_{\omega,ij})], & \text{otherwise} \\ \alpha_l \left(\frac{V_{\omega,i}}{\tau_t} \right)^2 - \frac{V_{\omega,i} V_{\omega,j}}{\tau_t} [\alpha_l \cos(\delta_{\omega,ij}) + \beta_l \sin(\delta_{\omega,ij})], & i \text{ tapped}, (i,j) \in \mathcal{L}_\omega, \omega \in \Omega \\ \alpha_l V_{\omega,i}^2 - \frac{V_{\omega,i} V_{\omega,j}}{\tau_t} [\alpha_l \cos(\delta_{\omega,ij}) + \beta_l \sin(\delta_{\omega,ij})], & j \text{ tapped} \end{cases} \quad (41d)$$

$$f_{\omega,(i,j)}^Q = \begin{cases} -\beta_l V_{\omega,i}^2 - V_{\omega,i} V_{\omega,j} [\alpha_l \sin(\delta_{\omega,ij}) - \beta_l \cos(\delta_{\omega,ij})], & \text{otherwise} \\ -\beta_l \left(\frac{V_{\omega,i}}{\tau_t} \right)^2 - \frac{V_{\omega,i} V_{\omega,j}}{\tau_t} [\alpha_l \sin(\delta_{\omega,ij}) - \beta_l \cos(\delta_{\omega,ij})], & i \text{ tapped}, (i,j) \in \mathcal{L}_\omega, \omega \in \Omega \\ -\beta_l V_{\omega,i}^2 - \frac{V_{\omega,i} V_{\omega,j}}{\tau_t} [\alpha_l \sin(\delta_{\omega,ij}) - \beta_l \cos(\delta_{\omega,ij})], & j \text{ tapped} \end{cases} \quad (41e)$$

$$\delta_{\omega,b_0} = 0, \omega \in \Omega \quad (41f)$$

$$(f_{\omega,(i,j)}^P)^2 + (f_{\omega,(i,j)}^Q)^2 \leq (f_{\omega,(i,j)}^+)^2, \quad (i,j) \in \mathcal{L}, \omega \in \Omega \quad (41g)$$

$$p_{\omega,g}^- \leq p_{\omega,g} \leq p_{\omega,g}^+, \quad g \in \mathcal{G}, \omega \in \Omega \quad (41h)$$

$$q_{\omega,g}^- \leq q_{\omega,g} \leq q_{\omega,g}^+, \quad g \in \mathcal{G}, \omega \in \Omega \quad (41i)$$

$$V_{\omega,b}^- \leq V_{\omega,b} \leq V_{\omega,b}^+, \quad b \in \mathcal{B}, \omega \in \Omega \quad (41j)$$

$$V_{\omega,b} = V_{base,b}, \quad b \in \mathcal{B}_{PV}, \omega \in \Omega \setminus \{base\} \quad (41k)$$

$$p_{\omega,g} = p_{base,g}, \quad g \in \{g|o_g \in \mathcal{B}_{PV} \setminus \{b_0\}\}. \quad (41l)$$

6 Conclusions

We have presented a new filter line-search algorithm that does not require inertia information. This inertia-free approach performs curvature tests along computed directions to guarantee descent when the constraint violation is sufficiently small. We proved that the approach yields global convergence and is competitive with the standard inertia-based strategy based on symmetric indefinite factorizations. Moreover, we demonstrate that the inertia-free approach can significantly reduce the amount of regularization needed. The availability of inertia-free strategies opens the possibility of using different types of linear algebra strategies and libraries and thus can enhance modularity of implementations. This was demonstrated through a distributed-memory Schur decomposition setting.

Acknowledgments

This material is based upon work supported by the U.S. Department of Energy, Office of Science, Office of Advanced Scientific Computing Research, Applied Mathematics program under Contract No. DE-AC02-06CH11357. We thank Frank Curtis and Jorge Nocedal for technical discussions. Victor M. Zavala acknowledges funding from the DOE Office of Science under the Early Career program. We also acknowledge the computing resources provided by the Laboratory Computing Resource Center at Argonne National Laboratory.

References

1. E. Agullo, J. Demmel, J. Dongarra, B. Hadri, J. Kurzak, J. Langou, H. Ltaief, P. Luszczek, and S. Tomov. Numerical linear algebra on emerging architectures: The PLASMA and MAGMA projects. In *Journal of Physics: Conference Series*, volume 180, page 012037. IOP Publishing, 2009.
2. P. R. Amestoy, A. Guermouche, J.Y. L'Excellent, and S. Pralet. Hybrid scheduling for the parallel solution of linear systems. *Parallel Computing*, 32(2):136–156, 2006.
3. Nikhil Arora and Lorenz T Biegler. A trust region sqp algorithm for equality constrained parameter estimation with simple parameter bounds. *Computational Optimization and Applications*, 28(1):51–86, 2004.
4. S. Balay, J. Brown, K. Buschelman, V. Eijkhout, W. Gropp, D. Kaushik, M. Knepley, L. McInnes, B. Smith, and H. Zhang. PETSc users manual revision 3.4, 2013.
5. M. Benzi, G.H. Golub, and J. Liesen. Numerical solution of saddle point problems. *Acta Numerica*, 14:1–137, 2005.
6. L.T. Biegler and V.M. Zavala. Large-scale nonlinear programming using IPOPT: An integrating framework for enterprise-wide dynamic optimization. *Computers & Chemical Engineering*, 33(3):575–582, 2009.
7. G. Biros and O. Ghattas. Parallel Lagrange–Newton–Krylov–Schur methods for PDE-constrained optimization. Part I: The Krylov–Schur solver. *SIAM Journal on Scientific Computing*, 27(2):687–713, 2005.
8. A. Borzi and V. Schulz. Multigrid methods for pde optimization. *SIAM Review*, 51(2):361–395, 2009.
9. J.R. Bunch and L. Kaufman. Some stable methods for calculating inertia and solving symmetric linear systems. *Mathematics of computation*, pages 163–179, 1977.
10. R. H. Byrd, J. Ch. Gilbert, and J. Nocedal. A trust-region method based on interior-point techniques for nonlinear programming. *Math. Program.*, 89:149–185, 2000.
11. R.H. Byrd, F.E. Curtis, and J. Nocedal. An inexact Newton method for nonconvex equality constrained optimization. *Mathematical programming*, volume=122, number=2, pages=273–299, year=2010, publisher=Springer.
12. A.M. Cervantes, A. Wächter, R.H. Tütüncü, and L.T. Biegler. A reduced space interior point strategy for optimization of differential algebraic systems. *Computers & Chemical Engineering*, 24(1):39–51, 2000.
13. N. Chiang and A. Grothey. Solving security constrained optimal power flow problems by a structure exploiting interior point method. *Optimization and Engineering*, pages 1–23, 2012.
14. N. Chiang, C.G. Petra, and V.M. Zavala. Structured nonconvex optimization of large-scale energy systems using PIPS-NLP. In *Proceedings of the 18th Power Systems Computation Conference (PSCC)*, Wroclaw, Poland, 2014.
15. Andrew R Conn, Nicholas IM Gould, and Ph L Toint. *Trust region methods*, volume 1. Siam, 2000.

16. M.P. Costa and E.M.G.P. Fernandes. Assessing the potential of interior point barrier filter line search methods: nonmonotone versus monotone approach. *Optimization*, 60(10-11):1251–1268, 2011.
17. F.E. Curtis, J. Nocedal, and A. Wächter. A matrix-free algorithm for equality constrained optimization problems with rank-deficient Jacobians. *SIAM Journal on Optimization*, 20(3):1224–1249, 2009.
18. F.E. Curtis, O. Schenk, and A. Wächter. An interior-point algorithm for large-scale nonlinear optimization with inexact step computations. *SIAM Journal on Scientific Computing*, 32(6):3447–3475, 2010.
19. E.D. Dolan and J.J. Moré. Benchmarking optimization software with performance profiles. *Mathematical Programming*, 91(2):201–213, 2002.
20. I. S. Duff. Ma57 - a code for the solution of sparse symmetric definite and indefinite systems. *ACM Transactions on Mathematical Software*, 30:118–144, 2004.
21. I.S. Duff and J.K. Reid. MA27-a set of Fortran subroutines for solving sparse symmetric sets of linear equations. UKAEA Atomic Energy Research Establishment, 1982.
22. J. Gondzio and R. Sarkissian. Parallel interior-point solver for structured linear programs. *Mathematical Programming*, 96(3):561–584, 2003.
23. Nicholas IM Gould, Mary E Hribar, and Jorge Nocedal. On the solution of equality constrained quadratic programming problems arising in optimization. *SIAM Journal on Scientific Computing*, 23(4):1376–1395, 2001.
24. Nicholas IM Gould, Stefano Lucidi, Massimo Roma, and Philippe L Toint. Solving the trust-region subproblem using the lanczos method. *SIAM Journal on Optimization*, 9(2):504–525, 1999.
25. N.I.M. Gould. On practical conditions for the existence and uniqueness of solutions to the general equality quadratic programming problem. *Mathematical Programming*, 32(1):90–99, 1985.
26. N. Haverbeke, M. Diehl, and B. De Moor. A structure exploiting interior-point method for moving horizon estimation. In *Proceedings of the 48th IEEE Conference on Decision and Control*, pages 1273–1278. IEEE, 2009.
27. E.V. Haynsworth. Determination of the inertia of a partitioned Hermitian matrix. *Linear Algebra and Its Applications*, 1(1):73 – 81, 1968.
28. Matthias Heinkenschloss and Denis Ridzal. A matrix-free trust-region sqp method for equality constrained optimization. *SIAM Journal on Optimization*, 24(3):1507–1541, 2014.
29. Michael Allen Heroux and James M Willenbring. *Trilinos users guide*. Citeseer, 2003.
30. Y. Kawajiri and L.T. Biegler. Optimization strategies for simulated moving bed and powerfeed processes. *AIChE Journal*, 52(4):1343–1350, 2006.
31. M. Lubin, C.G. Petra, and M. Anitescu. The parallel solution of dense saddle-point linear systems arising in stochastic programming. *Optimization Methods and Software*, 27(4-5):845–864, 2012.
32. M. Lubin, C.G. Petra, M. Anitescu, and V.M. Zavala. Scalable stochastic optimization of complex energy systems. In *High Performance Computing, Networking, Storage and Analysis (SC), 2011 International Conference for*, pages 1–10. IEEE, 2011.
33. C.G. Petra, O. Schenk, M. Lubin, and K. Gaertner. An augmented incomplete factorization approach for computing the schur complement in stochastic optimization. *SIAM Journal on Scientific Computing*, 36(2):C139–C162, 2014.
34. C.V. Rao, S.J. Wright, and J.B. Rawlings. Application of interior-point methods to model predictive control. *Journal of optimization theory and applications*, 99(3):723–757, 1998.
35. O. Schenk, A. Wächter, and M. Hagemann. Matching-based preprocessing algorithms to the solution of saddle-point problems in large-scale nonconvex interior-point optimization. *Computational Optimization and Applications*, 36:321–341, 2007.
36. O. Schenk, A. Wächter, and M. Weiser. Inertia-revealing preconditioning for large-scale nonconvex constrained optimization. *SIAM Journal on Scientific Computing*, 31(2):939–960, 2008.
37. M. Soler, A. Olivares, and E. Staffetti. Hybrid optimal control approach to commercial aircraft trajectory planning. *Journal of Guidance, Control, and Dynamics*, 33(3):985–991, 2010.
38. A. Wächter and L. T. Biegler. On the implementation of a primal-dual interior point filter line search algorithm for large-scale nonlinear programming. *Mathematical Programming*, 106:25–57, 2006.
39. A. Wächter and L.T. Biegler. Line search filter methods for nonlinear programming: Motivation and global convergence. *SIAM Journal on Optimization*, 16(1):1–31, 2005.
40. Richard A Waltz, José Luis Morales, Jorge Nocedal, and Dominique Orban. An interior algorithm for nonlinear optimization that combines line search and trust region steps. *Mathematical Programming*, 107(3):391–408, 2006.
41. Y. Wang and S. Boyd. Fast model predictive control using online optimization. *IEEE Transactions on Control Systems Technology*, 18(2):267–278, 2010.
42. V.M. Zavala. Stochastic optimal control model for natural gas networks. *Computers & Chemical Engineering*, 64:103–113, 2014.
43. V.M. Zavala and L.T. Biegler. Large-scale parameter estimation in low-density polyethylene tubular reactors. *Industrial & Engineering Chemistry Research*, 45(23):7867–7881, 2006.
44. V.M. Zavala, C.D. Laird, and L.T. Biegler. Interior-point decomposition approaches for parallel solution of large-scale nonlinear parameter estimation problems. *Chemical Engineering Science*, 63(19):4834–4845, 2008.
45. S. Zenios and R. Lasken. Nonlinear network optimization on a massively parallel connection machine. *Annals of Operations Research*, 14(1):147–165, 1988.

Appendix

Table A1: Performance of inertia-based and inertia-free strategies on small-scale instances.

Problem	n	IBR				IFRd				IFRt			
		Obj	Iter	Reg	time	Obj	Iter	Reg	time	Obj	Iter	Reg	time
3pk	30	1.7E+00	10	0	0.09	1.72E+00	10	0	0.08	1.72E+00	10	0	0.09
aircfta	5	0.00E+00	3	0	0.04	0.00E+00	3	2	0.05	0.00E+00	3	0	0.05
aircftb	8	3.34E-27	12	10	0.04	1.22E-19	18	5	0.04	1.22E-19	18	5	0.04
airport	84	4.80E+04	15	0	0.06	4.80E+04	15	0	0.05	4.80E+04	15	0	0.06
aljazaf	3	7.50E+01	34	5	0.07	7.50E+01	33	13	0.05	-	-	-	-
allinitc	4	3.05E+01	28	4	0.07	3.05E+01	26	5	0.04	3.05E+01	30	0	0.06
allinit	4	1.67E+01	11	0	0.07	1.67E+01	11	5	0.05	1.67E+01	11	0	0.05
allinitu	4	5.74E+00	13	15	0.07	5.74E+00	8	6	0.07	5.74E+00	8	6	0.06
alsotame	2	8.21E-02	8	0	0.06	8.21E-02	8	0	0.08	8.21E-02	8	0	0.05
arglina	100	1.00E+02	1	0	0.11	1.00E+02	1	0	0.12	1.00E+02	1	0	0.11
arglinb	10	4.63E+00	2	2	0.04	4.63E+00	1	0	0.07	4.63E+00	1	0	0.04
arglinc	8	6.14E+00	2	2	0.04	6.14E+00	1	0	0.05	6.14E+00	1	0	0.05
argtrig	100	0.00E+00	3	0	0.06	0.00E+00	3	2	0.07	0.00E+00	3	0	0.07
arwhead	5000	-2.66E-15	6	0	0.12	-2.66E-15	6	0	0.11	-2.66E-15	6	0	0.13
aug2dcqp	20200	6.50E+06	27	0	1.3	6.50E+06	27	0	1.2	6.50E+06	27	0	1.19
aug2dc	20200	1.82E+06	12	0	0.72	1.82E+06	12	0	0.72	1.82E+06	12	0	0.76
aug2dqp	20192	6.24E+06	26	0	1.18	6.24E+06	26	0	1.21	6.24E+06	26	0	1.14
aug2d	20192	1.69E+06	1	0	0.22	1.69E+06	1	0	0.21	1.69E+06	1	0	0.23
aug3dcqp	3873	9.93E+02	17	0	0.18	9.93E+02	17	0	0.19	9.93E+02	17	0	0.19
aug3dc	3873	7.71E+02	1	0	0.06	7.71E+02	1	0	0.06	7.71E+02	1	0	0.07
aug3dqp	3873	6.75E+02	18	0	0.17	6.75E+02	18	0	0.17	6.75E+02	18	0	0.18
aug3d	3873	5.54E+02	2	0	0.34	5.54E+02	2	0	0.36	5.54E+02	2	0	0.35
avgasa	8	-4.41E+00	9	0	0.05	-4.41E+00	9	0	0.04	-4.41E+00	9	0	0.06
avgasb	8	-4.48E+00	11	0	0.05	-4.48E+00	11	0	0.05	-4.48E+00	11	0	0.05
avion2	49	9.47E+07	40	45	0.05	9.47E+07	59	10	0.05	-	-	-	-
bard	3	8.21E-03	7	5	0.04	8.21E-03	8	0	0.05	8.21E-03	8	0	0.05
bdexp	5000	2.41E-04	12	0	0.24	2.41E-04	12	0	0.24	2.41E-04	12	0	0.26
bdqrtc	1000	3.98E+03	10	0	0.07	3.98E+03	10	0	0.09	3.98E+03	10	0	0.07
bdvalue	5000	0.00E+00	0	0	0.06	0.00E+00	0	0	0.13	0.00E+00	0	0	0.06
beale	2	4.34E-18	8	5	0.04	4.34E-18	8	5	0.05	4.34E-18	8	5	0.04
biggs3	6	9.99E-14	8	5	0.06	9.99E-14	8	5	0.05	9.99E-14	8	5	0.06
biggs5	6	1.08E-19	20	19	0.05	3.06E-01	19	3	0.05	3.06E-01	19	3	0.05
biggs6	6	8.91E-15	33	26	0.06	3.06E-01	18	0	0.05	3.06E-01	18	0	0.04
biggsb1	1000	1.52E-02	13	0	0.08	1.52E-02	13	0	0.08	1.52E-02	13	0	0.07
biggs4	4	-2.45E+01	23	11	0.05	-2.45E+01	22	8	0.05	-2.45E+01	22	8	0.04
blockqp1	2005	-9.96E+02	10	0	0.14	-9.96E+02	10	0	0.14	-9.96E+02	10	0	0.13
blockqp2	2005	-9.96E+02	9	0	0.12	-9.96E+02	9	0	0.12	-9.96E+02	9	0	0.11
blockqp3	2005	-4.97E+02	12	0	0.14	-4.97E+02	12	0	0.13	-4.97E+02	12	0	0.2
blockqp4	2005	-4.98E+02	9	0	0.12	-4.98E+02	9	0	0.12	-4.98E+02	9	0	0.13
blockqp5	2005	-4.97E+02	42	47	0.3	-4.97E+02	15	0	0.12	-4.97E+02	15	0	0.14
bloweya	2002	-4.55E+02	8	0	0.1	-4.55E+02	8	0	0.1	-4.55E+02	8	0	0.09
bloweyb	2002	-3.05E+02	6	0	0.1	-3.05E+02	6	0	0.09	-3.05E+02	6	0	0.09
bloweyc	2002	-3.04E+02	10	0	0.11	-3.04E+02	10	0	0.1	-3.04E+02	10	0	0.1
booth	2	0.00E+00	1	0	0.05	0.00E+00	2	2	0.04	0.00E+00	1	0	0.04
box2	3	7.34E-15	7	4	0.04	7.88E-13	11	5	0.05	7.88E-13	11	5	0.04
box3	3	2.87E-14	8	2	0.05	7.03E-14	7	0	0.04	7.03E-14	7	0	0.04
bqp1var	1	8.10E-08	5	0	0.06	8.10E-08	5	0	0.04	8.10E-08	5	0	0.07
bqpgabim	50	-3.53E-05	12	0	0.06	-3.53E-05	12	0	0.05	-3.53E-05	12	0	0.07
bqpgasim	50	-5.25E-05	12	0	0.06	-5.25E-05	12	0	0.04	-5.25E-05	12	0	0.07
brainpc2	13805	4.37E-04	68	83	170.84	-	-	-	-	-	-	-	
brainpc7	6905	3.87E-04	22	25	1.37	-	-	-	-	-	-	-	
brainpc9	6905	4.48E-04	20	23	1.26	-	-	-	-	-	-	-	
bratu1d	1001	-8.52E+00	5	0	0.06	-8.52E+00	5	0	0.06	-8.52E+00	9	7	0.07
bratu2d	4900	0.00E+00	6	0	0.9	0.00E+00	6	1	1.66	0.00E+00	6	0	1
bratu2d	4900	0.00E+00	2	0	0.45	0.00E+00	2	1	0.78	0.00E+00	2	0	0.42
bratu3d	3375	0.00E+00	3	0	4.15	0.00E+00	3	1	7.32	0.00E+00	3	0	5.64
brkmcc	450	1.69E-01	3	0	0.04	1.69E-01	3	0	0.05	1.69E-01	3	0	0.08
brownal	10	1.50E-16	7	0	0.04	1.50E-16	7	0	0.04	1.50E-16	7	0	0.08
brownsb	2	0.00E+00	8	4	0.04	0.00E+00	8	4	0.04	0.00E+00	8	4	0.08
brownden	4	8.58E+04	8	0	0.05	8.58E+04	8	0	0.04	8.58E+04	8	0	0.08
broydn3d	10000	0.00E+00	4	0	0.22	0.00E+00	4	1	0.2	0.00E+00	4	0	0.31
broydn7d	1000	3.45E+02	84	120	0.28	5.73E+02	49	16	0.17	5.63E+02	53	19	0.31
broydnbd	5000	0.00E+00	5	0	0.25	0.00E+00	5	1	0.24	0.00E+00	5	0	0.32
brybnd	5000	1.22E-26	8	0	0.3	1.22E-26	8	0	0.28	1.22E-26	8	0	0.39
bt10	2	-1.00E+00	6	0	0.05	-1.00E+00	6	1	0.05	-1.00E+00	6	0	0.07
bt11	5	8.25E-01	7	0	0.06	8.25E-01	7	0	0.05	8.25E-01	7	0	0.07
bt12	5	6.19E+00	4	0	0.06	6.19E+00	4	0	0.05	6.19E+00	4	0	0.07
bt13	5	8.09E-08	22	0	0.06	8.09E-08	22	0	0.05	8.09E-08	22	0	0.07
bt1	2	-1.00E+00	7	14	0.06	-1.00E+00	7	14	0.05	-1.00E+00	6	0	0.08
bt2	3	3.26E-02	12	0	0.06	3.26E-02	12	0	0.05	3.26E-02	12	0	0.08
bt3	5	4.09E+00	1	0	0.06	4.09E+00	1	0	0.04	4.09E+00	1	0	0.08
bt4	3	-4.55E+01	9	5	0.06	-4.55E+01	9	5	0.04	-4.55E+01	9	5	0.08
bt5	3	9.62E+02	7	3	0.06	9.62E+02	9	8	0.04	9.62E+02	7	3	0.08
bt6	5	2.77E-01	13	0	0.06	2.77E-01	13	0	0.04	2.77E-01	13	0	0.08
bt7	5	-	-	-	-	3.07E+02	37	1	0.04	-	-	-	-
bt8	5	1.00E+00	27	57	0.06	1.00E+00	11	0	0.04	1.00E+00	11	0	0.08
bt9	4	-1.00E+00	23	8	0.05	-1.00E+00	20	0	0.04	-1.00E+00	20	0	0.08
byrdsphr	3	-4.68E+00	22	9	0.06	-4.68E+00	22	9	0.04	-4.68E+00	22	9	0.08
camel6	2	-2.15E-01	11	9	0.06	2.23E+00	7	0	0.04	2.23E+00	7	0	0.08
cantilvr	5	1.34E+00	13	0	0.06	1.34E+00	13	0	0.05	1.34E+00	13	0	0.08
catenary	496	-3.48E+05	57	46	0.18	-3.48E+05	47	0	0.14	-3.48E+05	47	0	0.2
catena	32	-2.31E+04	20	11	0.06	-1.85E+04	32	11	0.07	-2.31E+04	30	12	0.09
cb2	3	1.95E+00	9	0	0.05	1.95E+00	9	0	0.04	1.95E+00	9	0	0.08
cb3	3	2.00E+00	9	0	0.06	2.00E+00	9	0	0.04	2.00E+00	9	0	0.06
cbratu2d	882	0.00E+00	1	0	0.1	0.00E+00	2	1	0.1	0.00E+00	1	0	0.15
cbratu3d	1024	0.00E+00	1	0	0.15	0.00E+00	1	1	0.17	0.00E+00	1	0	0.23
chaconn1	3	1.95E+00	7	0	0.06	1.95E+00	7	0	0.04	1.95E+00	7	0	0.08
chaconn2	3	2.00E+00	7	0	0.05	2.00E+00	7	0	0.04	2.00E+00	7	0	0.08
chainwo	1000	7.93E+01	99	97	0.22	5.26E+02	113	7	0.18	4.30E+02	114	6	0.32

chandheq	100	0.00E+00	11	0	0.14	0.00E+00	11	0	0.12	0.00E+00	11	0	0.19
chebyquad	50	5.39E-03	101	144	3.96	4.03E-01	72	49	2.47	6.27E-01	53	23	3.14
chemrcta	5000	-	-	-	-	-	-	-	-	0.00E+00	6	0	0.28
chenhark	1000	-2.00E+00	14	0	0.07	-2.00E+00	14	0	0.07	-2.00E+00	14	0	0.09
chmrosnb	50	1.82E-26	43	3	0.05	1.82E-26	43	3	0.05	1.82E-26	43	3	0.08
cliff	2	2.00E-01	27	0	0.05	2.00E-01	27	0	0.05	2.00E-01	27	0	0.07
cinlbeam	1499	3.45E+02	208	150	1.05	3.47E+02	92	54	0.58	3.46E+02	107	41	0.84
ciplatea	4970	-1.26E-02	5	0	0.19	-1.26E-02	5	0	0.15	-1.26E-02	5	0	0.24
ciplateb	4970	-6.99E+00	5	0	0.17	-6.99E+00	5	0	0.15	-6.99E+00	5	0	0.24
ciplatec	4970	-5.02E-03	1	0	0.11	-5.02E-03	1	0	0.1	-5.02E-03	1	0	0.17
cluster	2	0.00E+00	8	0	0.05	0.00E+00	8	0	0.04	0.00E+00	8	0	0.07
concon	15	-6.23E+03	9	0	0.08	-6.23E+03	9	0	0.04	-6.23E+03	9	0	0.07
congigmsz	3	2.80E+01	25	5	0.08	2.80E+01	30	10	0.04	2.80E+01	27	3	0.07
coolhans	9	0.00E+00	8	0	0.07	0.00E+00	9	2	0.04	0.00E+00	8	0	0.07
coshfun	61	-7.73E-01	190	243	0.1	-	-	-	-	-	-	-	-
core2	157	-	-	-	-	7.29E+01	76	12	0.08	-	-	-	-
cosine	10000	-1.00E+04	12	17	0.35	-1.35E+02	18	18	0.47	-2.36E+02	19	19	0.83
cragglyvy	5000	1.69E+03	14	0	0.22	1.69E+03	14	0	0.19	1.69E+03	14	0	0.31
csf1	5	-4.91E+01	14	4	0.05	-4.91E+01	18	9	0.05	-4.91E+01	14	1	0.09
csf2	5	-	-	-	-	-	-	-	-	5.50E+01	40	19	0.08
cube	2	1.75E-24	27	0	0.06	1.75E-24	27	0	0.04	1.75E-24	27	0	0.08
curly10	10000	-1.00E+06	21	25	1.13	-1.00E+06	18	20	0.95	-1.00E+06	18	20	1.55
curly20	10000	-1.00E+06	26	30	2.18	-1.00E+06	22	24	1.9	-1.00E+06	22	24	2.14
curly30	10000	-1.00E+06	29	36	3.66	-9.98E+05	28	27	3.38	-9.98E+05	28	27	3.46
cvxqp1	10000	2.25E+06	9	0	0.56	2.25E+06	9	0	0.53	2.25E+06	9	0	0.53
cvxqp2	1000	1.09E+06	38	0	0.85	1.09E+06	38	0	0.8	1.09E+06	38	0	0.79
cvxqp3	10000	8.18E+07	116	0	128.81	8.18E+07	116	0	123.7	8.18E+07	116	0	135.62
deconvb	10000	1.16E+08	54	0	351.97	1.16E+08	54	0	371.79	1.16E+08	54	0	373.3
deconvc	51	-	-	-	-	1.94E+03	432	30	0.18	-	-	-	-
deconvu	51	2.57E-03	103	56	0.11	3.35E+01	21	6	0.06	3.35E+01	21	6	0.09
degenlp	20	1.06E-10	41	58	0.09	5.20E-05	213	6	0.13	5.20E-05	150	6	0.16
degenlpb	20	3.05E+00	28	0	0.08	3.05E+00	28	0	0.05	3.05E+00	28	0	0.08
demyhalo	20	-3.08E+01	31	0	0.07	-3.08E+01	31	0	0.05	-3.08E+01	31	0	0.08
denschna	3	-3.00E+00	17	3	0.05	-3.00E+00	9	1	0.05	-3.00E+00	17	3	0.08
denschnc	2	1.10E-23	6	0	0.04	1.10E-23	6	0	0.05	1.10E-23	6	0	0.08
denschncb	2	9.99E-16	6	0	0.05	9.99E-16	6	0	0.05	9.99E-16	6	0	0.08
denschncd	2	2.18E-20	10	0	0.05	2.18E-20	10	0	0.05	2.18E-20	10	0	0.08
denschncd	3	2.00E-10	36	14	0.08	1.70E-10	35	4	0.05	1.70E-10	35	4	0.07
denschne	3	2.74E-23	10	10	0.08	1.00E+00	9	1	0.05	1.00E+00	9	1	0.06
denschnf	2	6.51E-22	6	0	0.08	6.51E-22	6	0	0.05	6.51E-22	6	0	0.08
dipigri	7	6.81E+02	12	0	0.08	6.81E+02	12	0	0.05	6.81E+02	12	0	0.08
ditter	327	-2.00E+00	22	28	0.23	-2.00E+00	23	0	0.22	-2.00E+00	23	0	0.23
dixchlng	10	2.47E+03	9	0	0.05	2.47E+03	9	0	0.08	2.47E+03	9	0	0.08
dixchlnv	100	0.00E+00	18	0	0.09	0.00E+00	18	0	0.12	0.00E+00	18	0	0.13
dixmaana	3000	1.00E+00	7	6	0.09	1.00E+00	5	0	0.12	1.00E+00	5	0	0.12
dixmaamb	3000	1.00E+00	11	10	0.16	1.00E+00	7	0	0.18	1.00E+00	7	0	0.17
dixmaanc	3000	1.00E+00	8	7	0.13	1.00E+00	168	16	2.43	1.00E+00	136	23	2.32
dixmaand	3000	1.00E+00	9	8	0.15	1.00E+00	195	26	3.1	1.00E+00	195	16	3.25
dixmaane	3000	1.00E+00	10	10	0.1	1.00E+00	137	9	1.26	1.00E+00	137	8	1.27
dixmaanf	3000	1.00E+00	19	20	0.23	1.00E+00	159	25	2.64	1.00E+00	156	15	2.64
dixmaang	3000	1.00E+00	16	17	0.2	1.00E+00	155	15	2.56	1.00E+00	198	17	3.29
dixmaanh	3000	1.00E+00	21	25	0.25	1.00E+00	168	19	2.42	1.00E+00	154	16	2.6
dixmaani	3000	1.00E+00	18	17	0.13	1.00E+00	212	23	1.67	1.00E+00	212	23	2
dixmaanj	3000	1.00E+00	20	23	0.24	1.00E+00	111	4	1.67	1.00E+00	87	8	1.39
dixmaank	3000	1.00E+00	24	28	0.29	1.00E+00	111	7	1.58	1.00E+00	108	9	1.67
dixma anl	3000	1.00E+00	28	36	0.32	1.00E+00	161	19	2.11	1.00E+00	174	18	2.12
dixon3dq	10	2.71E-30	1	0	0.04	2.71E-30	1	0	0.07	2.71E-30	1	0	0.04
djl	2	-8.95E+03	20	7	0.04	-8.95E+03	20	7	0.07	-8.95E+03	20	7	0.04
dnieper	61	1.87E+04	29	6	0.05	1.87E+04	30	0	0.08	1.87E+04	30	0	0.04
dqdrtc	5000	1.98E-25	1	0	0.1	1.98E-25	1	0	0.11	1.98E-25	1	0	0.07
drcavty1	10816	3.01E-11	137	185	78.84	-	-	-	-	-	-	-	-
drcavty2	10816	1.06E-05	765	301	293.87	-	-	-	-	-	-	-	-
drcavty3	10816	2.09E-04	198	302	121.66	-	-	-	-	-	-	-	-
dtoc1	14985	1.25E+02	6	0	0.36	1.25E+02	6	0	0.35	1.25E+02	6	0	0.57
dtoc1na	1485	1.27E+01	6	0	0.27	1.27E+01	6	0	0.26	1.27E+01	6	0	0.36
dtoc1nb	1485	1.59E+01	5	0	0.26	1.59E+01	5	0	0.22	1.59E+01	5	0	0.33
dtoc1nc	1485	2.50E+01	17	13	0.59	2.50E+01	8	3	0.31	2.50E+01	19	16	0.79
dtoc1nd	735	1.26E+01	22	18	0.35	1.27E+01	57	36	0.77	1.24E+01	70	52	1.42
dtoc2	5994	5.09E-01	10	4	0.49	5.13E-01	6	0	0.25	5.13E-01	6	0	0.41
dtoc3	14997	2.35E+02	1	0	0.2	2.35E+02	1	0	0.19	2.35E+02	1	0	0.3
dtoc4	14997	2.87E+00	3	0	0.36	2.87E+00	3	0	0.34	2.87E+00	3	0	0.55
dtoc5	9998	1.54E+00	3	0	0.14	1.54E+00	3	0	0.14	1.54E+00	3	0	0.22
dtoc6	10000	1.35E+05	11	0	0.28	1.35E+05	11	0	0.27	1.35E+05	11	0	0.44
dual1	85	3.50E-02	13	0	0.07	3.50E-02	13	0	0.07	3.50E-02	13	0	0.11
dual2	96	3.37E-02	11	0	0.07	3.37E-02	11	0	0.08	3.37E-02	11	0	0.12
dual3	111	1.36E-01	10	0	0.09	1.36E-01	10	0	0.1	1.36E-01	10	0	0.13
dual4	75	7.46E-01	10	0	0.06	7.46E-01	10	0	0.07	7.46E-01	10	0	0.1
dualc1	9	6.16E+03	30	0	0.07	6.16E+03	30	0	0.08	6.16E+03	30	0	0.11
dualc2	7	3.55E+03	21	0	0.07	3.55E+03	21	0	0.06	3.55E+03	21	0	0.09
dualc5	8	4.27E+02	12	0	0.07	4.27E+02	12	0	0.06	4.27E+02	12	0	0.09
dualc8	8	1.83E+04	16	0	0.09	1.83E+04	16	0	0.08	1.83E+04	16	0	0.11
edensch	2000	1.20E+04	7	0	0.08	1.20E+04	7	0	0.08	1.20E+04	7	0	0.12
eg1	3	-1.43E+00	7	0	0.05	-1.43E+00	7	0	0.05	-1.43E+00	7	0	0.07
eg2	1000	-9.99E+02	3	3	0.07	-9.99E+02	3	0	0.05	-9.99E+02	3	0	0.08
eg3	101	1.28E-10	17	6	0.06	6.89E-02	25	0	0.06	6.89E-02	25	0	0.08
eigena2	110	3.61E-30	2	0	0.05	3.61E-30	2	0	0.05	3.61E-30	2	0	0.05
eigenaco	110	7.89E-31	3	4	0.05	7.89E-31	2	0	0.05	7.89E-31	2	0	0.05
eigenals	110	2.53E-24	25	24	0.11	1.00E+01	18	8	0.1	1.00E+01	18	8	0.1
eigena	110	4.74E-06	25	6	0.09	4.70E-06	25	5	0.08	4.70E-06	25	5	0.08
eigenb2	110	1.80E+01	2	0	0.05	1.80E+01	2	0	0.06	1.80E+01	2	0	0.05
eigenbco	110	1.05E-15	77	87	0.33	9.00E+00	2	0	0.06	9.00E+00	2	0	0.05
eigenb1s	110	5.73E-20	109	91	0.41	6.69E-02	41	9	0.18	6.69E-02	41	9	0.18
eigenb	110	6.19E-15	110	87	0.26	6.69E-02	42	9	0.12	6.69E-02	42	9	0.13
eigenc2	462	5.42E-25	20	22	1.27	5.36E+00	96	70	5.37	1.04E+01	86	33	4.18
eigencco	30	5.76E-21	12	11	0.06	4.80E-21	9	3	0.04	4.80E-21	9	3	0.05
eigmaxb	101	-9.67E-04	11	0	0.06	-9.67E-04	11	6	0.05	-9.67E-04	11	6	0.06
eigmaxc	22	-1.00E+00	8	0	0.06	-1.00E+00	8	3	0.05	-1.00E+00	8	1	0.05

eigminb	101	9.67E-04	11	0	0.06	9.67E-04	11	8	0.06	9.67E-04	11	9	0.06
eigminc	22	1.00E+00	10	0	0.07	1.00E+00	10	7	0.06	1.00E+00	10	0	0.04
engval1	5000	5.55E+03	8	0	0.14	5.55E+03	8	0	0.13	5.55E+03	8	0	0.11
engval2	3	1.71E-17	19	13	0.06	1.65E-18	16	0	0.05	1.65E-18	16	0	0.04
errinos	50	4.04E+01	29	12	0.05	4.04E+01	36	10	0.06	4.04E+01	36	10	0.04
expfita	5	1.14E-03	34	19	0.05	1.14E-03	34	19	0.05	1.14E-03	34	19	0.04
expfitb	5	5.02E-03	54	26	0.07	5.02E-03	54	26	0.08	5.02E-03	54	26	0.06
expfitc	5	2.33E-02	81	26	0.17	2.33E-02	92	26	0.21	2.33E-02	93	26	0.2
expfit	2	2.41E-01	8	8	0.06	2.41E-01	11	7	0.05	2.41E-01	11	7	0.04
explin2	120	-7.24E+05	17	0	0.07	-7.24E+05	17	0	0.06	-7.24E+05	17	0	0.04
explin	120	-7.24E+05	17	0	0.04	-7.24E+05	17	0	0.06	-7.24E+05	17	0	0.04
expquad	120	-3.62E+06	21	15	0.06	-3.62E+06	31	0	0.06	-3.62E+06	31	0	0.04
extrasin	2	1.00E+00	5	0	0.06	1.00E+00	5	0	0.05	1.00E+00	5	0	0.06
extrosnb	10	0.00E+00	0	0	0.06	0.00E+00	0	0	0.05	0.00E+00	0	0	0.06
fccu	19	1.11E+01	1	0	0.05	1.11E+01	1	0	0.05	1.11E+01	1	0	0.07
fletcbv2	100	-5.14E-01	1	0	0.06	-5.14E-01	1	0	0.06	-5.14E-01	1	0	0.07
fletcher	100	2.48E-15	47	65	0.05	1.06E-16	170	69	0.07	1.48E-16	184	63	0.06
fletcher	4	-	-	-	-	1.07E-00	19	22	0.05	-	-	-	-
fminsr1f2	1024	1.00E+00	29	24	0.2	1.00E+00	24	0	0.16	1.00E+00	24	0	0.15
fminsr2f	1024	1.00E+00	50	26	11.49	1.00E+00	31	0	5.37	1.00E+00	35	0	7.38
freuroth	5000	6.08E+05	7	4	0.18	6.08E+05	7	4	0.18	6.08E+05	7	4	0.26
gausselm	1495	-	-	-	-	-1.00E+00	15	0	0.22	-1.00E+00	15	0	0.35
genhs28	10	9.27E-01	1	0	0.04	9.27E-01	1	0	0.04	9.27E-01	1	0	0.07
genhumps	5	4.65E-20	230	343	0.05	1.25E-20	86	68	0.05	1.25E-20	86	68	0.08
genrose	500	1.00E+00	744	10	0.34	1.00E+00	761	31	0.42	1.00E+00	761	31	0.65
gigomez1	3	-3.00E+00	16	5	0.04	-3.00E+00	16	5	0.06	-3.00E+00	16	5	0.08
gilbert	1000	4.82E+02	27	2	0.08	4.82E+02	27	2	0.08	4.82E+02	37	1	0.13
goffin	51	4.54E-06	7	4	0.07	4.54E-06	6	0	0.05	4.54E-06	6	0	0.08
gottfr	2	0.00E+00	5	0	0.05	0.00E+00	5	3	0.04	0.00E+00	5	0	0.09
gouldqp2	699	1.93E-04	9	0	0.05	1.93E-04	9	0	0.05	1.93E-04	9	0	0.09
gouldqp3	699	2.07E+00	12	0	0.07	2.07E+00	12	0	0.09	2.07E+00	12	0	0.11
spp	250	1.44E+04	18	0	0.35	1.44E+04	18	0	0.36	1.44E+04	18	0	0.5
gridneta	13284	3.05E+02	22	0	0.85	3.05E+02	22	0	0.79	3.05E+02	22	0	1.15
gridnetb	13284	1.43E+02	1	0	0.17	1.43E+02	1	0	0.17	1.43E+02	1	0	0.25
gridnetc	7564	1.62E+02	24	0	0.52	1.62E+02	24	0	0.44	1.62E+02	24	0	0.68
gridnetd	7565	5.66E+02	23	0	1	5.66E+02	23	0	0.89	5.66E+02	23	0	1.28
gridnete	7565	2.07E+02	5	0	0.43	2.07E+02	5	0	0.4	2.07E+02	5	0	0.59
gridnetf	7565	2.42E+02	24	0	0.98	2.42E+02	24	0	0.88	2.42E+02	24	0	1.3
gridnetg	61	7.33E+01	17	0	0.05	7.33E+01	17	0	0.05	7.33E+01	17	0	0.1
gridneti	61	3.96E+01	6	0	0.05	3.96E+01	6	0	0.05	3.96E+01	6	0	0.08
gridnetj	61	4.02E+01	13	0	0.06	4.02E+01	13	0	0.05	4.02E+01	13	0	0.08
grouping	100	1.39E+01	7	0	0.07	-	-	-	-	1.39E+01	8	0	0.1
growthls	3	1.00E+00	72	12	0.05	1.00E+00	70	1	0.06	1.00E+00	71	1	0.07
growth	3	1.00E+00	71	12	0.05	1.00E+00	70	1	0.06	1.00E+00	70	1	0.08
gulf	3	2.14E-16	21	11	0.05	5.01E-22	26	13	0.06	5.01E-22	26	13	0.08
hadamals	100	2.53E+01	155	204	0.37	8.13E-02	11	3	0.08	8.13E-02	11	3	0.11
hadamard	65	1.00E+00	6	0	0.06	1.00E+00	6	0	0.08	1.00E+00	7	0	0.1
hager1	10001	8.81E-01	1	0	0.1	8.81E-01	1	0	0.11	8.81E-01	1	0	0.15
hager2	10000	4.32E-01	1	0	0.5	4.32E-01	1	0	0.52	4.32E-01	1	0	0.82
hager3	10000	1.41E-01	1	0	0.25	1.41E-01	1	0	0.26	1.41E-01	1	0	0.4
hager4	10000	2.79E+00	7	0	0.33	2.79E+00	7	0	0.33	2.79E+00	7	0	0.5
haifam	85	-4.50E-01	69	66	0.13	-4.50E+01	138	58	0.2	-4.50E+01	89	35	0.24
haifas	7	-4.50E-01	28	32	0.04	-4.50E-01	19	6	0.06	-4.50E-01	19	6	0.07
hairy	2	2.00E-01	51	65	0.04	2.00E+01	29	29	0.06	2.00E+01	29	29	0.07
haldmads	6	3.30E-02	79	90	0.06	-	-	-	-	1.23E-04	283	101	0.17
harkerp2	300	-5.00E-01	15	0	0.08	-5.00E-01	15	0	0.07	-5.00E-01	15	0	0.12
hart6	100	-3.32E+00	8	5	0.06	-3.32E+00	8	5	0.05	-3.32E+00	8	5	0.08
hatfda	4	9.50E-13	9	0	0.05	9.50E-13	9	0	0.05	9.50E-13	9	0	0.08
hatfdb	4	5.57E-03	10	0	0.06	5.57E-03	10	0	0.05	5.57E-03	10	0	0.08
hatfdd	4	3.88E-15	5	0	0.05	3.88E-15	5	0	0.05	3.88E-15	5	0	0.08
hatfddc	3	6.62E-08	20	8	0.06	1.40E+01	18	0	0.05	1.40E+01	18	0	0.08
hatfde	3	4.43E-07	25	9	0.06	1.53E+01	18	0	0.05	1.53E+01	18	0	0.08
hatfdg	25	0.00E+00	7	0	0.06	0.00E+00	7	8	0.05	0.00E+00	7	0	0.08
hatfdh	4	-2.45E+01	14	0	0.05	-2.45E+01	14	0	0.05	-2.45E+01	14	0	0.08
heart6ls	6	2.11E-21	828	1225	0.08	4.98E-21	232	114	0.07	2.21E-25	232	110	0.1
heart6	6	0.00E+00	66	14	0.06	0.00E+00	67	49	0.06	0.00E+00	22	17	0.08
heart8ls	8	1.44E-16	78	109	0.06	4.92E-21	489	242	0.09	6.94E-28	498	237	0.13
heart8	8	0.00E+00	13	0	0.05	0.00E+00	13	24	0.06	0.00E+00	11	6	0.06
helix	3	3.72E-15	10	9	0.05	5.52E-17	14	0	0.06	5.52E-17	14	0	0.07
hilberta	10	4.66E-20	1	0	0.05	4.66E-20	1	0	0.06	4.66E-20	1	0	0.06
hilbertb	50	7.51E-28	1	0	0.05	7.51E-28	1	0	0.07	7.51E-28	1	0	0.07
himmelba	2	0.00E+00	1	0	0.05	0.00E+00	2	1	0.06	0.00E+00	1	0	0.06
himmelbb	2	1.60E-17	13	16	0.05	4.35E-10	19	0	0.06	4.35E-10	19	0	0.06
himmelbc	2	0.00E+00	5	0	0.06	0.00E+00	5	3	0.06	0.00E+00	5	0	0.06
himmelbe	3	0.00E+00	2	0	0.06	0.00E+00	3	3	0.05	0.00E+00	2	0	0.06
himmelbf	4	3.19E+02	10	7	0.05	3.19E+02	11	2	0.05	3.19E+02	11	2	0.06
himmelbg	2	3.63E-22	6	3	0.05	3.63E-22	6	3	0.05	3.63E-22	6	3	0.07
himmelbh	2	-1.00E+00	4	0	0.05	-1.00E+00	4	0	0.05	-1.00E+00	4	0	0.07
himmelbi	100	-1.76E+03	18	0	0.06	-1.76E+03	18	0	0.06	-1.76E+03	18	0	0.08
himmelbk	24	5.18E-02	18	0	0.06	5.18E-02	18	0	0.06	5.18E-02	18	0	0.08
himmelp1	2	-6.21E+01	13	14	0.06	-2.39E+01	17	14	0.05	-5.17E+01	16	11	0.07
himmelp2	2	-8.20E+00	18	15	0.06	-6.21E+01	23	19	0.05	-8.20E+00	26	24	0.07
himmelp3	2	-5.90E+01	13	2	0.06	-5.90E+01	13	2	0.05	-5.90E+01	13	2	0.08
himmelp4	2	-5.90E+01	15	2	0.06	-5.90E+01	15	2	0.05	-5.90E+01	15	2	0.07
himmelp5	2	-5.90E+01	24	5	0.06	-5.90E+01	25	6	0.05	-5.90E+01	24	5	0.07
himmelp6	2	-5.90E+01	8	0	0.06	-5.90E+01	8	0	0.05	-5.90E+01	8	0	0.07
hong	4	1.35E+00	13	0	0.05	1.35E+00	13	0	0.05	1.35E+00	13	0	0.06
hs001	2	1.33E-15	26	0	0.05	1.33E-15	26	0	0.06	1.33E-15	26	0	0.07
hs002	2	4.94E+00	11	0	0.06	4.94E+00	11	0	0.05	4.94E+00	11	0	0.06
hs003	2	8.09E-08	4	0	0.06	8.09E-08	4	0	0.05	8.09E-08	4	0	0.06
hs004	2	2.67E+00	6	0	0.06	2.67E+00	6	0	0.06	2.67E+00	6	0	0.06
hs005	2	-1.91E+00	8	3	0.05	-1.91E+00	8	3	0.06	-1.91E+00	8	3	0.06
hs006	2	0.00E+00	2	0	0.06	0.00E+00	4	1	0.06	0.00E+00	2	0	0.06
hs007	2	-1.73E+00	47	49	0.06	-1.73E+00	15	5	0.06	-1.73E+00	47	49	0.07
hs008	2	-1.00E+00	5	0	0.06	-1.00E+00	5	4	0.06	-1.00E+00	5	0	0.07
hs009	2	-5.00E-01	3	0	0.05	-5.00E-01	3	0	0.06	-5.00E-01	3	0	0.07
hs010	2	-1.00E+00	20	0	0.06	-1.00E+00	20	0	0.06	-1.00E+00	20	0	0.06

hs011	2	-8.50E+00	8	0	0.06	-8.50E+00	8	0	0.06	-8.50E+00	8	0	0.06
hs012	2	-3.00E+01	11	0	0.06	-3.00E+01	11	0	0.06	-3.00E+01	11	0	0.07
hs013	2	9.95E-01	31	0	0.05	9.95E-01	33	23	0.06	9.95E-01	31	0	0.07
hs014	2	1.39E+00	7	0	0.05	1.39E+00	7	0	0.06	1.39E+00	7	0	0.08
hs015	2	3.06E+02	15	10	0.06	3.06E+02	12	8	0.06	3.06E+02	19	9	0.08
hs016	2	2.31E+01	11	0	0.06	2.31E+01	11	0	0.06	2.31E+01	11	0	0.08
hs017	2	1.00E+00	20	0	0.06	1.00E+00	20	0	0.06	1.00E+00	20	0	0.11
hs018	2	5.00E+00	12	0	0.06	5.00E+00	13	3	0.06	5.00E+00	12	0	0.09
hs019	2	-6.96E+03	15	7	0.05	-6.96E+03	18	17	0.06	-6.96E+03	15	7	0.07
hs020	2	4.02E+01	12	0	0.06	4.02E+01	12	0	0.06	4.02E+01	12	0	0.08
hs021	2	-1.00E+02	9	0	0.06	-1.00E+02	9	0	0.06	-1.00E+02	9	0	0.08
hs022	2	1.00E+00	7	0	0.06	1.00E+00	7	0	0.06	1.00E+00	7	0	0.08
hs023	2	2.00E+00	10	0	0.06	2.00E+00	10	0	0.05	2.00E+00	10	0	0.08
hs024	2	-1.00E+00	12	8	0.06	-1.00E+00	12	8	0.05	-1.00E+00	12	8	0.08
hs025	3	1.14E-12	33	26	0.05	1.14E-12	36	33	0.06	1.14E-12	36	33	0.08
hs026	3	1.65E-12	18	0	0.05	1.65E-12	18	0	0.06	1.65E-12	18	0	0.07
hs027	3	-	-	-	-	4.00E-02	21	1	0.06	-	-	-	-
hs028	3	4.93E-32	1	0	0.05	4.93E-32	1	0	0.06	4.93E-32	1	0	0.06
hs029	3	-2.26E+01	11	7	0.05	-2.26E+01	11	11	0.06	-2.26E+01	11	7	0.06
hs030	3	1.00E+00	14	0	0.05	1.00E+00	14	0	0.06	1.00E+00	14	0	0.06
hs031	3	6.00E+00	7	0	0.05	6.00E+00	7	0	0.06	6.00E+00	7	0	0.07
hs032	3	1.00E+00	12	0	0.05	1.00E+00	12	0	0.06	1.00E+00	12	0	0.07
hs033	3	-4.59E+00	9	0	0.05	-4.59E+00	9	3	0.06	-4.59E+00	9	0	0.07
hs034	3	-8.34E-01	9	0	0.05	-8.34E-01	9	0	0.06	-8.34E-01	9	0	0.06
hs035	3	1.11E-01	7	0	0.05	1.11E-01	7	0	0.06	1.11E-01	7	0	0.07
hs036	3	-3.30E+03	13	11	0.06	-3.30E+03	13	11	0.06	-3.30E+03	13	11	0.06
hs037	3	-3.46E+03	11	9	0.04	-3.46E+03	11	9	0.06	-3.46E+03	11	9	0.07
hs038	4	1.91E-19	40	5	0.05	1.91E-19	40	5	0.06	1.91E-19	40	5	0.11
hs039	4	-1.00E+00	23	8	0.05	-1.00E+00	20	0	0.06	-1.00E+00	20	0	0.11
hs040	4	-2.50E-01	4	0	0.04	-2.50E-01	5	5	0.06	-2.50E-01	4	0	0.09
hs041	4	1.93E+00	10	2	0.04	1.93E+00	10	2	0.06	1.93E+00	10	2	0.08
hs042	4	1.39E+01	6	0	0.05	1.39E+01	6	0	0.06	1.39E+01	6	0	0.07
hs043	4	-4.40E-01	9	0	0.06	-4.40E-01	9	0	0.06	-4.40E-01	9	0	0.07
hs044	4	-1.30E+01	18	15	0.06	-3.00E+00	11	0	0.06	-3.00E+00	11	0	0.07
hs045	5	1.00E+00	23	24	0.06	1.00E+00	27	24	0.06	1.00E+00	27	24	0.07
hs046	5	4.08E-12	18	0	0.06	4.08E-12	18	0	0.06	4.08E-12	18	0	0.08
hs047	5	3.15E-11	17	3	0.06	3.15E-11	17	3	0.05	3.15E-11	17	3	0.08
hs048	5	1.60E-29	1	0	0.06	1.60E-29	1	0	0.05	1.60E-29	1	0	0.07
hs049	5	1.38E-09	16	0	0.06	1.38E-09	16	0	0.05	1.38E-09	16	0	0.08
hs050	5	1.23E-32	9	0	0.06	1.23E-32	9	0	0.05	2.10E-31	9	0	0.07
hs051	5	2.59E-31	1	0	0.06	2.59E-31	1	0	0.05	2.59E-31	1	0	0.08
hs052	5	5.33E+00	1	0	0.06	5.33E+00	1	0	0.05	5.33E+00	1	0	0.08
hs053	5	4.09E+00	6	0	0.06	4.09E+00	6	0	0.05	4.09E+00	6	0	0.07
hs054	6	1.93E-01	7	0	0.06	1.93E-01	7	0	0.05	1.93E-01	7	0	0.07
hs055	6	6.67E+00	7	0	0.06	6.67E+00	7	0	0.05	6.67E+00	7	0	0.07
hs056	7	-3.46E+00	13	11	0.05	-3.46E+00	24	22	0.05	-3.46E+00	13	11	0.07
hs057	2	3.06E-02	21	1	0.06	3.06E-02	20	5	0.05	3.06E-02	20	5	0.08
hs059	2	-7.80E+00	75	45	0.05	-7.80E+00	18	6	0.05	-7.80E+00	88	55	0.09
hs060	3	3.26E-02	6	0	0.04	3.26E-02	6	0	0.05	3.26E-02	6	0	0.08
hs061	3	-1.44E-02	10	0	0.05	-1.44E-02	9	10	0.06	-1.44E-02	5	0	0.07
hs062	3	-2.63E+04	8	0	0.05	-2.63E+04	8	0	0.05	-2.63E+04	8	0	0.07
hs063	3	9.62E-02	7	3	0.05	9.62E-02	8	7	0.05	9.62E-02	7	3	0.08
hs064	3	6.30E+03	17	0	0.05	6.30E+03	17	0	0.05	6.30E+03	17	0	0.07
hs065	3	9.54E-01	10	0	0.05	9.54E-01	10	0	0.06	9.54E-01	10	0	0.09
hs066	3	5.18E-01	7	0	0.05	5.18E-01	7	0	0.05	5.18E-01	7	0	0.08
hs067	10	-1.16E+03	12	0	0.07	-1.16E+03	12	0	0.05	-1.16E+03	12	0	0.08
hs070	4	9.40E-03	23	23	0.05	9.40E-03	54	32	0.06	9.40E-03	54	32	0.09
hs071	4	1.70E+01	8	0	0.05	1.70E+01	8	0	0.06	1.70E+01	8	0	0.08
hs072	4	7.28E+02	16	0	0.05	7.28E+02	16	0	0.05	7.28E+02	16	0	0.09
hs073	4	2.99E+01	8	0	0.04	2.99E+01	8	0	0.06	2.99E+01	8	0	0.08
hs074	4	5.13E+03	9	0	0.04	5.13E+03	9	0	0.06	5.13E+03	9	0	0.06
hs075	4	5.17E+03	8	0	0.04	5.17E+03	8	0	0.06	5.17E+03	8	0	0.06
hs076	4	-4.68E+00	7	0	0.05	-4.68E+00	7	0	0.06	-4.68E+00	7	0	0.08
hs077	5	2.42E-01	12	0	0.05	2.42E-01	12	0	0.06	2.42E-01	12	0	0.07
hs078	5	-2.92E+00	4	0	0.05	-2.92E+00	6	5	0.06	-2.92E+00	4	0	0.07
hs079	5	7.88E-02	4	0	0.05	7.88E-02	4	0	0.05	7.88E-02	4	0	0.07
hs080	5	5.39E-02	6	0	0.05	5.39E-02	6	0	0.06	5.39E-02	6	0	0.07
hs081	5	5.39E-02	9	3	0.08	5.39E-02	7	4	0.06	5.39E-02	8	0	0.07
hs083	5	-3.07E+04	15	0	0.04	-3.07E+04	15	0	0.06	-3.07E+04	15	0	0.07
hs084	5	-5.28E+06	19	16	0.04	-5.28E+06	19	16	0.06	-5.28E+06	19	16	0.07
hs085	5	-1.91E+00	33	0	0.05	-1.91E+00	33	2	0.07	-1.91E+00	33	0	0.09
hs086	5	-3.23E+01	10	0	0.04	-3.23E+01	10	0	0.06	-3.23E+01	10	0	0.08
hs087	9	8.83E+03	17	0	0.05	8.83E+03	17	0	0.06	8.83E+03	17	0	0.08
hs088	2	1.36E+00	16	4	0.05	1.36E+00	18	3	0.07	1.36E+00	24	0	0.09
hs089	3	1.36E+00	13	6	0.06	1.36E+00	30	16	0.07	1.36E+00	31	17	0.09
hs090	4	1.36E+00	19	9	0.05	1.36E+00	21	3	0.06	1.36E+00	22	5	0.1
hs091	5	1.36E+00	26	26	0.06	1.36E+00	20	5	0.07	1.36E+00	64	31	0.11
hs092	6	1.36E+00	19	16	0.06	1.36E+00	16	0	0.07	1.36E+00	16	0	0.09
hs095	6	1.56E-02	19	5	0.05	1.56E-02	23	3	0.06	1.56E-02	23	3	0.08
hs096	6	1.56E-02	18	5	0.06	1.56E-02	18	5	0.05	1.56E-02	18	5	0.08
hs097	6	4.07E+00	19	6	0.06	4.07E+00	21	3	0.06	4.07E+00	21	3	0.08
hs098	6	3.14E+00	31	22	0.06	4.07E+00	23	1	0.06	4.07E+00	23	1	0.08
hs099	23	-8.31E+08	7	0	0.05	-8.31E+08	7	0	0.05	-8.31E+08	7	0	0.08
hs100lnp	7	6.81E+02	16	0	0.06	6.81E+02	16	0	0.06	6.81E+02	16	0	0.08
hs100mod	7	6.79E+02	13	0	0.04	6.79E+02	13	0	0.06	6.79E+02	13	0	0.07
hs100	7	6.81E+02	12	0	0.04	6.81E+02	12	0	0.05	6.81E+02	12	0	0.07
hs101	7	1.81E+03	65	88	0.06	1.81E+03	24	0	0.06	-	-	-	-
hs102	7	9.12E+02	32	26	0.05	9.12E+02	41	11	0.06	-	-	-	-
hs103	7	5.44E+02	74	42	0.07	5.44E+02	60	6	0.07	-	-	-	-
hs104	8	3.95E+00	9	0	0.05	3.95E+00	9	0	0.06	3.95E+00	9	0	0.08
hs105	8	1.14E+03	23	6	0.1	1.14E+03	24	4	0.1	1.14E+03	24	4	0.15
hs106	8	7.05E+03	15	0	0.04	7.05E+03	15	0	0.06	7.05E+03	15	0	0.08
hs108	9	-6.75E-01	27	28	0.06	-6.75E-01	15	3	0.05	-6.75E-01	15	3	0.07
hs109	9	5.33E+03	22	0	0.05	5.33E+03	22	1	0.05	5.33E+03	22	0	0.08
hs110	10	-4.58E+01	6	0	0.04	-4.58E+01	6	0	0.05	-4.58E+01	6	0	0.08
hs111lnp	10	-4.78E+01	22	12	0.04	-4.74E+01	27	9	0.05	-	-	-	-
hs111	10	-4.78E+01	22	12	0.05	-4.75E+01	66	52	0.06	-	-	-	-

hs112	10	-4.78E+01	17	0	0.05	-4.78E+01	17	0	0.05	-4.78E+01	17	0	0.07
hs113	10	2.43E+01	11	0	0.05	2.43E+01	11	0	0.05	2.43E+01	11	0	0.07
hs114	10	-1.77E+03	19	0	0.05	-1.77E+03	19	0	0.05	-1.77E+03	19	0	0.07
hs116	13	9.76E+01	25	0	0.05	9.76E+01	25	0	0.06	9.76E+01	25	0	0.08
hs117	15	3.23E+01	25	10	0.05	3.23E+01	27	6	0.06	3.23E+01	27	6	0.08
hs118	15	6.65E+02	11	0	0.05	6.65E+02	11	0	0.05	6.65E+02	11	0	0.07
hs119	16	2.45E+02	16	0	0.05	2.45E+02	16	0	0.05	2.45E+02	16	0	0.07
hs21mod	7	-9.60E+01	13	0	0.05	-9.60E+01	13	0	0.05	-9.60E+01	13	0	0.07
hs268	5	1.63E-07	14	0	0.05	1.63E-07	14	0	0.05	1.63E-07	14	0	0.07
hs35mod	3	2.50E-01	11	0	0.05	2.50E-01	11	0	0.05	2.50E-01	11	0	0.07
hs3mod	2	8.09E-08	5	0	0.06	8.09E-08	5	0	0.05	8.09E-08	5	0	0.07
hs4new	4	-1.50E+01	13	11	0.08	-1.30E+01	12	9	0.05	-1.30E+01	12	9	0.04
hs99exp	31	-1.01E+09	16	5	0.08	-1.01E+09	36	32	0.06	-1.01E+09	30	26	0.05
hubfit	2	1.69E-02	7	0	0.08	1.69E-02	7	0	0.06	1.69E-02	7	0	0.04
hues-mod	10000	3.48E+07	25	0	0.45	3.48E+07	25	0	0.45	3.48E+07	25	0	0.44
huestis	10000	3.48E+11	24	0	0.43	3.48E+11	24	0	0.42	3.48E+11	24	0	0.42
humps	2	3.41E-12	124	173	0.04	3.88E-13	219	229	0.05	3.88E-13	219	229	0.05
hypcir	2	0.00E+00	5	0	0.06	0.00E+00	5	3	0.05	0.00E+00	5	0	0.05
integreq	100	0.00E+00	2	0	0.08	0.00E+00	2	2	0.08	0.00E+00	2	0	0.07
jensmp	2	1.24E+02	10	0	0.05	1.24E+02	10	0	0.05	1.24E+02	10	0	0.05
kiwcrese	3	1.72E-07	15	5	0.06	1.72E-07	15	5	0.06	1.72E-07	15	5	0.05
kowosb	4	3.08E-04	8	5	0.05	3.08E-04	10	1	0.05	3.08E-04	10	1	0.05
ksp	20	5.76E-01	22	0	0.17	5.76E-01	22	0	0.16	5.76E-01	22	0	0.17
lakes	90	3.51E+05	15	7	0.05	3.51E+05	16	8	0.06	3.51E+05	16	5	0.06
lch	600	-4.32E+00	63	93	0.15	-3.10E+00	1	0	0.06	-3.10E+00	1	0	0.06
liarwhd	10000	8.20E-22	12	0	0.37	8.20E-22	12	0	0.37	8.20E-22	12	0	0.36
linspant	97	-7.70E+01	13	5	0.05	-7.70E+01	15	0	0.05	-7.70E+01	15	0	0.05
liswet10	10002	3.93E-01	79	0	1.96	3.93E-01	79	0	2	3.93E-01	77	0	1.89
liswet11	10002	4.65E-01	57	0	1.5	4.65E-01	57	0	1.57	4.65E-01	57	0	1.44
liswet12	10002	-3.38E+03	88	0	2.18	-3.38E+03	88	0	2.24	-3.38E+03	88	0	2.1
liswet1	10002	2.93E+01	20	0	0.68	2.93E+01	20	0	0.73	2.93E+01	20	0	0.68
liswet2	10002	2.50E+01	26	0	0.85	2.50E+01	26	0	0.83	2.50E+01	26	0	0.8
liswet3	10002	2.50E+01	27	0	0.83	2.50E+01	27	0	0.85	2.50E+01	27	0	0.83
liswet4	10002	2.50E+01	27	0	0.83	2.50E+01	27	0	0.83	2.50E+01	27	0	0.84
liswet5	10002	2.50E+01	27	0	0.82	2.50E+01	27	0	0.87	2.50E+01	27	0	0.82
liswet6	10002	2.50E+01	25	0	0.78	2.50E+01	25	0	0.87	2.50E+01	25	0	0.79
liswet7	10002	4.21E+02	18	0	0.62	4.21E+02	18	0	0.7	4.21E+02	18	0	0.63
liswet8	10002	6.51E+02	65	0	1.66	6.51E+02	65	0	1.79	6.51E+02	65	0	1.61
liswet9	10002	1.90E+03	57	0	1.51	1.90E+03	57	0	1.62	1.90E+03	57	0	1.43
lminsurf	15625	9.00E+00	2	0	0.49	9.00E+00	2	0	0.51	9.00E+00	2	0	0.5
loadbal	31	4.53E-01	13	0	0.04	4.53E-01	13	0	0.05	4.53E-01	13	0	0.05
logros	2	1.87E-14	54	7	0.05	1.87E-14	54	7	0.05	1.87E-14	54	7	0.04
lootsma	3	1.41E+00	9	0	0.04	1.41E+00	9	3	0.07	1.41E+00	9	0	0.04
lotschd	12	2.40E+03	14	0	0.05	2.40E+03	14	0	0.08	2.40E+03	14	0	0.07
lsmnodoc	5	1.23E+02	14	0	0.07	1.23E+02	14	0	0.08	1.23E+02	14	0	0.07
lsqfit	2	3.38E-02	7	0	0.08	3.38E-02	7	0	0.05	3.38E-02	7	0	0.06
madsen	3	6.16E-01	20	6	0.07	1.00E+00	16	3	0.05	6.16E-01	16	3	0.06
madschj	81	-7.97E+02	52	48	0.28	-7.97E+02	27	12	0.16	-7.97E+02	27	9	0.14
makela1	3	-1.41E+00	16	14	0.04	-1.41E+00	11	9	0.05	-1.41E+00	11	9	0.04
makela2	3	7.20E+00	7	0	0.04	7.20E+00	7	0	0.06	7.20E+00	7	0	0.05
makela3	21	1.81E-06	36	24	0.05	1.81E-06	26	0	0.08	1.81E-06	26	0	0.05
makela4	21	3.63E-06	7	0	0.07	3.63E-06	7	0	0.08	3.63E-06	7	0	0.05
mancino	100	1.26E-21	5	0	0.17	1.26E-21	5	0	0.17	1.26E-21	5	0	0.14
manne	1094	-9.68E-01	390	548	2.69	-	-	-	-	-	-	-	-
maratosb	2	-1.00E+00	32	48	0.04	-1.00E+00	31	45	0.06	-1.00E+00	31	45	0.06
maratos	2	-1.00E+00	19	0	0.04	-1.00E+00	19	0	0.06	-1.00E+00	19	0	0.05
matrix2	6	3.39E-07	16	0	0.05	3.39E-07	16	0	0.06	3.39E-07	16	0	0.05
maxlika	8	1.14E+03	23	6	0.09	1.14E+03	25	8	0.1	1.14E+03	25	8	0.09
mc McCormck	50000	-4.57E+04	7	0	1.95	-4.57E+04	7	0	2.05	-4.57E+04	7	0	1.96
mconcon	15	-6.23E+03	10	0	0.04	-6.23E+03	10	0	0.05	-6.23E+03	10	0	0.05
mdhole	2	8.09E-08	47	12	0.05	8.09E-08	38	3	0.06	8.09E-08	38	3	0.04
methanb8	31	2.14E-14	6	4	0.05	6.77E-23	19	1	0.06	6.64E-23	19	1	0.04
methan18	31	7.93E-14	44	53	0.06	7.85E-22	591	279	0.24	1.67E-18	597	295	0.23
meshat	2	-4.01E-02	3	2	0.08	-4.01E-02	4	0	0.04	-4.01E-02	4	0	0.06
mifflin1	3	-1.00E+00	16	0	0.05	-1.00E+00	16	0	0.05	-1.00E+00	16	0	0.05
mifflin2	3	-	-	-	-	-1.00E+00	16	5	0.05	-1.00E+00	16	5	0.04
mine44	311	2.57E-03	14	8	0.14	2.57E-03	20	4	0.15	2.57E-03	21	3	0.14
minmaxbd	5	1.16E+02	66	20	0.05	1.16E+02	49	17	0.06	1.16E+02	56	2	0.05
minmaxrb	3	3.54E-07	9	0	0.04	3.54E-07	9	0	0.05	3.54E-07	9	0	0.04
minperm	1113	3.63E-04	6	10	1.65	3.63E-04	6	6	1.24	3.63E-04	6	5	1.12
minsurf	64	1.00E+00	1	0	0.04	1.00E+00	2	1	0.04	1.00E+00	1	0	0.04
mistake	9	-1.00E+00	17	8	0.05	-1.00E+00	54	29	0.05	-1.00E+00	54	29	0.05
model	1831	5.74E+03	37	0	0.11	5.74E+03	37	0	0.12	5.74E+03	37	0	0.1
morebv	5002	1.04E-11	0	0	0.09	1.04E-11	0	0	0.09	1.04E-11	0	0	0.08
mosarqp1	2500	-9.53E+02	13	0	0.12	-9.53E+02	13	0	0.14	-9.53E+02	13	0	0.12
mosarqp2	900	-1.60E+03	12	0	0.09	-1.60E+03	12	0	0.1	-1.60E+03	12	0	0.08
msqrals	1024	4.22E-16	24	27	8.88	-	-	-	-	-	-	-	-
msqrta	1024	0.00E+00	4	0	3.92	0.00E+00	4	5	6.93	0.00E+00	4	0	4.72
msqrbls	1024	3.64E-12	27	32	10.26	1.02E-14	678	334	223.29	1.30E-14	606	285	177.35
msqrtrb	1024	0.00E+00	4	0	3.97	0.00E+00	4	5	7	0.00E+00	4	0	4.92
mwright	5	2.50E+01	7	0	0.04	2.50E+01	7	0	0.05	2.50E+01	7	0	0.05
nasty	2	1.53E-72	1	0	0.05	1.53E-72	1	0	0.04	1.53E-72	1	0	0.04
ncvxbqp1	10000	-1.99E+10	259	388	20.7	-	-	-	-	-	-	-	-
ncvxqp1	1000	-7.15E+07	312	473	13.21	-7.15E+07	597	881	26.24	-7.15E+07	573	854	33.63
ncvxqp2	1000	-5.78E+07	393	594	16.8	-5.78E+07	749	1066	31.17	-5.78E+07	728	1018	33.52
ncvxqp3	1000	-3.05E+07	463	692	21.96	-	-	-	-	-3.07E+07	962	1214	54.64
ncvxqp4	1000	-9.40E+07	282	430	4.64	-9.40E+07	657	961	11.06	-9.40E+07	615	904	11.11
ncvxqp5	1000	-6.63E+07	347	526	5.73	-6.62E+07	760	1029	12.95	-6.62E+07	713	981	19.08
ncvxqp6	1000	-3.41E+07	439	662	7.28	-	-	-	-	-3.45E+07	860	1070	16.88
ncvxqp7	1000	-4.34E+07	243	368	18.18	-4.34E+07	317	475	24.21	-4.34E+07	322	483	26.45
ncvxqp8	1000	-3.04E+07	338	513	27.23	-3.04E+07	608	869	48.41	-3.05E+07	581	832	55.25
ncvxqp9	1000	-2.15E+07	321	478	27.41	-	-	-	-	-2.15E+07	526	684	51.04
ngone	100	-6.36E-01	30	22	0.21	-6.38E-01	124	35	0.62	-6.39E-01	133	31	0.75
noncvxu2	1000	2.32E+03	400	605	11.99	2.36E+03	765	416	17.51	2.35E+03	874	540	22.12
noncvxu	1000	2.32E+03	34	48	0.09	2.35E+03	76	52	0.17	2.33E+03	83	65	0.23
nondia	9999	2.31E-25	5	0	0.26	2.31E-25	5	0	0.25	2.31E-25	5	0	0.29
nondquar	10000	1.62E-11	21	0	0.37	1.62E-11	21	0	0.37	1.62E-11	21	0	0.46

nonmsqrt	9	7.52E-01	121	12	0.05	3.32E+00	152	8	0.06	3.22E+00	139	0	0.07
nonscomp	10000	3.98E-04	17	0	0.43	3.98E-04	17	0	0.43	3.98E-04	17	0	0.49
nuffield2	2382	-	-	-	-	-1.82E-02	148	6	4.02	-	-	-	-
nuffield_continuum	2	2.50E+00	9	0	0.06	2.50E+00	9	0	0.05	2.50E+00	9	0	0.06
obstclal	96	1.40E+00	9	0	0.06	1.40E+00	9	0	0.05	1.40E+00	9	0	0.06
obstclbl	96	2.88E+00	10	0	0.06	2.88E+00	10	0	0.05	2.88E+00	10	0	0.05
obstclbu	96	2.88E+00	15	0	0.06	2.88E+00	15	0	0.05	2.88E+00	15	0	0.06
odfits	10	-2.38E+03	10	0	0.05	-2.38E+03	10	0	0.05	-2.38E+03	10	0	0.06
oet1	3	5.38E-01	26	0	0.1	5.38E-01	26	0	0.1	5.38E-01	26	0	0.14
oet2	3	8.72E-02	70	35	0.23	-	-	-	-	-	-	-	-
oet3	4	4.51E-03	14	0	0.07	4.51E-03	14	0	0.1	4.51E-03	14	0	0.11
oet7	7	9.97E-05	160	169	0.92	-	-	-	-	8.72E-02	81	25	0.48
optcdcg2	1199	2.30E+02	25	0	0.1	2.30E+02	25	0	0.1	2.30E+02	25	0	0.14
optcdcg3	1199	4.61E+01	23	0	0.1	4.61E+01	23	0	0.09	4.61E+01	23	0	0.13
optcntrl	32	5.50E+02	42	0	0.06	5.50E+02	42	0	0.05	5.50E+02	42	0	0.08
optmass	66	-1.90E-01	23	24	0.06	-1.74E-01	20	17	0.08	-1.90E-01	20	18	0.06
optprloc	30	-1.64E+01	20	0	0.06	-1.64E+01	20	0	0.08	-1.64E+01	20	0	0.06
orthrdm2	4003	1.56E+02	5	0	0.18	1.56E+02	5	0	0.19	1.56E+02	5	0	0.19
orthrds2	203	1.54E+03	38	64	0.09	1.46E+03	61	15	0.1	-	-	-	-
orthrega	517	1.41E+03	65	78	0.3	1.66E+03	28	16	0.13	1.66E+03	28	16	0.19
orthregb	27	4.52E-20	2	2	0.06	1.58E-17	2	1	0.04	0.00E+00	1	0	0.07
orthregc	10005	1.90E+02	13	13	2.74	1.90E+02	126	63	14.56	1.90E+02	94	47	14.04
orthregd	10003	1.52E+03	12	5	0.8	1.52E+03	18	5	1.24	1.52E+03	16	5	0.98
orthrege	36	6.07E-01	44	24	0.05	1.84E+00	60	42	0.05	2.23E+00	10	3	0.04
osbornea	5	5.46E-05	35	11	0.06	5.46E-05	22	0	0.05	5.46E-05	22	0	0.06
osborneb	11	4.01E-02	18	12	0.06	-	-	-	-	-	-	-	-
oslbqp	8	6.25E+00	11	0	0.06	6.25E+00	11	0	0.06	6.25E+00	11	0	0.05
palmer1a	6	8.99E-02	43	21	0.05	8.99E-02	39	6	0.06	8.99E-02	39	6	0.05
palmer1b	4	-	-	-	-	-	-	-	-	3.45E+00	21	7	0.05
palmer1c	8	9.76E-02	1	0	0.04	9.76E-02	1	0	0.05	9.76E-02	1	0	0.05
palmer1d	7	6.53E-01	1	0	0.05	6.53E-01	1	0	0.05	6.53E-01	1	0	0.05
palmer1e	8	8.35E-04	37	15	0.08	8.35E-04	32	13	0.05	8.35E-04	31	13	0.05
palmer1	4	1.18E+04	746	7	0.11	1.18E+04	755	11	0.08	1.18E+04	732	11	0.08
palmer2a	6	1.72E-02	132	47	0.08	1.72E-02	94	6	0.06	1.72E-02	95	6	0.06
palmer2b	4	6.23E-01	18	15	0.07	6.23E-01	21	14	0.05	6.23E-01	21	14	0.06
palmer2c	8	1.44E-02	1	0	0.05	1.44E-02	1	0	0.05	1.44E-02	1	0	0.06
palmer2e	8	2.15E-04	36	19	0.05	2.15E-04	97	5	0.05	2.15E-04	98	4	0.06
palmer2	4	-	-	-	-	4.58E+03	23	8	0.05	4.58E+03	23	8	0.06
palmer3a	6	2.04E-02	129	19	0.05	2.04E-02	105	3	0.05	2.04E-02	105	3	0.06
palmer3b	4	4.23E+00	16	14	0.05	4.23E+00	16	11	0.04	4.23E+00	16	11	0.06
palmer3c	8	1.95E-02	1	0	0.05	1.95E-02	1	0	0.04	1.95E-02	1	0	0.05
palmer3e	8	5.07E-05	73	7	0.06	5.07E-05	28	5	0.04	5.07E-05	28	5	0.05
palmer3	4	2.27E+03	211	23	0.08	2.27E+03	466	4	0.06	2.27E+03	469	4	0.07
palmer4a	6	4.06E-02	98	20	0.08	4.06E-02	39	5	0.07	4.06E-02	39	5	0.06
palmer4b	4	6.84E+00	16	14	0.07	6.84E+00	22	15	0.07	6.84E+00	22	15	0.06
palmer4c	8	5.03E-02	1	0	0.05	5.03E-02	1	0	0.07	5.03E-02	1	0	0.05
palmer4e	8	1.48E-04	30	17	0.06	1.48E-04	119	5	0.08	1.48E-04	119	3	0.06
palmer4	4	2.29E+03	246	23	0.09	2.29E+03	132	7	0.08	2.29E+03	134	7	0.05
palmer5b	9	9.75E-03	75	46	0.06	-	-	-	-	-	-	-	-
palmer5c	6	2.13E+00	1	0	0.06	2.13E+00	1	0	0.06	2.13E+00	1	0	0.04
palmer5d	4	8.73E+01	1	0	0.05	8.73E+01	1	0	0.05	8.73E+01	1	0	0.04
palmer6a	6	5.59E-02	273	20	0.07	5.59E-02	115	3	0.05	5.59E-02	112	3	0.05
palmer6c	8	1.64E-02	1	0	0.05	1.64E-02	1	0	0.05	1.64E-02	1	0	0.05
palmer6e	8	2.24E-04	27	9	0.06	2.24E-04	334	10	0.06	2.24E-04	330	7	0.05
palmer7c	8	6.02E-01	1	0	0.08	6.02E-01	1	0	0.05	6.02E-01	1	0	0.05
palmer8a	6	7.40E-02	83	31	0.08	7.40E-02	43	6	0.05	7.40E-02	43	6	0.07
palmer8c	8	1.60E-01	1	0	0.05	1.60E-01	1	0	0.05	1.60E-01	1	0	0.07
palmer8e	8	6.34E-03	27	18	0.04	6.34E-03	172	2	0.06	6.34E-03	172	2	0.08
penalty2	100	9.71E+04	19	0	0.07	9.71E+04	19	0	0.06	9.71E+04	19	0	0.09
pentagon	6	1.37E-04	15	10	0.05	1.47E-04	16	0	0.04	1.47E-04	16	0	0.08
pentdi	1000	-7.50E-01	11	0	0.07	-7.50E-01	11	0	0.06	-7.50E-01	11	0	0.08
pf11s	3	-	-	-	-	4.91E-18	247	13	0.05	4.91E-18	247	13	0.06
pf11	3	-	-	-	-	4.91E-18	247	13	0.05	4.91E-18	247	13	0.05
pf12s	3	2.29E-21	122	16	0.07	6.39E-26	98	13	0.04	6.39E-26	98	13	0.05
pf12	3	2.29E-21	122	16	0.08	6.39E-26	98	13	0.05	6.39E-26	98	13	0.05
pf13s	3	1.51E-21	114	15	0.08	1.71E-21	126	9	0.04	1.01E-25	126	9	0.06
pf13	3	1.51E-21	114	15	0.08	1.71E-21	126	9	0.06	1.01E-25	126	9	0.07
pf14s	3	4.85E-27	199	18	0.07	2.64E-22	220	15	0.06	3.16E-21	219	15	0.06
pf14	3	4.85E-27	199	18	0.07	2.64E-22	220	15	0.06	3.16E-21	219	15	0.06
polak4	3	2.53E-07	64	0	0.07	2.53E-07	45	3	0.07	2.53E-07	45	3	0.05
polak5	3	5.00E+01	33	0	0.06	5.00E+01	33	0	0.08	5.00E+01	33	0	0.05
polak6	5	-4.40E+01	56	52	0.07	-4.40E+01	54	16	0.08	-4.40E+01	63	29	0.06
porous1	4900	0.00E+00	13	0	1.94	0.00E+00	13	3	2.46	0.00E+00	13	0	1.77
porous2	4900	0.00E+00	7	0	1.23	0.00E+00	7	5	1.94	0.00E+00	7	0	1.08
portf11	12	2.05E-02	8	0	0.07	2.05E-02	8	0	0.05	2.05E-02	8	0	0.05
portf12	12	2.97E-02	7	0	0.06	2.97E-02	7	0	0.05	2.97E-02	7	0	0.05
portf13	12	3.28E-02	8	0	0.1	3.28E-02	8	0	0.06	3.28E-02	8	0	0.05
portf14	12	2.63E-02	7	0	0.09	2.63E-02	7	0	0.05	2.63E-02	7	0	0.06
portf6	12	2.58E-02	7	0	0.08	2.58E-02	7	0	0.06	2.58E-02	7	0	0.08
powell20	1000	5.21E+07	255	0	0.74	5.21E+07	255	0	0.57	5.21E+07	255	0	0.58
powellbs	2	0.00E+00	46	0	0.06	0.00E+00	46	1	0.06	0.00E+00	46	0	0.05
power	1000	0.00E+00	1	0	0.06	0.00E+00	1	0	0.05	3.34E-24	1	0	0.05
propbpenl	500	-2.09E-07	5	0	0.23	-2.09E-07	5	0	0.21	-2.09E-07	5	0	0.22
prodp10	60	6.09E+01	15	0	0.05	6.09E+01	15	0	0.04	6.09E+01	15	0	0.05
prodp11	60	5.30E+01	15	0	0.08	5.30E+01	15	0	0.05	5.30E+01	15	0	0.05
pspdoc	4	2.41E+00	8	0	0.08	2.41E+00	8	0	0.04	2.41E+00	8	0	0.05
pt	2	1.78E-01	19	0	0.1	1.78E-01	19	0	0.07	1.78E-01	19	0	0.09
qpcboe2	143	8.29E+06	92	0	0.14	8.29E+06	92	0	0.15	8.29E+06	92	0	0.12
qpcstair	467	6.20E+06	159	0	0.46	6.20E+06	159	0	0.46	6.20E+06	159	0	0.45
qpnstair	467	5.15E+06	186	15	0.59	5.15E+06	208	0	0.59	5.15E+06	193	0	0.55
qr3dbd	127	1.34E-13	26	14	0.1	1.34E-13	58	21	0.15	1.34E-13	55	19	0.15
qr3dls	155	1.34E-13	49	49	0.26	1.34E-13	63	25	0.26	1.34E-13	63	25	0.29
qr3d	155	1.34E-13	49	49	0.26	1.34E-13	67	23	0.22	1.34E-13	67	23	0.24
qrtquad	120	-3.65E+06	27	22	0.07	-3.65E+06	40	18	0.06	-3.65E+06	40	18	0.06
qudlin	12	-7.20E+03	23	23	0.07	-7.20E+03	21	0	0.05	-7.20E+03	21	0	0.05
reading1	10001	-1.60E-01	19	0	0.99	-1.60E-01	19	0	0.95	-1.60E-01	19	0	1
reading2	15003	-1.10E-02	5	0	0.48	-1.10E-02	5	0	0.49	-1.10E-02	5	0	0.49

reading3	202	-9.85E-09	20	0	0.05	-9.85E-09	20	0	0.07	-9.85E-09	20	0	0.06
recipe	3	0.00E+00	2	0	0.05	0.00E+00	3	3	0.04	0.00E+00	2	0	0.04
res	18	0.00E+00	11	0	0.05	0.00E+00	11	0	0.04	0.00E+00	11	0	0.05
rk23	17	8.33E-02	9	8	0.07	8.33E-02	44	38	0.05	4.44E-01	231	335	0.1
robot	14	1.34E+01	8	16	0.08	1.34E+01	8	11	0.04	1.34E+01	6	0	0.07
rosenbr	2	3.74E-21	21	0	0.07	3.74E-21	21	0	0.05	3.74E-21	21	0	0.06
rosenmmx	5	-	-	-	-	-4.40E+01	21	1	0.07	-4.40E+01	21	1	0.07
s332	2	2.99E+01	15	0	0.05	2.99E+01	15	0	0.08	2.99E+01	15	0	0.05
s365mod	7	5.21E+01	21	12	0.05	5.21E+01	20	6	0.05	5.21E+01	29	4	0.05
s368	100	6.65E-20	5	4	0.25	3.37E-18	5	0	0.25	3.37E-18	5	0	0.24
scon1dls	1000	1.65E-08	366	170	0.98	1.65E-08	389	183	1.03	1.65E-08	393	210	1.29
scosine	10000	-1.00E+04	134	194	2.84	-	-	-	-	-	-	-	-
semicon1	1000	0.00E+00	55	0	0.17	0.00E+00	59	22	0.21	0.00E+00	55	0	0.17
semicon2	1000	0.00E+00	21	0	0.09	0.00E+00	21	16	0.11	0.00E+00	21	0	0.09
sensors	1000	-1.96E+05	65	94	260.47	-	-	-	-	-1.48E+05	47	50	219.08
sim2bqp	2	8.09E-08	7	0	0.05	8.09E-08	7	0	0.08	8.09E-08	7	0	0.07
simbqp	2	8.09E-08	7	0	0.05	8.09E-08	7	0	0.05	8.09E-08	7	0	0.07
simpllpa	2	1.00E+00	10	0	0.05	1.00E+00	10	0	0.04	1.00E+00	10	0	0.07
simpllpb	2	1.10E+00	8	0	0.05	1.10E+00	8	0	0.05	1.10E+00	8	0	0.07
sineval	20	2.05E+40	42	0	0.08	2.05E+40	42	0	0.07	2.10E+40	42	0	0.07
sinqrad	2	4.40E-11	20	5	0.82	3.06E-11	18	0	0.72	1.75E-11	19	0	1
sinrosnb	1000	-9.99E+04	5	5	0.08	-9.99E+04	5	0	0.09	-9.99E+04	5	0	0.13
sipow1m	2	-1.00E+00	22	0	0.66	-1.00E+00	22	0	0.66	-1.00E+00	23	0	1.1
sipow1	2	-1.00E+00	22	0	0.67	-1.00E+00	22	0	0.66	-1.00E+00	23	0	1.07
sipow2m	2	-1.00E+00	26	0	0.34	-1.00E+00	26	0	0.33	-1.00E+00	26	0	0.53
sipow2	2	-1.00E+00	28	0	0.35	-1.00E+00	28	0	0.36	-1.00E+00	26	0	0.52
sipow3	4	5.36E+01	11	0	0.6	5.36E+01	11	0	0.59	5.36E+01	11	0	0.93
sisser	4	5.33E+10	16	8	0.05	4.10E+10	14	0	0.06	4.10E+10	14	0	0.08
smbank	117	-7.13E+06	13	0	0.06	-7.13E+06	13	0	0.06	-7.13E+06	13	0	0.08
smmpsf	720	1.05E+06	103	7	0.17	1.05E+06	104	0	0.16	1.05E+06	104	0	0.24
snake	2	-1.96E+04	7	0	0.05	-1.96E+04	7	1	0.05	-1.96E+04	7	0	0.08
sosap2	20000	-5.00E+03	13	0	3.28	-5.00E+03	13	0	3.37	-5.00E+03	13	0	3.35
spanhyd	97	-	-	-	-	2.40E+02	344	148	0.29	2.40E+02	386	168	0.31
sreadin3	10001	-2.76E-05	6	0	0.35	-2.76E-05	6	0	0.36	-2.76E-05	6	0	0.33
srosenbr	10000	1.87E-17	21	0	0.27	1.87E-17	21	0	0.27	1.87E-17	21	0	0.27
sseblin	194	1.62E+07	124	0	0.09	1.62E+07	124	0	0.08	1.62E+07	124	0	0.08
ssnlbeam	33	3.38E+02	19	13	0.06	3.47E+02	14	6	0.06	3.47E+02	9	3	0.05
stancmin	3	4.25E+00	10	0	0.06	4.25E+00	10	0	0.06	4.25E+00	10	0	0.05
static3	434	-	-	-	-	-1.53E+03	23	0	0.09	-1.53E+03	23	0	0.07
stsenbra	432	1.70E+04	23	0	0.26	1.70E+04	23	0	0.21	1.70E+04	23	0	0.19
stsenbrb	468	9.08E+03	61	0	0.69	9.09E+03	46	6	0.39	9.09E+03	44	0	0.31
stsenbrd	468	-	-	-	-	-	-	-	-	1.06E+04	63	10	0.48
stsenbre	540	2.89E+04	91	49	1.63	-	-	-	-	-	-	-	-
stsenbrf	468	-	-	-	-	2.83E+02	561	565	0.81	2.83E+02	306	269	0.42
stsenbrg	540	-	-	-	-	2.85E+04	132	75	1.82	2.83E+04	61	14	0.6
supersim	2	6.67E-01	6	0	0.05	6.67E-01	6	0	0.05	6.67E-01	6	0	0.05
svanberg	5000	8.36E+03	20	4	1.05	8.36E+03	20	4	1.07	8.36E+03	20	4	1.05
swopf	83	6.79E-02	15	0	0.05	6.79E-02	15	0	0.05	6.79E-02	15	0	0.05
synthes1	6	7.59E-01	9	0	0.05	7.59E-01	9	0	0.05	7.59E-01	9	0	0.04
tame	2	0.00E+00	5	0	0.05	0.00E+00	5	0	0.05	0.00E+00	5	0	0.04
tfi2	3	6.49E-01	13	0	0.53	6.49E-01	13	0	0.54	6.49E-01	13	0	0.52
tointgor	50	1.18E+03	1	0	0.07	1.18E+03	1	0	0.04	1.18E+03	1	0	0.04
trainf	20008	3.10E+00	41	0	1.69	3.10E+00	41	0	1.76	3.10E+00	41	0	2.16
trainh	20008	1.23E+01	71	0	7.88	1.23E+01	71	0	8.22	1.23E+01	71	0	12.16
tridia	10000	2.72E-24	1	0	0.13	2.72E-24	1	0	0.14	6.12E-24	1	0	0.22
trimloss	142	9.06E+00	32	0	0.06	9.06E+00	32	0	0.07	9.06E+00	32	0	0.09
try-b	2	2.07E-15	10	3	0.05	2.07E-15	26	25	0.05	2.07E-15	10	3	0.06
twobars	2	1.51E+00	9	0	0.05	1.51E+00	9	0	0.08	1.51E+00	9	0	0.07
ubh1	17997	1.12E+00	5	0	0.41	1.12E+00	5	0	0.4	1.12E+00	5	0	0.61
ubh5	19997	1.12E+00	5	0	0.48	1.12E+00	5	0	0.46	1.12E+00	5	0	0.76
vardim	100	7.27E-27	25	0	0.07	7.27E-27	25	0	0.07	0.00E+00	25	0	0.11
watson	31	7.02E-13	12	12	0.07	4.15E-06	12	3	0.05	4.09E-06	12	1	0.07
weeds	3	9.21E+03	19	1	0.06	9.21E+03	18	8	0.05	9.21E+03	18	8	0.06
woods	10000	6.85E-15	40	5	0.56	6.85E-15	40	5	0.58	6.85E-15	40	5	0.79
yao	2002	1.96E+02	27	0	0.18	1.96E+02	27	0	0.19	1.96E+02	27	0	0.25
yfit	3	6.69E-13	47	4	0.05	6.69E-13	47	4	0.06	6.69E-13	47	4	0.07
yfitu	3	6.67E-13	36	4	0.05	6.67E-13	36	4	0.06	6.67E-13	36	4	0.07
zangwil2	2	-1.82E+01	1	0	0.05	-1.82E+01	1	0	0.06	-1.82E+01	1	0	0.06
zangwil3	3	0.00E+00	1	0	0.06	0.00E+00	2	1	0.06	0.00E+00	1	0	0.06
zecevic2	2	-4.12E+00	8	0	0.06	-4.12E+00	8	0	0.06	-4.12E+00	8	0	0.07
zecevic3	2	9.73E+01	16	3	0.06	9.73E+01	14	6	0.06	9.73E+01	16	3	0.07
zecevic4	2	7.56E+00	10	0	0.07	7.56E+00	10	0	0.06	7.56E+00	10	0	0.07
zigzag	64	3.16E+00	27	17	0.08	3.16E+00	40	16	0.07	3.16E+00	41	13	0.09
zy2	3	2.00E+00	9	5	0.05	2.00E+00	10	4	0.06	2.00E+00	10	4	0.07
s201	2	0.00E+00	1	0	0.08	0.00E+00	1	0	0.11	0.00E+00	1	0	0.09
s202	2	4.90E+01	7	0	0.04	4.90E+01	7	0	0.05	4.90E+01	7	0	0.04
s203	5	1.74E-18	4	0	0.05	1.74E-18	4	0	0.06	1.74E-18	4	0	0.04
s204	2	1.84E-01	4	0	0.04	1.84E-01	4	0	0.06	1.84E-01	4	0	0.04
s205	2	2.15E-21	11	7	0.04	2.91E-25	11	6	0.06	2.91E-25	11	6	0.04
s206	2	3.08E-29	4	0	0.05	3.08E-29	4	0	0.05	3.08E-29	4	0	0.04
s207	2	1.40E-24	7	0	0.04	1.40E-24	7	0	0.06	1.40E-24	7	0	0.04
s208	2	3.74E-21	21	0	0.04	3.74E-21	21	0	0.05	3.74E-21	21	0	0.04
s209	2	6.18E-17	79	0	0.04	6.18E-17	79	0	0.05	7.69E-29	80	0	0.04
s210	2	4.25E-19	348	0	0.05	4.25E-19	348	0	0.06	7.30E-19	346	0	0.05
s211	2	1.75E-24	27	0	0.04	1.75E-24	27	0	0.05	1.75E-24	27	0	0.04
s212	2	1.16E-22	11	6	0.04	1.16E-22	11	6	0.05	1.16E-22	11	6	0.04
s213	2	1.10E-09	29	0	0.04	1.10E-09	29	0	0.05	1.10E-09	29	0	0.04
s215	2	1.26E-07	8	0	0.05	1.26E-07	8	0	0.05	1.26E-07	8	0	0.05
s216	2	9.99E-01	6	0	0.06	9.99E-01	6	0	0.05	9.99E-01	6	0	0.04
s217	2	-8.00E-01	9	0	0.05	-8.00E-01	9	0	0.05	-8.00E-01	9	0	0.04
s219	4	-1.00E+00	60	28	0.05	-1.00E+00	21	0	0.07	-1.00E+00	21	0	0.05
s220	2	1.00E+00	29	0	0.06	1.00E+00	31	15	0.05	1.00E+00	29	0	0.05
s221	2	-	-	-	-	-1.00E+00	35	20	0.05	-1.00E+00	65	10	0.04
s222	2	-1.50E+00	6	0	0.06	-1.50E+00	6	0	0.05	-1.50E+00	6	0	0.05
s223	2	-8.34E-01	9	0	0.05	-8.34E-01	9	0	0.04	-8.34E-01	9	0	0.04
s224	2	-3.04E+02	9	0	0.05	-3.04E+02	9	0	0.05	-3.04E+02	9	0	0.05
s225	2	2.00E+00	10	0	0.06	2.00E+00	10	0	0.07	2.00E+00	10	0	0.05

s226	2	-5.00E-01	8	0	0.05	-5.00E-01	8	0	0.05	-5.00E-01	8	0	0.05
s227	2	1.00E+00	7	0	0.05	1.00E+00	7	0	0.04	1.00E+00	7	0	0.04
s228	2	-3.00E+00	8	0	0.04	-3.00E+00	8	0	0.05	-3.00E+00	8	0	0.05
s229	2	8.28E-15	21	0	0.04	8.28E-15	21	0	0.05	8.28E-15	21	0	0.05
s230	2	3.75E-01	9	3	0.04	3.75E-01	10	0	0.05	3.75E-01	10	0	0.05
s231	2	2.99E-14	27	0	0.05	2.99E-14	27	0	0.05	2.99E-14	27	0	0.05
s232	2	-1.00E+00	7	4	0.04	-1.00E+00	7	4	0.05	-1.00E+00	7	4	0.05
s233	2	2.43E-14	9	0	0.04	2.43E-14	9	0	0.05	2.43E-14	9	0	0.04
s234	2	-8.00E-01	12	0	0.05	-8.00E-01	12	0	0.05	-8.00E-01	12	0	0.04
s235	3	-	-	-	-	-	-	-	-	4.00E-02	39	1	0.04
s236	2	-8.20E+00	19	14	0.06	-8.20E+00	12	4	0.04	-8.20E+00	29	24	0.05
s237	2	-5.89E+01	29	5	0.05	-5.89E+01	30	14	0.05	-5.89E+01	29	5	0.05
s238	2	-8.20E+00	41	19	0.05	-8.20E+00	27	24	0.05	-	-	-	-
s239	2	-8.20E+00	19	12	0.05	-5.89E+01	18	7	0.05	-5.89E+01	22	13	0.05
s240	3	1.62E-27	1	0	0.05	1.62E-27	1	0	0.04	1.62E-27	1	0	0.05
s241	8	1.14E-16	11	3	0.05	1.83E-18	10	4	0.04	4.85E-13	12	0	0.05
s242	3	9.63E-08	17	7	0.05	5.06E-08	24	1	0.04	5.06E-08	24	1	0.05
s243	3	7.97E-01	4	0	0.05	7.97E-01	4	0	0.04	7.97E-01	4	0	0.05
s244	3	2.44E-07	13	0	0.05	2.44E-07	13	0	0.04	2.44E-07	13	0	0.05
s245	3	1.59E-14	11	8	0.05	4.95E-13	8	0	0.05	4.95E-13	8	0	0.05
s246	3	1.04E-21	10	0	0.05	1.04E-21	10	0	0.04	1.04E-21	10	0	0.05
s247	4	1.72E-16	15	0	0.05	1.72E-16	15	0	0.06	1.72E-16	15	0	0.05
s248	3	-8.00E-01	15	5	0.05	-8.00E-01	15	5	0.04	-8.00E-01	15	5	0.05
s249	3	1.00E+00	7	0	0.05	1.00E+00	7	0	0.04	1.00E+00	7	0	0.05
s250	3	-3.30E+03	14	11	0.05	-3.30E+03	14	11	0.04	-3.30E+03	14	11	0.05
s251	3	-3.46E+03	12	9	0.05	-3.46E+03	12	9	0.04	-3.46E+03	12	9	0.05
s252	3	4.00E-02	20	0	0.05	4.00E-02	20	1	0.05	4.00E-02	20	0	0.07
s253	3	6.93E+01	14	0	0.05	6.93E+01	14	0	0.06	6.93E+01	14	0	0.05
s254	3	-1.73E+00	7	0	0.05	-1.73E+00	8	6	0.07	-1.73E+00	7	7	0.05
s256	4	1.71E-10	17	0	0.05	1.71E-10	17	0	0.06	1.71E-10	17	0	0.05
s257	4	7.54E-17	16	6	0.05	7.54E-17	17	5	0.04	7.54E-17	17	5	0.05
s258	4	2.74E-18	40	5	0.05	2.74E-18	40	5	0.04	2.74E-18	40	5	0.05
s259	4	-8.54E+00	11	0	0.05	-8.54E+00	11	0	0.04	-8.54E+00	11	0	0.05
s260	4	2.74E-18	40	5	0.05	2.74E-18	40	5	0.05	2.74E-18	40	5	0.05
s261	4	6.37E-10	14	0	0.05	6.37E-10	14	0	0.04	6.37E-10	14	0	0.05
s262	4	-1.00E+01	8	0	0.05	-1.00E+01	8	0	0.04	-1.00E+01	8	0	0.05
s263	4	-1.00E+00	18	0	0.05	-1.00E+00	18	1	0.05	-1.00E+00	18	0	0.05
s264	4	-4.41E+01	9	0	0.05	-4.41E+01	9	0	0.04	-4.41E+01	9	0	0.05
s265	4	1.90E+00	6	8	0.04	1.90E+00	6	8	0.04	1.90E+00	6	8	0.05
s266	5	1.00E+00	7	0	0.05	1.00E+00	7	0	0.05	1.00E+00	7	0	0.07
s267	5	1.42E-18	33	32	0.05	1.50E-02	31	4	0.04	1.50E-02	31	4	0.05
s268	5	1.63E-07	14	0	0.04	1.63E-07	14	0	0.05	1.63E-07	14	0	0.05
s269	5	4.09E+00	1	0	0.05	4.09E+00	1	0	0.04	4.09E+00	1	0	0.04
s270	5	9.03E-08	15	15	0.05	9.22E-08	21	1	0.09	9.22E-08	21	1	0.04
s271	6	1.23E-30	1	0	0.05	1.23E-30	1	0	0.06	1.23E-30	1	0	0.04
s272	6	1.53E-14	75	81	0.07	5.66E-03	19	6	0.06	5.66E-03	19	6	0.04
s273	6	7.01E-18	10	0	0.07	7.01E-18	10	0	0.05	7.01E-18	10	0	0.04
s274	2	1.05E-30	1	0	0.07	1.05E-30	1	0	0.04	1.05E-30	1	0	0.04
s275	4	1.64E-28	1	0	0.07	1.64E-28	1	0	0.04	1.64E-28	1	0	0.04
s276	6	6.40E-25	1	0	0.07	6.40E-25	1	0	0.05	6.40E-25	1	0	0.04
s277	4	5.08E+00	10	0	0.07	5.08E+00	10	0	0.05	5.08E+00	10	0	0.04
s278	6	7.84E+00	11	0	0.07	7.84E+00	11	0	0.06	7.84E+00	11	0	0.04
s279	8	1.06E+01	10	0	0.07	1.06E+01	10	0	0.05	1.06E+01	10	0	0.04
s280	10	1.34E+01	12	0	0.06	1.34E+01	12	0	0.06	1.34E+01	12	0	0.07
s282	10	1.27E-18	60	2	0.06	1.27E-18	60	2	0.06	1.27E-18	60	2	0.09
s283	10	1.23E-10	35	0	0.05	1.23E-10	35	0	0.05	1.23E-10	35	0	0.09
s286	20	3.74E-20	21	0	0.05	3.74E-20	21	0	0.04	3.74E-20	21	0	0.06
s287	20	1.37E-17	40	5	0.05	1.37E-17	40	5	0.04	1.37E-17	40	5	0.05
s288	20	8.54E-10	17	0	0.05	8.54E-10	17	0	0.04	8.54E-10	17	0	0.05
s289	30	0.00E+00	8	6	0.05	0.00E+00	8	6	0.05	0.00E+00	8	6	0.04
s290	2	0.00E+00	1	0	0.05	0.00E+00	1	0	0.04	0.00E+00	1	0	0.04
s291	10	3.82E-31	1	0	0.05	3.82E-31	1	0	0.04	3.82E-31	1	0	0.04
s292	30	4.62E-30	1	0	0.05	4.62E-30	1	0	0.04	4.62E-30	1	0	0.06
s293	50	7.64E-30	1	0	0.05	7.64E-30	1	0	0.04	7.64E-30	1	0	0.05
s294	6	3.97E+00	19	3	0.05	3.97E+00	19	3	0.04	3.97E+00	19	3	0.04
s295	10	3.99E+00	29	7	0.05	1.54E-16	39	10	0.04	1.54E-16	39	10	0.05
s296	16	3.99E+00	38	7	0.11	3.91E-19	47	10	0.04	3.91E-19	47	10	0.04
s297	30	4.59E-27	60	0	0.07	4.59E-27	60	0	0.04	4.59E-27	60	0	0.05
s298	50	2.28E-21	89	0	0.06	2.28E-21	89	0	0.05	2.28E-21	89	0	0.04
s299	100	1.30E-20	162	0	0.06	1.30E-20	162	0	0.06	1.30E-20	162	0	0.06
s300	20	-2.00E+01	1	0	0.08	-2.00E+01	1	0	0.04	-2.00E+01	1	0	0.05
s301	50	-5.00E+01	1	0	0.05	-5.00E+01	1	0	0.06	-5.00E+01	1	0	0.04
s302	100	-1.00E+02	1	0	0.05	-1.00E+02	1	0	0.06	-1.00E+02	1	0	0.04
s303	20	1.12E-32	11	0	0.05	1.12E-32	11	0	0.07	1.12E-32	11	0	0.04
s304	50	1.62E-20	15	0	0.05	1.62E-20	15	0	0.05	1.62E-20	15	0	0.04
s305	100	1.24E-38	19	0	0.07	1.24E-38	19	0	0.06	1.24E-38	19	0	0.06
s307	2	1.24E+02	12	0	0.05	1.24E+02	12	0	0.04	1.24E+02	12	0	0.04
s308	2	7.73E-01	9	0	0.04	7.73E-01	9	0	0.04	7.73E-01	9	0	0.04
s309	2	2.89E-01	7	0	0.04	2.89E-01	7	0	0.04	2.89E-01	7	0	0.05
s311	2	5.80E-25	6	5	0.04	3.18E-17	7	4	0.04	3.18E-17	7	4	0.05
s312	2	5.92E+00	19	0	0.04	5.92E+00	19	0	0.04	5.92E+00	19	0	0.07
s314	2	1.69E-01	3	0	0.06	1.69E-01	3	0	0.04	1.69E-01	3	0	0.07
s315	2	-8.00E-01	13	8	0.07	-8.00E-01	12	6	0.04	-8.00E-01	12	6	0.07
s316	2	3.34E+02	7	8	0.07	3.34E+02	7	8	0.04	3.34E+02	6	0	0.07
s317	2	3.72E+02	9	8	0.07	3.72E+02	9	8	0.04	3.72E+02	7	0	0.07
s318	2	4.13E+02	10	8	0.06	4.13E+02	10	8	0.04	4.13E+02	7	0	0.04
s319	2	4.52E+02	11	8	0.07	4.52E+02	11	8	0.04	4.52E+02	8	0	0.04
s320	2	4.86E+02	13	8	0.07	4.86E+02	13	8	0.04	4.86E+02	9	0	0.04
s321	2	4.96E+02	14	10	0.06	4.96E+02	16	9	0.04	4.96E+02	11	0	0.04
s322	2	5.00E+02	38	32	0.05	5.00E+02	23	13	0.04	5.00E+02	16	0	0.04
s323	2	3.80E+00	7	0	0.05	3.80E+00	7	0	0.07	3.80E+00	7	0	0.04
s324	2	5.00E+00	13	0	0.05	5.00E+00	14	3	0.04	5.00E+00	13	0	0.04
s325	2	3.79E+00	8	0	0.05	3.79E+00	9	4	0.05	3.79E+00	8	0	0.04
s326	2	-7.98E+01	12	3	0.05	-7.98E+01	10	4	0.06	-7.98E+01	12	3	0.04
s327	2	3.06E-02	18	2	0.05	3.06E-02	22	4	0.04	3.06E-02	22	4	0.04
s328	2	1.74E+00	16	0	0.05	1.74E+00	16	0	0.04	1.74E+00	16	0	0.04
s329	2	-6.96E+03	16	9	0.05	-6.96E+03	16	9	0.04	-6.96E+03	16	9	0.04

s330	2	1.62E+00	10	0	0.08	1.62E+00	10	0	0.05	1.62E+00	10	0	0.05
s331	2	4.26E+00	6	0	0.06	4.26E+00	6	0	0.05	4.26E+00	6	0	0.07
s333	3	4.33E-02	7	3	0.05	4.33E-02	7	0	0.04	4.33E-02	7	0	0.06
s334	3	8.21E-03	7	5	0.05	8.21E-03	8	0	0.05	8.21E-03	8	0	0.06
s335	3	-4.47E-03	26	0	0.05	-4.47E-03	26	0	0.05	-4.47E-03	26	0	0.05
s336	3	-3.38E-01	17	12	0.05	-3.38E-01	18	11	0.05	-3.38E-01	25	0	0.05
s337	3	6.00E+00	7	0	0.06	6.00E+00	7	0	0.05	6.00E+00	7	0	0.05
s338	3	-7.21E+00	13	18	0.05	-7.21E+00	19	20	0.05	-7.21E+00	11	9	0.05
s339	3	3.36E+00	8	0	0.05	3.36E+00	8	0	0.05	3.36E+00	8	0	0.05
s340	3	-5.40E-02	8	3	0.06	-5.40E-02	8	4	0.05	-5.40E-02	8	3	0.05
s341	3	-2.26E+01	7	0	0.05	-2.26E+01	10	4	0.04	-2.26E+01	7	0	0.05
s342	3	-2.26E+01	12	0	0.05	-2.26E+01	13	6	0.05	-2.26E+01	12	0	0.05
s343	3	-5.68E+00	13	1	0.05	-5.68E+00	13	1	0.06	-5.68E+00	13	1	0.05
s344	3	3.26E-02	6	0	0.06	3.26E-02	6	0	0.04	3.26E-02	6	0	0.05
s345	3	3.26E-02	9	0	0.05	3.26E-02	9	0	0.04	3.26E-02	9	0	0.05
s346	3	-5.68E+00	13	1	0.05	-5.68E+00	13	1	0.04	-5.68E+00	13	1	0.05
s348	3	3.70E+01	14	0	0.04	3.70E+01	14	0	0.04	3.70E+01	14	0	0.04
s350	4	3.08E-04	8	5	0.05	3.08E-04	10	1	0.04	3.08E-04	10	1	0.04
s351	4	3.19E+02	10	7	0.07	3.19E+02	11	2	0.04	3.19E+02	11	2	0.04
s352	4	9.03E+02	1	0	0.07	9.03E+02	1	0	0.04	9.03E+02	1	0	0.04
s353	4	-3.99E+01	7	0	0.07	-3.99E+01	7	0	0.05	-3.99E+01	7	0	0.04
s354	4	1.14E-01	10	0	0.05	1.14E-01	10	0	0.04	1.14E-01	10	0	0.04
s355	4	6.97E+01	47	35	0.05	6.97E+01	49	24	0.04	6.97E+01	49	24	0.05
s356	4	1.88E+00	15	10	0.05	1.88E+00	40	11	0.04	1.88E+00	40	11	0.04
s357	4	3.58E-01	10	0	0.05	3.58E-01	10	0	0.05	3.58E-01	10	0	0.05
s358	5	5.46E-05	24	7	0.04	5.46E-05	20	0	0.04	5.46E-05	20	0	0.04
s359	5	-5.50E+06	16	0	0.04	-5.50E+06	16	0	0.04	-5.50E+06	16	0	0.04
s360	5	-5.28E+06	22	21	0.04	-5.28E+06	35	22	0.04	-5.28E+06	35	22	0.04
s361	5	-1.53E+04	18	5	0.05	-1.53E+04	26	1	0.05	-1.53E+04	26	1	0.05
s365	7	5.21E+01	14	4	0.08	-	-	-	-	5.22E+01	24	8	0.05
s366	7	1.23E+03	20	3	0.08	1.23E+03	20	3	0.05	1.23E+03	20	3	0.05
s367	7	-	-	-	-	-3.74E+01	16	9	0.05	-3.74E+01	13	0	0.05
s368	8	-1.42E-14	13	20	0.07	1.07E-14	5	0	0.05	-7.11E-15	5	0	0.05
s369	8	7.05E+03	12	0	0.07	7.05E+03	12	0	0.05	7.05E+03	12	0	0.05
s370	6	2.29E+03	12	0	0.05	2.29E+03	12	0	0.05	2.29E+03	12	0	0.05
s371	9	1.40E+06	12	0	0.05	1.40E+06	12	0	0.07	1.40E+06	12	0	0.05
s372	9	-	-	-	-	-	-	-	-	1.10E+05	28	0	0.05
s373	9	1.34E+04	3	0	0.04	1.34E+04	3	0	0.07	1.34E+04	3	0	0.05
s374	10	2.33E-01	54	69	0.07	2.33E-01	60	11	0.07	2.33E-01	39	2	0.06
s375	10	-1.52E+01	19	18	0.05	-1.52E+01	19	19	0.05	-1.52E+01	19	18	0.06
s377	10	-7.95E+02	23	0	0.05	-7.95E+02	23	0	0.08	-7.95E+02	23	0	0.06
s378	10	-4.78E+01	22	12	0.07	-4.74E+01	27	9	0.07	-	-	-	-
s379	11	4.01E-02	18	12	0.05	-	-	-	-	-	-	-	-
s380	12	3.17E+00	69	13	0.06	3.17E+00	45	1	0.06	3.17E+00	56	0	0.05
s381	13	1.01E+00	10	0	0.06	1.01E+00	10	0	0.05	1.01E+00	10	0	0.05
s382	13	1.04E+00	10	0	0.05	1.04E+00	10	0	0.05	1.04E+00	10	0	0.05
s383	14	7.29E+05	10	0	0.05	7.29E+05	10	0	0.05	7.29E+05	10	0	0.05
s386	2	0.00E+00	1	0	0.05	0.00E+00	1	0	0.05	0.00E+00	1	0	0.05
s387	15	-8.25E+03	17	10	0.05	-8.25E+03	17	10	0.05	-8.25E+03	21	12	0.05
s388	15	-5.82E+03	62	76	0.06	-5.82E+03	30	10	0.04	-5.82E+03	63	36	0.05
s389	15	-5.81E+03	182	254	0.08	-5.81E+03	40	18	0.05	-5.81E+03	33	14	0.05
s392	33	-1.10E+06	34	0	0.06	-1.10E+06	34	0	0.04	-1.10E+06	34	0	0.05
s393	48	8.63E-01	27	18	0.06	1.03E+00	14	2	0.05	1.03E+00	14	2	0.06
s394	20	1.92E+00	14	9	0.05	4.97E+00	13	0	0.04	4.97E+00	13	0	0.05
s395	50	1.92E+00	14	11	0.04	1.92E+00	14	3	0.04	1.92E+00	14	3	0.05
IEEE_57	738	8.96E-05	20	0	0.16	8.96E-05	20	0	0.12	8.96E-05	20	0	0.17
IEEE_162	369	1.64E+00	109	132	0.85	1.64E+00	23	0	0.2	1.64E+00	23	0	0.18
IEEE_300	3910	1.17E-02	34	17	0.82	1.17E-02	31	0	0.55	1.17E-02	31	0	0.58

Table A2: Percentage of steps accepted by different criteria in the filter.

Problem	IBR			IFRd			IFRt		
	SAC	SRCO	SRCC	SAC	SRCO	SRCC	SAC	SRCO	SRCC
aircfta	0	0	100	0	0	100	0	0	100
aircftb	92	8	0	94	6	0	94	6	0
airport	27	0	73	27	0	73	27	0	73
aljazzaf	3	47	50	6	48	45	-	-	-
allinit	91	0	9	82	0	18	82	9	9
allinitc	25	18	57	27	12	62	27	23	50
alsotame	63	25	13	63	25	13	63	25	13
argtrig	0	0	100	0	0	100	0	0	100
aug2d	0	0	100	0	0	100	0	0	100
aug2dc	92	0	8	92	0	8	92	0	8
aug2dcqp	48	33	19	48	33	19	48	33	19
aug2dqp	38	31	31	38	31	31	38	31	31
aug3d	0	100	0	0	100	0	0	100	0
aug3dc	0	100	0	0	100	0	0	100	0
aug3dcqp	65	35	0	65	35	0	65	35	0
aug3dqp	67	33	0	67	33	0	67	33	0
avgasa	56	11	33	56	11	33	56	11	33
avgasb	73	0	27	73	0	27	73	0	27
avion2	38	38	25	34	47	19	-	-	-
bdvalue	-	-	-	-	-	-	-	-	-
biggs3	100	0	0	100	0	0	100	0	0
biggs5	100	0	0	100	0	0	100	0	0
biggsb1	92	8	0	92	8	0	92	8	0
biggsb4	91	4	4	91	5	5	91	5	5
blockqp1	90	10	0	90	10	0	90	10	0
blockqp2	89	11	0	89	11	0	89	11	0
blockqp3	92	8	0	92	8	0	92	8	0
blockqp4	89	11	0	89	11	0	89	11	0
blockqp5	93	7	0	87	13	0	87	13	0
bloweya	88	13	0	88	13	0	88	13	0
bloweyb	83	17	0	83	17	0	83	17	0
bloweyc	90	10	0	90	10	0	90	10	0
booth	0	0	100	0	0	50	0	0	100
box2	100	0	0	100	0	0	100	0	0
bqp1var	100	0	0	100	0	0	100	0	0
bqpgabim	100	0	0	100	0	0	100	0	0
brainpc2	0	72	28	-	-	-	-	-	-
brainpc7	0	95	5	-	-	-	-	-	-
brainpc9	0	100	0	-	-	-	-	-	-
bratu2d	0	0	100	0	0	100	0	0	100
bratu2dt	0	0	100	0	0	100	0	0	100
bratu3d	0	0	100	0	0	100	0	0	100
broydn3d	0	0	100	0	0	100	0	0	100
broydnbd	0	0	100	0	0	100	0	0	100
bt1	0	71	29	0	71	29	0	67	33
bt10	0	0	100	0	0	100	0	0	100
bt11	0	43	57	0	43	57	0	43	57
bt12	0	25	75	0	25	75	0	25	75
bt13	0	41	59	0	41	59	0	41	59
bt2	0	92	8	0	92	8	0	92	8
bt3	0	100	0	0	100	0	0	100	0
bt4	0	33	67	0	33	67	0	33	67
bt5	0	14	86	0	33	67	0	14	86
bt6	15	62	23	15	62	23	15	62	23
bt7	-	-	-	0	38	62	-	-	-
bt8	0	100	0	0	100	0	0	100	0
bt9	0	9	91	0	5	95	0	5	95
byrdsphr	0	18	82	0	18	82	0	18	82
camel6	82	18	0	100	0	0	100	0	0
cantilvr	0	69	31	0	69	31	0	69	31
catena	0	20	80	0	31	69	0	30	70
catenary	0	19	81	0	15	85	0	15	85
cb2	0	44	56	0	44	56	0	44	56
cb3	0	67	33	0	67	33	0	67	33
cbratu2d	0	0	100	0	0	100	0	0	100
cbratu3d	0	0	100	0	0	100	0	0	100
chaconn1	0	57	43	0	57	43	0	57	43
chaconn2	0	71	29	0	71	29	0	71	29
chandheq	0	100	0	0	100	0	0	100	0
chemrcta	-	-	-	-	-	-	0	17	83
chenhark	100	0	0	100	0	0	100	0	0
clnlbeam	70	30	0	65	23	12	60	27	13
cluster	0	0	100	0	0	100	0	0	100
concon	11	33	56	11	33	56	11	33	56
congigmz	0	40	60	0	40	60	0	44	56
coolhans	0	0	100	0	0	100	0	0	100
core2	-	-	-	4	42	54	-	-	-
coshfun	0	58	42	-	-	-	-	-	-
csfi1	0	86	14	6	72	22	7	71	21
csfi2	-	-	-	-	-	-	3	60	38
cvxqp1	18	13	68	18	13	68	18	13	68
cvxqp2	5	35	59	5	35	59	5	35	59
cvxqp3	7	0	93	7	0	93	7	0	93
deconvc	19	65	16	0	95	5	0	95	5
degenlpa	43	25	32	43	25	32	43	25	32
degenlpb	16	6	77	16	6	77	16	6	77
demyalo	0	41	59	0	67	33	0	41	59
dipigri	8	67	25	8	67	25	8	67	25
dittert	9	91	0	13	78	9	13	78	9
dixchlng	11	44	44	11	44	44	11	44	44
dixchlnv	0	94	0	0	94	0	0	94	0
dnieper	7	10	83	7	10	83	7	10	83
dracvty1	99	1	1	-	-	-	-	-	-

drcavty2	48	52	1	-	-	-	-	-	-
drcavty3	92	7	1	-	-	-	-	-	-
dtoc1l	83	17	0	83	17	0	83	17	0
dtoc1na	17	50	33	17	50	33	17	50	33
dtoc1nb	20	20	60	20	20	60	20	20	60
dtoc1nc	6	71	24	13	63	25	5	74	21
dtoc1nd	5	82	14	2	82	16	1	89	10
dtoc2	0	70	30	0	50	50	0	50	50
dtoc3	0	0	100	0	0	100	0	0	100
dtoc4	0	33	67	0	33	67	0	33	67
dtoc5	0	0	100	0	0	100	0	0	100
dtoc6	0	0	100	0	0	100	0	0	100
dual1	85	15	0	85	15	0	85	15	0
dual2	91	0	9	91	0	9	91	0	9
dual3	90	0	10	90	0	10	90	0	10
dual4	90	10	0	90	10	0	90	10	0
dualc1	10	67	23	10	67	23	10	67	23
dualc2	19	57	24	19	57	24	19	57	24
dualc5	33	25	42	33	25	42	33	25	42
dualc8	25	6	69	25	6	69	25	6	69
eg3	0	100	0	0	96	4	0	96	4
eigena2	50	0	0	50	0	0	50	0	0
eigenaco	67	0	0	50	0	0	50	0	0
eigenb2	50	0	0	50	0	0	50	0	0
eigenbco	42	57	1	50	0	50	50	0	50
eigenc2	5	95	0	3	75	22	1	55	44
eigencco	25	75	0	11	89	0	11	89	0
eigmaxb	0	55	36	0	55	27	0	55	27
eigmaxc	0	63	13	0	63	13	0	63	13
eigminb	0	73	9	0	73	9	0	73	9
eigminc	0	50	30	0	40	40	0	50	30
expflia	97	3	0	97	3	0	97	3	0
expflib	94	6	0	94	6	0	94	6	0
expfltc	95	5	0	95	5	0	95	4	1
expquad	90	10	0	55	45	0	55	45	0
extrasim	80	20	0	80	20	0	80	20	0
fccu	0	100	0	0	100	0	0	100	0
fletcher	-	-	-	26	21	47	-	-	-
gausselm	-	-	-	47	47	7	47	47	7
genhs28	0	100	0	0	100	0	0	100	0
gigomez1	0	44	56	0	44	56	0	44	56
gilbert	0	11	89	0	11	89	0	27	73
goffin	86	0	14	83	0	17	83	0	17
gottfr	0	0	100	0	0	100	0	0	100
gouldqp2	67	33	0	67	33	0	67	33	0
gouldqp3	67	33	0	67	33	0	67	33	0
gpp	6	83	11	6	83	11	6	83	11
gridneta	50	14	36	50	14	36	50	14	36
gridnetb	0	0	100	0	0	100	0	0	100
gridnetc	75	25	0	75	25	0	75	25	0
gridnetd	48	26	26	48	26	26	48	26	26
gridnete	40	40	20	40	40	20	40	40	20
gridnetf	75	25	0	75	25	0	75	25	0
gridnetg	12	24	65	18	18	65	18	18	65
gridneth	50	33	17	67	17	17	67	17	17
gridneti	85	8	8	85	8	8	85	8	8
hadamard	50	0	50	50	0	50	43	14	43
hager1	0	0	100	0	0	100	0	0	100
hager2	0	0	100	0	0	100	0	0	100
hager3	0	0	100	0	0	100	0	0	100
hager4	86	14	0	86	14	0	86	14	0
haifam	1	65	33	1	52	47	1	66	33
haifas	7	32	61	0	63	37	0	63	37
haldmads	3	81	16	-	-	-	1	53	46
hatfdb	100	0	0	100	0	0	100	0	0
hatfdc	100	0	0	100	0	0	100	0	0
hatfdg	0	0	100	0	0	100	0	0	100
hatfdh	86	7	7	86	7	7	86	7	7
heart6	0	0	100	0	0	100	0	0	100
heart8	0	0	100	0	0	100	0	0	100
himmelba	0	0	100	0	0	50	0	0	100
himmelbc	0	0	100	0	0	100	0	0	100
himmelbe	0	0	100	0	0	67	0	0	100
himmelbi	94	6	0	94	6	0	94	6	0
himmelbk	0	83	17	0	83	17	0	83	17
himmelp1	92	8	0	94	6	0	94	6	0
himmelp2	0	78	22	0	91	9	0	85	15
himmelp3	15	77	8	15	77	8	15	77	8
himmelp4	7	87	7	7	87	7	7	87	7
himmelp5	0	100	0	0	84	16	0	100	0
himmelp6	13	88	0	13	88	0	13	88	0
hong	85	15	0	85	15	0	85	15	0
hs001	100	0	0	100	0	0	100	0	0
hs002	91	9	0	91	9	0	91	9	0
hs003	100	0	0	100	0	0	100	0	0
hs004	100	0	0	100	0	0	100	0	0
hs005	88	13	0	88	13	0	88	13	0
hs006	0	50	50	0	75	25	0	50	50
hs007	30	40	30	0	20	80	30	40	30
hs008	0	0	100	0	0	100	0	0	100
hs009	100	0	0	100	0	0	100	0	0
hs010	0	20	80	0	20	80	0	20	80
hs011	13	38	50	13	38	50	13	38	50
hs012	9	27	64	9	27	64	9	27	64
hs013	48	29	23	61	30	9	48	29	23
hs014	0	57	43	0	57	43	0	57	43
hs015	20	47	33	17	58	25	16	74	11

hs016	18	64	18	18	64	18	18	64	18
hs017	0	95	5	0	95	5	0	95	5
hs018	0	67	33	8	54	38	0	67	33
hs019	13	47	40	11	39	50	13	47	40
hs020	17	75	8	17	75	8	17	75	8
hs021	78	11	11	78	11	11	78	11	11
hs022	0	71	29	0	71	29	0	71	29
hs023	0	100	0	0	100	0	0	100	0
hs024	100	0	0	100	0	0	100	0	0
hs025	97	3	0	94	6	0	94	6	0
hs026	6	94	0	6	94	0	6	94	0
hs027	-	-	-	5	43	52	-	-	-
hs028	100	0	0	100	0	0	100	0	0
hs029	9	73	18	9	73	18	9	73	18
hs030	21	21	57	21	21	57	21	21	57
hs031	0	86	14	0	86	14	0	86	14
hs032	17	83	0	17	83	0	17	83	0
hs033	11	89	0	11	89	0	11	89	0
hs034	11	67	22	11	67	22	11	67	22
hs035	100	0	0	100	0	0	100	0	0
hs036	100	0	0	100	0	0	100	0	0
hs037	100	0	0	100	0	0	100	0	0
hs039	0	9	91	0	5	95	0	5	95
hs040	0	0	100	0	0	100	0	0	100
hs041	80	0	20	80	0	20	80	0	20
hs042	0	17	83	0	17	83	0	17	83
hs043	11	33	56	11	33	56	11	33	56
hs044	100	0	0	100	0	0	100	0	0
hs046	6	94	0	6	94	0	6	94	0
hs047	6	94	0	6	94	0	6	94	0
hs048	100	0	0	100	0	0	100	0	0
hs049	100	0	0	100	0	0	100	0	0
hs050	100	0	0	100	0	0	89	11	0
hs051	100	0	0	100	0	0	100	0	0
hs052	0	100	0	0	100	0	0	100	0
hs053	33	67	0	33	67	0	50	50	0
hs054	86	14	0	86	14	0	86	14	0
hs055	71	14	14	71	14	14	71	14	14
hs056	8	54	38	4	54	42	8	54	38
hs057	5	90	5	5	80	15	5	80	15
hs059	3	63	35	0	94	6	7	61	32
hs060	0	100	0	0	100	0	0	100	0
hs061	20	10	70	11	11	78	0	20	80
hs062	100	0	0	100	0	0	100	0	0
hs063	0	29	71	13	25	63	0	29	71
hs064	6	65	29	6	65	29	6	65	29
hs065	0	80	20	0	80	20	0	80	20
hs066	0	86	14	0	86	14	0	86	14
hs067	25	75	0	25	75	0	17	83	0
hs070	9	83	9	28	61	11	28	61	11
hs071	0	63	38	0	63	38	0	63	38
hs072	0	0	100	0	0	100	0	0	100
hs073	13	88	0	13	88	0	13	88	0
hs074	11	11	78	11	11	78	11	11	78
hs075	25	38	38	25	38	38	25	38	38
hs076	100	0	0	100	0	0	100	0	0
hs077	0	75	25	0	75	25	0	75	25
hs078	0	0	100	0	0	100	0	0	100
hs079	0	100	0	0	100	0	0	100	0
hs080	0	33	67	0	33	67	0	33	67
hs081	0	33	67	0	29	71	0	25	75
hs083	27	33	40	27	33	40	27	33	40
hs084	11	79	11	11	79	11	11	79	11
hs085	0	64	36	0	64	36	0	64	36
hs086	100	0	0	100	0	0	100	0	0
hs087	0	29	71	0	29	71	0	29	71
hs088	13	38	50	11	17	72	8	21	71
hs089	8	23	69	17	23	60	13	32	55
hs090	11	37	53	10	38	52	14	32	55
hs091	12	31	58	10	15	75	2	28	70
hs092	16	42	42	6	38	56	6	38	56
hs095	11	68	21	9	70	22	9	70	22
hs096	11	72	17	11	72	17	11	72	17
hs097	16	47	37	14	48	38	14	48	38
hs098	10	61	29	17	57	26	17	57	26
hs099	0	57	43	0	57	43	0	57	43
hs100	8	67	25	8	67	25	8	67	25
hs100lnp	13	75	13	13	75	13	13	75	13
hs100mod	8	85	8	8	85	8	8	85	8
hs101	2	60	38	4	67	29	-	-	-
hs102	3	50	47	2	39	59	-	-	-
hs103	1	26	73	3	40	57	-	-	-
hs104	0	56	44	0	56	44	0	56	44
hs105	91	9	0	83	17	0	88	13	0
hs106	13	53	33	13	53	33	13	53	33
hs108	0	81	19	0	80	20	0	80	20
hs109	9	18	73	9	18	73	9	18	73
hs111	5	9	86	5	44	52	-	-	-
hs111lnp	5	9	86	4	7	89	-	-	-
hs112	71	29	0	71	29	0	71	29	0
hs113	9	91	0	9	91	0	9	91	0
hs114	0	84	16	0	84	16	0	84	16
hs116	20	72	8	20	72	8	20	72	8
hs117	4	96	0	4	96	0	4	96	0
hs118	45	55	0	45	55	0	45	55	0
hs119	63	38	0	63	38	0	63	38	0
hs21mod	85	0	15	85	0	15	85	0	15

hs268	93	7	0	93	7	0	93	7	0
hs35mod	100	0	0	100	0	0	100	0	0
hs3mod	100	0	0	100	0	0	100	0	0
hs44new	100	0	0	100	0	0	100	0	0
hs99exp	6	69	25	3	56	42	3	63	33
hubfit	100	0	0	100	0	0	100	0	0
hues-mod	92	4	4	92	4	4	92	4	4
huestis	25	4	71	25	4	71	25	4	71
hypcir	0	0	100	0	0	100	0	0	100
integreq	0	0	100	0	0	100	0	0	100
kiwcresc	0	27	73	0	27	73	0	27	73
ksip	91	9	0	91	9	0	91	9	0
lakes	7	80	13	13	56	31	6	63	31
lch	38	44	17	100	0	0	100	0	0
linspanh	54	38	8	73	20	7	73	20	7
liswet1	25	5	70	25	5	70	25	5	70
liswet10	81	1	18	81	1	18	81	1	18
liswet11	75	2	23	75	2	23	75	2	23
liswet12	81	1	18	81	1	18	81	1	18
liswet2	46	4	50	46	4	50	46	4	50
liswet3	44	0	56	44	0	56	44	0	56
liswet4	44	0	56	44	0	56	44	0	56
liswet5	44	7	48	44	7	48	44	7	48
liswet6	44	4	52	44	4	52	44	4	52
liswet7	11	6	83	11	6	83	11	6	83
liswet8	75	2	23	75	2	23	75	2	23
liswet9	70	2	28	70	2	28	70	2	28
lminsurf	0	50	50	0	50	50	0	50	50
loadbal	100	0	0	100	0	0	100	0	0
lootsma	11	89	0	11	89	0	11	89	0
lotschd	86	7	7	86	7	7	86	7	7
lstmmodoc	79	21	0	79	21	0	79	21	0
lsqfit	100	0	0	100	0	0	100	0	0
madsen	0	55	45	0	88	13	0	63	38
madseschj	13	46	40	7	63	30	7	67	26
makela1	0	81	19	0	73	27	0	73	27
makela2	0	57	43	0	57	43	0	57	43
makela3	8	22	69	12	19	69	12	19	69
makela4	86	14	0	86	14	0	86	14	0
manne	44	52	4	-	-	-	-	-	-
maratos	0	21	79	0	21	79	0	21	79
matrix2	0	100	0	0	100	0	0	100	0
maxlika	91	9	0	92	8	0	92	8	0
mconcon	0	40	60	0	40	60	0	40	60
mifflin1	6	25	69	6	25	69	6	25	69
mifflin2	-	-	-	0	63	38	0	63	38
minc44	0	71	29	0	75	25	0	62	38
minmaxbd	0	33	67	0	27	73	0	29	71
minmaxrb	44	44	11	44	44	11	44	44	11
minperm	0	17	67	0	0	50	0	50	50
minsurf	0	0	100	0	50	50	0	0	100
mistake	0	71	29	0	59	41	0	59	41
model	19	70	11	19	70	11	19	70	11
morebv	-	-	-	-	-	-	-	-	-
mosarqp1	85	15	0	85	15	0	85	15	0
mosarqp2	67	33	0	67	33	0	67	33	0
msqrta	0	0	100	0	0	100	0	0	100
msqrta	0	0	100	0	0	100	0	0	100
msqrta	0	0	100	0	0	100	0	0	100
mwright	0	57	43	0	57	43	0	57	43
ncvxqp1	100	0	0	100	0	0	100	0	0
ncvxqp2	100	0	0	100	0	0	83	17	0
ncvxqp3	100	0	0	-	-	-	63	37	0
ncvxqp4	100	0	0	100	0	0	100	0	0
ncvxqp5	100	0	0	100	0	0	100	0	0
ncvxqp6	100	0	0	-	-	-	100	0	0
ncvxqp7	100	0	0	100	0	0	100	0	0
ncvxqp8	100	0	0	100	0	0	100	0	0
ncvxqp9	100	0	0	-	-	-	57	43	0
ngone	0	80	20	0	68	32	0	73	27
nuffield_continuum	100	0	0	100	0	0	100	0	0
nuffield2	-	-	-	6	57	37	-	-	-
odfits	80	10	10	80	10	10	50	40	10
oet1	85	12	4	85	12	4	85	12	4
oet2	1	73	26	-	-	-	-	-	-
oet3	93	7	0	93	7	0	93	7	0
oet7	9	61	29	-	-	-	1	72	27
optcdeg2	48	40	12	48	40	12	48	40	12
optcdeg3	43	57	0	43	57	0	43	57	0
optcntrl	10	10	81	10	10	81	10	10	81
optmass	0	91	9	5	60	35	0	65	35
optprloc	0	95	5	0	95	5	0	95	5
orthdm2	0	60	40	0	60	40	0	60	40
orthdm2	0	0	100	0	13	87	-	-	-
orthrega	54	29	17	75	11	14	75	11	14
orthregb	0	50	50	0	50	50	0	0	100
orthregc	0	77	23	5	75	20	5	82	13
orthregd	0	75	25	0	56	44	0	88	13
orthrege	2	80	18	5	72	23	0	50	50
oslbqp	91	0	9	91	0	9	91	0	9
pentagon	93	7	0	94	6	0	94	6	0
polak4	3	59	38	2	56	42	2	56	42
polak5	0	82	18	0	82	18	0	82	18
polak6	0	41	59	0	59	41	0	51	49
porous1	0	0	100	0	0	100	0	0	100
porous2	0	0	100	0	0	100	0	0	100
portfl1	100	0	0	100	0	0	100	0	0
portfl2	100	0	0	100	0	0	100	0	0

portf3	100	0	0	100	0	0	100	0	0
portf4	100	0	0	100	0	0	100	0	0
portf6	100	0	0	100	0	0	100	0	0
powell20	1	37	62	1	37	62	1	37	62
powellbs	0	0	100	0	0	100	0	0	100
prodp10	33	20	47	33	20	47	33	20	47
prodp11	13	40	47	13	40	47	13	40	47
pspdoc	88	0	13	88	0	13	88	0	13
pt	89	5	5	89	5	5	89	5	5
qpcboei2	5	1	93	5	1	93	5	1	93
qpcstair	6	6	88	6	6	88	6	6	88
qpnstair	5	5	90	5	4	90	6	5	90
qrquad	96	4	0	98	3	0	98	3	0
reading1	5	95	0	5	95	0	5	95	0
reading2	80	20	0	80	20	0	80	20	0
reading3	15	10	75	15	10	75	15	10	75
recipe	0	0	100	0	0	67	0	0	100
res	45	27	27	45	27	27	45	27	27
rk23	11	63	22	7	75	18	0	96	4
robot	0	63	38	0	63	38	0	50	50
rosenmx	-	-	-	0	62	38	0	62	38
s32	7	80	13	7	80	13	7	80	13
s365mod	5	48	48	5	25	70	3	34	62
s368	92	8	0	80	20	0	80	20	0
semicon1	0	100	0	0	100	0	0	100	0
semicon2	0	100	0	0	100	0	0	100	0
simbap	86	14	0	86	14	0	86	14	0
simplpa	80	0	20	80	0	20	80	0	20
simplpb	75	0	25	75	0	25	75	0	25
simrosnb	20	80	0	20	80	0	20	80	0
sipow1	91	9	0	91	9	0	91	4	4
sipow1m	91	9	0	91	9	0	91	4	4
sipow2	96	4	0	96	4	0	100	0	0
sipow2m	96	0	4	96	0	4	96	0	4
sipow3	91	9	0	91	9	0	91	9	0
smbank	77	23	0	77	23	0	77	23	0
smmpsf	17	6	77	17	6	77	17	6	77
snake	14	14	71	14	29	57	14	14	71
sosqp2	77	8	15	77	8	15	77	8	15
spanhyd	-	-	-	68	28	3	65	31	5
sreadin3	50	33	17	50	33	17	50	33	17
sseblin	5	1	94	5	1	94	5	1	94
ssnlbeam	21	79	0	36	57	7	33	67	0
stancmin	50	0	50	50	0	50	50	0	50
static3	-	-	-	87	13	0	87	13	0
steenbra	43	0	57	43	0	57	39	4	57
steenbrb	69	11	20	70	4	26	68	5	27
steenbrd	-	-	-	-	-	-	51	14	35
steenbre	51	21	29	-	-	-	-	-	-
steenbrf	-	-	-	95	1	4	91	3	7
steenbrg	-	-	-	20	54	27	43	10	48
supersim	0	0	17	0	0	17	0	0	17
svanberg	5	60	35	5	60	35	5	60	35
swopf	0	60	40	0	60	40	0	60	40
synthes1	11	78	11	11	78	11	11	78	11
tame	0	20	0	0	20	0	0	20	0
tfi2	92	8	0	92	8	0	92	8	0
trainf	59	41	0	59	41	0	59	41	0
trainh	41	46	13	41	46	13	41	46	13
trimloss	0	97	3	0	97	3	0	97	3
try-b	0	100	0	4	96	0	0	100	0
twobars	0	67	33	0	67	33	0	67	33
ubh1	40	40	20	40	40	20	40	40	20
ubh5	0	0	100	0	0	100	0	0	100
woods	100	0	0	100	0	0	100	0	0
yfit	100	0	0	100	0	0	100	0	0
zangwil3	0	0	100	0	0	50	0	0	100
zecevic2	88	13	0	88	13	0	88	13	0
zecevic3	0	63	38	0	64	36	0	63	38
zecevic4	10	80	10	10	80	10	10	80	10
zigzag	0	93	7	0	75	25	0	71	29
zy2	11	89	0	10	90	0	10	90	0
s203	0	75	25	0	75	25	0	75	25
s215	13	38	50	13	38	50	13	38	50
s216	0	67	33	0	67	33	0	67	33
s217	0	33	67	0	33	67	0	33	67
s219	0	35	65	0	5	95	0	5	95
s220	59	34	7	55	35	10	59	34	7
s221	-	-	-	51	40	9	34	11	55
s222	0	67	33	0	67	33	0	67	33
s223	11	78	11	11	78	11	11	78	11
s224	100	0	0	100	0	0	100	0	0
s225	0	100	0	0	100	0	0	100	0
s226	13	63	25	13	63	25	13	63	25
s227	14	29	57	14	29	57	14	29	57
s228	13	88	0	13	88	0	13	88	0
s229	95	5	0	95	5	0	95	5	0
s230	11	44	44	0	80	20	0	80	20
s231	93	7	0	93	7	0	93	7	0
s232	100	0	0	100	0	0	100	0	0
s233	11	78	11	11	78	11	11	78	11
s234	0	100	0	0	100	0	0	100	0
s235	-	-	-	-	-	-	5	59	36
s236	5	84	11	0	100	0	3	90	7
s237	0	97	3	7	80	13	0	97	3
s238	5	61	34	7	85	7	-	-	-
s239	5	79	16	0	89	11	0	95	5

s241	0	73	27	0	80	20	0	75	25
s242	94	6	0	96	4	0	96	4	0
s244	100	0	0	100	0	0	100	0	0
s247	13	73	13	13	73	13	13	73	13
s248	0	47	53	0	47	53	0	47	53
s249	0	100	0	0	100	0	0	100	0
s250	100	0	0	100	0	0	100	0	0
s251	100	0	0	100	0	0	100	0	0
s252	5	65	30	5	70	25	5	65	30
s253	100	0	0	100	0	0	100	0	0
s254	0	14	86	0	25	75	0	14	86
s257	75	25	0	76	24	0	76	24	0
s259	82	18	0	82	18	0	82	18	0
s262	50	50	0	50	50	0	50	50	0
s263	0	17	83	0	17	83	0	17	83
s264	11	44	44	11	44	44	11	44	44
s265	17	67	17	17	67	17	50	33	17
s268	93	7	0	93	7	0	93	7	0
s269	0	100	0	0	100	0	0	100	0
s270	7	93	0	5	86	10	5	86	10
s277	80	0	20	80	0	20	80	0	20
s278	82	0	18	82	0	18	82	0	18
s279	80	0	20	80	0	20	80	0	20
s280	83	0	17	83	0	17	83	0	17
s307	100	0	0	100	0	0	100	0	0
s315	8	77	15	8	83	8	8	83	8
s316	0	14	86	0	14	86	0	14	86
s317	22	11	67	22	11	67	0	14	86
s318	20	10	70	20	10	70	0	14	86
s319	9	9	82	9	9	82	0	13	88
s320	15	8	77	15	8	77	0	11	89
s321	7	14	79	13	6	81	0	9	91
s322	5	16	79	0	22	78	0	6	94
s323	0	71	29	0	71	29	0	71	29
s324	0	62	38	7	57	36	0	62	38
s325	13	50	38	11	67	22	13	50	38
s326	8	58	33	10	60	30	8	58	33
s327	6	83	11	9	77	14	9	77	14
s328	81	19	0	81	19	0	81	19	0
s329	13	56	31	13	56	31	13	56	31
s330	0	50	50	0	50	50	0	50	50
s331	83	17	0	83	17	0	83	17	0
s335	0	8	92	0	8	92	0	8	92
s336	6	12	82	6	11	83	0	24	76
s337	0	86	14	0	86	14	0	86	14
s338	15	15	69	21	16	63	0	36	64
s339	13	88	0	13	88	0	13	88	0
s340	88	0	13	88	0	13	88	0	13
s341	14	43	43	10	40	50	14	43	43
s342	0	33	67	0	23	77	0	33	67
s343	0	69	31	0	69	31	0	69	31
s344	0	100	0	0	100	0	0	100	0
s345	0	89	11	0	89	11	0	89	11
s346	0	69	31	0	69	31	0	69	31
s348	7	36	57	7	36	57	7	36	57
s353	0	71	29	0	71	29	0	71	29
s354	100	0	0	100	0	0	100	0	0
s355	4	89	6	0	86	14	0	86	14
s356	0	87	13	0	55	45	0	55	45
s357	0	100	0	0	100	0	0	100	0
s358	92	8	0	95	5	0	90	10	0
s359	100	0	0	100	0	0	100	0	0
s360	9	91	0	6	94	0	6	94	0
s361	22	78	0	19	77	4	19	77	4
s365	0	43	57	-	-	-	0	46	54
s366	5	75	20	5	75	20	5	75	20
s367	-	-	-	0	88	13	0	85	15
s369	8	58	33	8	58	33	8	58	33
s372	-	-	-	-	-	-	11	54	36
s373	0	67	33	0	67	33	0	67	33
s374	0	72	28	2	70	28	3	72	26
s375	32	16	53	32	16	53	32	16	53
s377	48	48	4	48	48	4	48	48	4
s378	5	9	86	4	7	89	-	-	-
s380	1	42	57	0	42	58	2	50	48
s381	90	0	10	90	0	10	90	0	10
s382	0	80	20	0	80	20	0	80	20
s383	80	20	0	80	20	0	80	20	0
s387	6	53	41	6	53	41	5	57	38
s388	2	63	35	3	50	47	2	62	37
s389	5	44	51	3	53	45	3	58	39
s392	9	38	53	9	38	53	9	38	53
s393	15	85	0	21	71	7	21	71	7
s394	7	93	0	0	100	0	0	100	0
s395	0	93	7	0	100	0	0	100	0
IEEE_57	0	80	20	0	80	20	0	80	20
IEEE_162	4	94	2	0	96	4	0	96	4
IEEE_300	3	53	44	0	61	39	0	61	39
Average	46	30	24	49	26	25	51	28	21